ROLE AND MECHANISMS OF BACTERIAL BIOFILMS IN SILVER NANOPARTICLE RESISTANCE

Mr. Pumis Thuptimdang

A Dissertation Submitted in Partial Fulfillment of the Requirements
for the Degree of Doctor of Philosophy Program in Environmental Management
(Interdisciplinary Program)
Graduate School
Chulalongkorn University
Academic Year 2014

บทบาทและกลไกของไบโอฟิล์มของแบคทีเรียในการต้านทานอนุภาคซิลเวอร์นาโน

นายภูมิศร์ ทับทิมแดง

วิทยานิพนธ์นี้เป็นส่วนหนึ่งของการศึกษาตามหลักสูตรปริญญาวิทยาศาสตรดุษฎีบัณฑิต
สาขาวิชาการจัดการสิ่งแวดล้อม (สหสาขาวิชา)
บัณฑิตวิทยาลัย จุฬาลงกรณ์มหาวิทยาลัย
ปีการศึกษา 2557

Thesis Title	ROLE AND MECHANISMS OF BACTERIAL BIOFILMS IN SILVER NANOPARTICLE RESISTANCE
By	Mr. Pumis Thuptimdang
Field of Study	Environmental Management
Thesis Advisor	Professor Eakalak Khan, Ph.D.
Thesis Co-Advisor	Associate Professor Tawan Limpiyakorn, Ph.D.

Accepted by the Graduate School, Chulalongkorn University in Partial Fulfillment of the Requirements for the Doctoral Degree

.....Dean of the Graduate School
(Associate Professor Sunait Chutintaranond, Ph.D.)

THESIS COMMITTEE

.....Chairman
(Assistant Professor Ekawan Luepromchai, Ph.D.)
.....Thesis Advisor
(Professor Eakalak Khan, Ph.D.)
.....Thesis Co-Advisor
(Associate Professor Tawan Limpiyakorn, Ph.D.)
.....Examiner
(Assistant Professor Benjaporn Suwannasilp, Ph.D.)
.....Examiner
(Assistant Professor Onruthai Pinyakong, Ph.D.)
.....Examiner
(Assistant Professor Sumana Ratpukdi, Ph.D.)
.....External Examiner
(Sorawit Powtongsook, Ph.D.)

ภูมิศร์ ทับทิมแดง : บทบาทและกลไกของไบโอฟิล์มของแบคทีเรียในการต้านทานอนุภาคซิลเวอร์นาโน (ROLE AND MECHANISMS OF BACTERIAL BIOFILMS IN SILVER NANOPARTICLE RESISTANCE) อ.ที่ปรึกษาวิทยานิพนธ์หลัก: ศ. ดร.เอกลักษณ์ คาน, อ.ที่ปรึกษาวิทยานิพนธ์ร่วม: รศ. ดร.ตะวัน ลิมปิยากร, 132 หน้า.

การใช้ผลิตภัณฑ์ซิลเวอร์นาโนอย่างแพร่หลายในปัจจุบัน อาจก่อให้เกิดการปนเปื้อนสู่สิ่งแวดล้อม และส่งผลกระทบต่อไบโอฟิล์มในระบบบำบัดน้ำเสียหรือแหล่งน้ำธรรมชาติ ซึ่งความรุนแรงของผลกระทบขึ้นกับความต้านทานซิลเวอร์นาโนของไบโอฟิล์ม อย่างไรก็ตาม กลไกการต้านทานซิลเวอร์นาโนในไบโอฟิล์มนั้นซับซ้อนและยังไม่มีการศึกษาอย่างชัดเจน งานวิจัยนี้มีวัตถุประสงค์เพื่อศึกษากลไกการต้านทานซิลเวอร์นาโนของไบโอฟิล์ม เมื่อไบโอฟิล์มอยู่ในระยะการเจริญเติบโตที่ต่างกัน, ไบโอฟิล์มมีลักษณะทางกายภาพที่ต่างกัน, และซิลเวอร์นาโนมีคุณสมบัติที่ต่างกัน งานวิจัยนี้ใช้ซิลเวอร์นาโนที่สังเคราะห์ขึ้นเองในห้องปฏิบัติการ และใช้แบคทีเรีย *Pseudomonas putida* KT2440 เป็นตัวแทนของแบคทีเรียในสิ่งแวดล้อม ทำการกำหนดและเลือกไบโอฟิล์มในสามระยะการเจริญเติบโตด้วยปริมาณ Adenosine triphosphate (ATP) , extracellular polymeric substances (EPS), และการแสดงออกของยีนที่เกี่ยวข้องกับการสร้างไบโอฟิล์ม (*csgA* และ *alg8*) เมื่อศึกษาผลกระทบของซิลเวอร์นาโนต่อไบโอฟิล์มที่ระยะต่าง ๆ พบว่าไบโอฟิล์มในระยะที่โตขึ้น (ระยะ 2 และ 3) มีความต้านทานซิลเวอร์นาโนสูงขึ้น (ปริมาณ ATP ลดลงน้อยหรือไม่ลด) เมื่อเทียบกับไบโอฟิล์มระยะแรก (ปริมาณ ATP ลดลงกว่า 90%) เมื่อดึงเอา EPS บางส่วนออกจากไบโอฟิล์มพบว่าความต้านทานซิลเวอร์นาโนลดลง แสดงถึงบทบาทสำคัญของ EPS ต่อความต้านทานซิลเวอร์นาโนของไบโอฟิล์ม นอกจากระยะการเจริญเติบโตแล้ว ยังพบว่าลักษณะทางกายภาพของไบโอฟิล์มส่งผลต่อความต้านทานซิลเวอร์นาโนอีกด้วย เมื่อเลี้ยงไบโอฟิล์มในแหล่งคาร์บอน (กลูโคส กลูตามิกแอซิด และซิเตรท) ปริมาณแหล่งคาร์บอน (ความเข้มข้นกลูโคส 5 และ 50 มิลลิโมลาร์) และอุณหภูมิ (25 และ 30 องศาเซลเซียส) ต่าง ๆ และวิเคราะห์ไบโอฟิล์มจากกล้องจุลทรรศน์เลเซอร์แบบคอนโฟคัลและโปรแกรม COMSTAT พบว่าในสภาวะที่มีกลูโคสเป็นแหล่งคาร์บอน, ความเข้มข้นของกลูโคสมากขึ้น, หรืออุณหภูมิสูงขึ้น ไบโอฟิล์มจะมีความหนาและปริมาตรมากขึ้น, อัตราส่วนพื้นผิวต่อปริมาตรน้อยลง, และความขรุขระของผิวไบโอฟิล์มน้อยลง ซึ่งส่งผลให้มีความต้านทานซิลเวอร์นาโนที่มากขึ้น อย่างไรก็ตาม ความต้านทานซิลเวอร์นาโนของไบโอฟิล์มจะลดลง เมื่อซิลเวอร์นาโนปล่อยไอออนซิลเวอร์มากขึ้นและมีประจุเป็นลบหรือบวกมากขึ้น การทดลองทำโดยสังเคราะห์ซิลเวอร์นาโนสามชนิด ที่มีขนาดใกล้เคียงกัน แต่ปล่อยไอออนซิลเวอร์ต่างกัน (5.3% ในซิลเวอร์นาโนชนิดที่หนึ่ง, 7.7% ในซิลเวอร์นาโนชนิดที่สอง, และ 9.1% ในซิลเวอร์นาโนชนิดที่สาม) ซิลเวอร์นาโนทั้งสามชนิดมีประจุเฉลี่ยที่เป็นกลาง (-1.4 มิลลิโวลต์ในซิลเวอร์นาโนชนิดที่หนึ่ง, -5.5 มิลลิโวลต์ในซิลเวอร์นาโนชนิดที่สอง, และ -2.4 มิลลิโวลต์ในซิลเวอร์นาโนชนิดที่สาม) แต่พบว่าเฉพาะซิลเวอร์นาโนชนิดที่สาม มีประจุเฉลี่ยที่เกิดจากประจุสองชนิด คือประจุลบ (-60 ถึง -95 มิลลิโวลต์) และประจุบวก (+140 มิลลิโวลต์) เมื่อศึกษาผลกระทบของซิลเวอร์นาโนทั้งสามชนิดต่อไบโอฟิล์ม พบว่าซิลเวอร์นาโนปลดปล่อยไอออนซิลเวอร์มากขึ้นเมื่อเวลาการทดลองผ่านไป 24 ชั่วโมง (7% ในซิลเวอร์นาโนชนิดที่หนึ่ง, 13% ในซิลเวอร์นาโนชนิดที่สอง, และ 12% ในซิลเวอร์นาโนชนิดที่สาม) ผลการทดสอบความต้านทานของไบโอฟิล์มต่อซิลเวอร์นาโนทั้งสามชนิดแสดงให้เห็นว่า ซิลเวอร์นาโนชนิดที่สามมีความเป็นพิษต่อไบโอฟิล์มมากที่สุดเนื่องมาจากประจุบวกและลบและปริมาณไอออนซิลเวอร์ที่มากกว่า จากผลการทดลองทั้งหมดในงานวิจัยนี้สรุปได้ว่า การประเมินผลกระทบของซิลเวอร์นาโนต่อไบโอฟิล์มในสิ่งแวดล้อม จำเป็นต้องคำนึงถึงระยะการเจริญเติบโต, ลักษณะทางกายภาพของไบโอฟิล์ม, และคุณสมบัติของซิลเวอร์นาโนไปพร้อมกัน

สาขาวิชา การจัดการสิ่งแวดล้อม ลายมือชื่อนิสิต .....

ปีการศึกษา 2557 ลายมือชื่อ อ.ที่ปรึกษาหลัก .....

ลายมือชื่อ อ.ที่ปรึกษาร่วม .....

5287809420 : MAJOR ENVIRONMENTAL MANAGEMENT
KEYWORDS: BIOFILMS / EXTRACELLULAR POLYMERIC SUBSTANCES / BIOFILM MATURITY / BIOFILM PHYSICAL CHARACTERISTICS / SILVER NANOPARTICLES / SILVER NANOPARTICLE PROPERTIES / SILVER IONS

PUMIS THUPTIMDANG: ROLE AND MECHANISMS OF BACTERIAL BIOFILMS IN SILVER NANOPARTICLE RESISTANCE. ADVISOR: PROF. EAKALAK KHAN, Ph.D., CO-ADVISOR: ASSOC. PROF. TAWAN LIMPIYAKORN, Ph.D., 132 pp.

The use silver nanoparticles (AgNPs) may release AgNPs into wastewater and natural water systems where they can be harmful to biofilms. Therefore, it is important to understand the mechanisms of biofilm resistance to AgNPs. This research aims to investigate the mechanisms of AgNP resistance in biofilms by focusing on the roles of biofilm maturity, biofilm physical characteristics, and AgNP properties. A representative for environmental bacteria used in this study was *Pseudomonas putida* KT2440. Biofilms at three stages of maturity were identified and selected based on adenosine triphosphate (ATP) activity, extracellular polymeric substance (EPS) amount, and expression of EPS-associated genes (*csgA* and *alg8*). Exposing to synthesized AgNPs, more mature biofilms (stages 2 and 3) showed little to no reduction in ATP activity whereas the same treatment reduced more than 90% of ATP activity in the less mature biofilms (stage 1). The biofilms stripped of their EPS were more susceptible to AgNPs than controls with intact EPS, showing the critical role of EPS in AgNP resistance. Not only was the AgNP resistance of biofilms related to the stage but also physical characteristics. The mature biofilms forming in different carbon sources (glucose, glutamic acid, and citrate), glucose concentrations (5 and 50 mM of glucose), and temperature (25° and 30°C) had different physical characteristics. Biofilms with more thickness, more biomass volume, less surface/volume ratio, and less roughness are more resistant to AgNPs. The AgNP resistance of biofilms forming in glucose was similar to glutamic acid (1-log reduction in cell number), which was higher than citrate (2-log reduction in cell number). At 25°C, biofilms forming at higher glucose concentrations exhibited higher AgNP resistance (3-log reduction for 5 mM biofilms and less than 1-log reduction for 50 mM biofilms). Similarly, when the temperature was increased, the 5 mM glucose biofilms had higher AgNP resistance (3 log reduction at 25°C and 1 log reduction at 30°C). The toxicity of AgNPs in this study was mostly from the nanosized AgNPs combining with some toxicity from the released Ag^+. The released Ag^+ showed less toxicity (<1-log reduction) than AgNPs (3 to 4-log reduction) to biofilms in 5 mM of glucose at 25°C. The effect of AgNPs on biofilms increased when AgNPs had more Ag^+ release and highly negative or positive charges. Three AgNPs were synthesized to have different Ag^+ release, which are listed as AgNPs#1, AgNPs#2, and AgNPs#3, respectively. The sizes of the AgNPs were similar while the Ag^+ releases were different, which are 5.3% for AgNPs#1, 7.7% for AgNPs#2, and 9.1% for AgNPs#3. On average, all AgNPs exhibited nearly neutral charge (-1.4 mV for AgNPs#1, -5.5 mV for AgNPs#2, and -2.4 mV for AgNPs#3). However, AgNPs#3 had mainly highly negative (-60 to -95 mV) and positive charges (+140 mV) (but the average charge is close to neutral). After exposing biofilms to AgNPs, the Ag^+ release increased to 7% for AgNPs#1, 13% for AgNPs#2, and 12% for AgNPs#3. The AgNPs#3 exhibited highest toxicity to biofilms. The effect of AgNPs#1 on biofilms was less (1 to 2-log reduction) than that of AgNPs#2 and AgNPs#3 (3-log reduction). Overall, this study demonstrates that biofilm stage, physical characteristics, and AgNP properties must be considered altogether when determining the impact of AgNPs on environmental biofilms.

Field of Study: Environmental Management
Academic Year: 2014

Student's Signature .....
Advisor's Signature .....
Co-Advisor's Signature .....

ACKNOWLEDGEMENTS

I would like to thank my advisors: Prof. Dr. Eakalak Khan, who patiently guides, motivates, and always helps me to reach my potential, and Assoc. Prof. Dr. Tawan Limpiyakorn, who also teaches me and encourages me to do better. Both of them are so experienced and supportive, and I am glad to have them as my mentors. Also, I would like to thank Assoc. Prof. Dr. John McEvoy, who allows me to work in his lab and teaches me about microbiology, and Assoc. Prof. Dr. Birgit Prüβ, who opens the world of biofilms for me and eagerly helps me when I struggle. I am very fortunate to have them as my extra two advisors while I was staying at North Dakota State University. In addition to my advisors, I am very blessed to receive suggestions and comments to improve this dissertation from the skillful and expert committee members: Assist. Prof. Dr. Ekawan Luepromchai, Assist. Prof. Dr. Benjaporn Suwannasilp, Assist. Prof. Dr. Onruthai Pinyakong, Assist. Prof. Dr. Sumana Ratpukdi, and Dr. Sorawit Powtongsook.

I would like to acknowledge the technicians and researchers who have helped me completing my research. Cathy Giddings, for helping me in the lab with her kindness; Dr. Shelly Horne, for teaching and helping me on qPCR; Shane Stafslien, for suggesting the CDC reactor and allowing me to learn from his lab, Justin Daniels, for training me on the CDC reactor operation; Dr. Pawel Borowicz, for teaching me about CLSM; Ms. Numfon Khemthongcharoen for helping me on CLSM. I also have to thank my friends who had been working with me in the lab. Tanush Wadhawan, for being a coach in both research and life, Tu Thi Anh Le, for sharing the lab problems and your delicious food with me, Adam Edwinson, for being a helping hand every time I asked for. I would like to thank all of my friends from Civil Engineering lab and VMS lab at NDSU, and HSM lab at CU, who have shared memories of being a graduate student together.

Lastly, I have to thank my dad, my mom, and my sister, who always cheer me up and supports every decision I made. Without your support, I would not have come this far.

CONTENTS

Page

Page

Page

LIST OF FIGURES

LIST OF TABLES

Chapter 1
Introduction

1.1) Rationale

Due to their strong antimicrobial activity and low risk to human health, silver nanoparticles (AgNPs) are the most prominent metal nanoparticles applied into various manufactured products including medical devices, detergents, clothing, and cosmetics **[1]**. AgNPs are widely known for their effective antibacterial toxicity. AgNPs exhibit an inhibitory effect against various kinds of bacteria when used as a water disinfectant **[2]**. Medical device coated with AgNPs can reduce infection to patients **[3, 4]**. The AgNP-applied wound dressing promotes wound healing while the AgNP-finished fabric shows long-lasting antibacterial efficacy **[5, 6]**.

The widespread use of AgNP products unavoidably releases great amounts of AgNPs to the water environment, mainly through wastewater systems **[7]**. The AgNP-coated fabric can leach up to 20% of total Ag due to washing **[8, 9]**. In the sewer systems, AgNPs can be transported through a long distance to wastewater treatment plants, where a small fraction of them is not removed and gets discharged to environment **[10, 11]**. AgNPs in a river or lake can persist for a long period of time while slowly releasing toxic Ag^+ **[12]**. The toxicity from AgNPs may be minimized due to reactions with other chemical species such as Cl^-, S^{2-}, or organic acids **[13-15]**. However, the transformation process might not be completed while the transformed AgNPs still show toxicity and Ag^+ release **[16]**.

The mechanisms of AgNP toxicity to bacteria involve growth inhibition, activity suppression, cell wall and cell membrane damage, and DNA and protein

damage **[17-20]**. The level of AgNP toxicity not only depends on species of bacteria **[21]**, but also varies with the properties of the particles. Smaller AgNPs exhibit higher toxicity due to more ROS generation **[22, 23]**. The toxicity also increases when the zeta potential or surface charge highly deviated from neutral state. More positive charge increases the toxicity by better interaction of AgNPs with bacterial cell membrane, while more negative charge increases the stability and reduces the agglomeration of AgNPs **[24, 25]**. Amount of Ag^{+} release is another key to the toxicity of AgNPs in water systems **[26]**. In wastewater treatment systems, AgNPs can change the bacterial community in the activated sludge system, reduce nitrifying activity, and affect nitrifying-gene expression **[27-29]**. In natural water systems, the effect of AgNPs on environmental bacteria includes adverse effect on protein synthesis, disruption of enzymatic affinity, and change in community structure **[30]**.

Bacterial biofilms are a community of single- or multi-species of bacteria attached on surface by living in the organized structure of extracellular polymeric substances (EPS) **[31, 32]**. When in environment, bacteria normally form biofilms as an adaptive response to survive in diverse environments **[33]**. Since biofilms are the abundant form of environmental bacteria, the adverse effect of AgNPs in environment should be studied on biofilms. AgNPs have an ability to inhibit the formation of biofilms, diffuse into the biofilms, kill the cells inside biofilms, and reduce the biomass of biofilms **[34-36]**. However, biofilms show greater resistance to AgNPs compared with free-floating cells **[37, 38]**.

Studies on the effect of AgNPs have focused only on the biofilms at a single-time point. This might lead to the inaccurate assessment of biofilm resistance to AgNPs since biofilms at different time points may be in different stages of maturity

[39-42]. Bacteria produce different organelles and EPS to attach to surface, form various phenotypes, and construct mature biofilms **[43-45]**. Biofilms at different maturity levels will have different cell densities, EPS amounts, and degrees of resistance to antimicrobial agents **[46-48]**. Various studies proved that resistance to sanitizers and antibiotics depends on the stage of biofilm maturity **[48-51]**. However, there has been no investigation on AgNP resistance of biofilms at different maturity stages. The mechanism of AgNP resistance of biofilms at different stages of maturity needs to be understood in order to better evaluate the effect of AgNPs on biofilms.

Biofilm characteristics also play a role in the resistance of biofilms **[52, 53]**. Different growth conditions, i.e., nutrient level, type of carbon source, carbon availability, and temperature can contribute to the biomass, EPS production, structure, and metabolic activity of biofilms **[54-58]**. When growing under different conditions, biofilms probably exhibit different AgNP resistance due to the characteristic variations even though they are in the same stage of maturity.

To evaluate the toxicity of AgNPs on environmental biofilms, the question on how biofilms resist to AgNPs must be answered. The findings from this research will provide more understandings on the biofilm resistance to AgNPs and roles of stage of maturity, biofilm characteristics, and AgNP properties in the resistance to AgNPs of biofilms.

1.2) Objectives

The main objective of this research is to investigate the AgNP resistance in biofilms. The specific objectives include:

1. To investigate the impact of AgNPs on biofilms at different stages of maturity;
2. To determine the effect of AgNPs on biofilms with different physical characteristics; and
3. To determine the effect of AgNP properties on the toxicity to biofilms.

1.3) Hypotheses

1. Biofilms in older stages are more resistant to AgNPs than biofilms in earlier stages.
2. Mature biofilms that have higher thickness, higher biomass volume, less surface to volume ratio, and less roughness are more resistant to AgNPs.
3. Biofilms are less resistant to AgNPs with more positive or negative surface charges and higher Ag^{+} release.

Chapter 2
Literature Review

2.1) Silver nanoparticles

Silver nanoparticles are the nanoparticles of zero valent silver in a size range of 1 to 100 nm. Due to their small size, the surface area of AgNPs is relatively high, which substantially enhances their antibacterial property **[59]**. AgNPs have been widely used because of their high antimicrobial property and flexible applications than Ag^+ **[60]**.

2.1.1) Synthesis of AgNPs

AgNPs can be produced via many reactions such as the reaction between sodium borohydride ($NaBH_4$) and silver nitrate ($AgNO_3$) **[22, 61-63],** the reaction between $AgNO_3$, hydrazine hydrate, sodium citrate, and SDS **[64]**, or the UV-photoreduction method **[65]**. AgNPs can also be synthesized on material such as fabric **[66]**. To increase the stability of AgNPs, a polymer is normally used as a stabilizing agent in the synthesis **[67]**.

2.1.2) AgNP applications

Various applications of AgNPs include medical device coating, textile fabrics medical products, and water disinfection **[68]**.

2.1.2.1) Coatings

AgNPs are coated on the surface of material for the purpose of inhibition of cell growth and biofilm formation. Rivero et al. **[69]** fabricated AgNPs on the top of the fiber membrane. The AgNP-coated membrane showed high antibacterial efficiency over 99.99%. Medical devices coated with AgNPs can reduce

the chance of infection to patients. Roe et al. **[70]** found that the catheters coated with AgNPs are able to inhibit both cell growth and biofilm formation. Although some Ag^+ was released during the implanting period on a mouse, the catheters were considerably safe since no organ accumulation was observed and low accumulation was found at the implanted area.

2.1.2.2) Fabrication

El-Rafie et al. **[66]** synthesized and applied AgNPs on cotton fabric. The fabric showed high antibacterial properties, which were reduced after repeated washing. Therefore, a binder was incorporated into the fabric to withstand the washing process and enhance the antibacterial property. The AgNPs proved to be useful for medical purposes. The Ag wound cloth showed an effective treatment of biofilms **[71]**. The cell viability was reduced after the treatment. Even though some cells survived the treatment and were able to re-grow, they were susceptible to antibiotic treatment while the non Ag-treated biofilms were resistant.

2.1.2.3) Medicine

AgNPs can be used along with antibiotics to enhance their antibacterial activity. Fayaz et al. **[72]** observed the synergistic effects of AgNPs and antibiotics and found the increased antibacterial activities of ampicillin, erythromycin, kanamycin, and chloramphenicol against the Gram-positive and Gram-negative strains of bacteria.

2.1.2.4) Water disinfection

AgNPs are used in water treatment systems as a disinfectant. The application of AgNP-paper in percolation can reduce the cell number and inhibit the

re-growth of bacteria **[73]**. The Ag^+ amount left in the effluent was below the standard level and considered safe.

2.1.3) Fate and transport of AgNPs

The release of AgNPs from commercial clothing is possible as shown in the study of Benn and Werterhoff **[74]** on commercial socks, which represent the household sources of AgNPs. Higher numbers and longer time of washing led to higher amounts of silver released from the socks. Ag was observed in both ion and colloidal forms. Geranio et al. **[75]** reported that Ag can be released from the coated textiles in the washing conditions (high pH and the presence of surfactants). The use of bleaching agents can also induce the rate of release. The form and the amount of released Ag depend on the types of fabric and how Ag was incorporated into the fabric.

Apart from household products, AgNPs can be released from laboratories, film and print production, dentists and hospitals, galvanic and electroplating work, production of circuit boards, and catalyst production **[76]**. Blaser et al. **[77]** presented the Ag flows from the use of AgNPs incorporated plastics and textiles (Figure 1). The use of AgNP products causes the release of Ag^+ and nanoparticles into water. AgNPs can travel further to the sewer system. Kaegi et al. **[11]** found that AgNPs did not aggregate in the sewer system but attached on larger organic constituents, and can be transported to the wastewater treatment plant.

Wang et al. **[78]** stated that the nanomaterial should have less to no adverse effect on the biological wastewater treatment systems. However, it should be noted that the concentrations used in the study were relatively low and may not involve all of the situations of nanoparticle release. Another study shows that the AgNPs not

removed by the sedimentation process can enter the activated sludge system and possibly affect the ammonia-oxidizing population and reduce their nitrification activity **[27]**.

In the conditions where there is a reduced and sulfur-rich environment, AgNPs will aggregate with sulfur to form nanosized silver sulfide crystals (Ag_2S) **[79]**. This process is called sulfidation. AgNPs in the sewer system will be sulfidized while they are transported to the wastewater treatment plant. However, the sulfidation may not be complete, and a small fraction of AgNPs can be released to the surface water **[11]**.

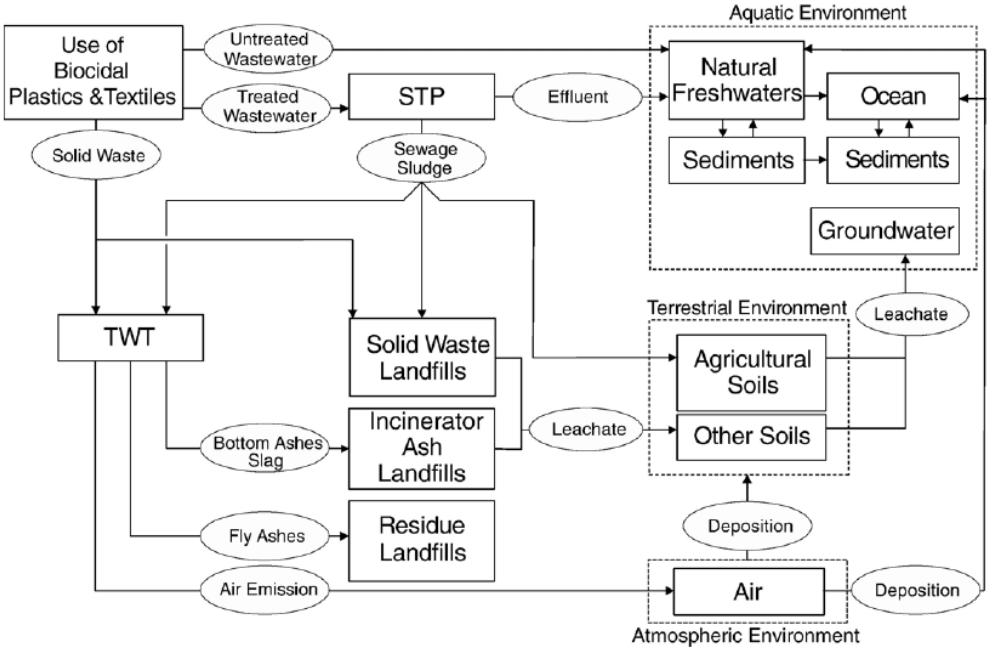

Figure 1 The flows of Ag from AgNP applications. TWT = thermal waste treatment; STP = sewage treatment plant.

When released into natural freshwater, AgNPs can be transformed to Ag_2S, AgCl or nano-Ag^0 species depending on the transformation process by organic/inorganic ligands **[80]**. An increase in ionic strength can induce AgNP aggregation, fractal dimension, and release of Ag^+ **[14]**. However, high toxicity of AgNPs was found in the high ionic strength conditions.

AgNPs can interact with other natural compounds such as clays, biomass, and natural organic matter (NOM). The effect of NOM on the stability and toxicity of AgNPs was studied by Gao et al. **[15]**. Suwannee River humic acid (SRHA) was used as the NOM in the study. The properties or stability of AgNPs were determined from zeta potential, particle size distribution, and suspended particle concentration after mixing with SRHA. The results showed that low concentrations of SRHA helped stabilizing AgNPs whereas higher concentrations induced aggregation. SRHA was not found to significantly influence Ag dissolution. The toxicity of AgNPs also decreased with higher SRHA concentrations.

2.1.4) AgNP toxicity

2.1.4.1) Toxicity to humans

One of the reasons that AgNPs are applied in many consumer products is that they have been considered safe for human health. However, many studies have found the effect of AgNPs on human cells. Gaiser et al. **[81]** observed the in vivo and in vitro toxicity of AgNPs on human and animal cells. The results showed the dose-dependent toxicity and the uptake of AgNPs into the human cells.

Beer et al. **[82]** studied the toxicity of AgNPs on lung cells by focusing on the Ag^+ fraction. The AgNPs with higher Ag^+ fraction exhibited higher toxicity. When the Ag^+ fraction was high, the toxicity from AgNPs and Ag^+ was similar. No

significantly different apoptosis and necrosis were observed between Ag^+-treated, AgNP-treated, and control cells. The accumulation of Ag might cause a group of diseases called Amyloidoses; however, only limited data for Ag^+ were provided while the data for AgNPs is yet to be obtained **[59]**.

2.1.4.2) Toxicity to aquatic organisms

AgNPs accumulate and cause abnormal swimming to the crustacean, *D. magna* **[83]**. AgNPs in a colloidal form showed similar toxicity to Ag^+, which is higher than the toxicity of AgNPs in a powder form. Even though the Ag^+ is an important mechanism of AgNP toxicity to aquatic organisms, it was found that some organisms can accumulate different degree of Ag^+, resulting in different toxicity **[84]**.

2.1.4.3) Toxicity to microorganisms

Similar to Ag^+, AgNPs show high toxicity to microorganisms. Guzman et al. **[64]** observed the antibacterial activity of synthesized AgNPs on different species of bacteria. The concentrations of reducing agents used for the synthesis contributed to the antibacterial activity. The AgNPs showed good antibacterial activity on all of the bacteria. The smaller size particles had more toxicity.

The toxicity of AgNPs to bacterial community was observed by Das et al. **[30]**. After the exposure, four responses of the phenotypes were observed: intolerant, impacted but recovering, tolerant, and stimulated phenotypes. AgNPs affected the total bacteria number, metabolic respiration, bacterial production, and the community structure.

Some bacteria are tolerant to AgNPs. Khan et al. **[85]** investigated the tolerance of bacteria from the sewage environment to AgNPs. No AgNP toxicity was

observed on the tolerant strain isolated from the sewage. Also, the released Ag^+ did not cause growth reduction.

2.2) Effect of AgNPs on bacteria

2.2.1) Mechanisms of AgNP toxicity to bacteria

The mechanisms of AgNP toxicity include cell wall and membrane damage, DNA and protein damage, activity inhibition, growth inhibition, and inhibition of biofilm formation.

2.2.1.1) Cell wall and cell membrane damage

AgNPs can cause the formation of pits on the cell wall of bacteria **[86]**. However, they can not rupture the outer and cytoplasmic membrane **[87]**. Song et al. **[67]** found the separation of cytoplasm from the cell wall, and AgNPs could inhibit the cell wall synthesis. Also, AgNPs in cytoplasm induced the metabolic disturbance in the cell. The hydrophobicity of cells plays a role in AgNP diffusion into the cell. Habimana et al. **[88]** used an enzyme to adjust the cell wall surface from hydrophilic to be more hydrophobic. Smaller fraction of AgNPs was able to diffuse through the cell wall in the presence of the enzyme, suggesting that the change in cell wall property to be more hydrophobic can reduce the toxicity of AgNPs.

2.2.1.2) DNA and protein damage

AgNPs caused the DNA strand-breaking activity on the plasmid DNA, which was observed by the change of plasmid from the dense forms to the open forms **[89]**. The effect of AgNPs on DNA of Gram-negative bacteria (*Escherichia coli*) was reported by Radzig et al. **[20]**. The mechanism of DNA damage was observed by determining the resistance of the mutants deficient in genes relating to DNA repair. Bacteria are less resistant to AgNPs when they had mutation in these genes.

Moreover, AgNPs can affect membrane protein of bacteria as observed by the gene responded to AgNP exposure **[90]**. For nitrifying bacteria, AgNPs can inhibit the functions of proteins responsible for biosynthesis, energy production, and nitrification **[28]**.

2.2.1.3) Activity inhibition

AgNPs can inhibit the respiration and biogas production of bacterial community in wastewater **[18]**. In the activated sludge system, AgNPs can inhibit nitrification activity, leading to the change of ammonia-oxidizing bacteria population **[27]**. The AgNP toxicity to the nitrifying activity can vary depending on the coating materials, which affect the aggregation of AgNPs and the Ag^+ release **[28]**.

AgNPs were found to be less toxic to nitrogen-cycling bacteria (denitrifier, nitrogen fixer, and nitrifier groups) than Ag^+ **[29]**. Among three types of bacteria, nitrifying bacteria was the most susceptible to AgNPs. No significant effect of AgNPs was observed in the expression of denitrifying genes, whereas the nitrifying genes (ammonia monooxygenase) were upregulated after exposed to a sublethal dose of AgNPs.

In natural water conditions, AgNPs can affect the protein synthesis and hydrolysis affinity of two extracellular enzymes (aminopeptidase and alkaline phosphatase) **[91]**. The effect of AgNPs does not differ significantly among different water types. The effect of AgNPs is also influenced by the adenosine triphosphate (ATP) activity of the cells; the addition of ATP inhibitors increases the toxicity of AgNPs **[92]**.

2.2.1.4) Growth inhibition

Staphylococcus aureus, *E. coli*, and *Pseudomonas aeruginosa* showed extended lag phase after the cells are exposed to AgNPs. The longer lag phase was observed at higher AgNP concentrations **[93]**. The growth of bacteria is also dependent on AgNP concentration. The higher concentration results in the extended lag phase of growth; however, the cells recovery from AgNP exposure have higher growth rate when compared to the unexposed cells **[17]**. Siddhartha et al. **[94]** found a clear extended lag phase in Gram-negative bacteria but not in Gram-positive in the presence of AgNPs. Only partial growth inhibition was found in Gram-positive bacteria. Higher doses resulted in longer lag phase in Gram negative but shorter lag phase in Gram positive. When AgNPs are sulfidized, the size and aggregation state of AgNPs affect the properties and products from sulfidation, which influence the bacterial growth inhibition **[13]**.

2.2.1.5) Inhibition of biofilm formation

The planktonic bacterial cells pretreated with AgNPs form less amount of biofilms compared to the non-treated cells. The biofilms have less biomass and viability when forming in higher AgNP concentrations **[95]**. The effect of AgNPs on biofilms is not only dose-dependent but also cell number-dependent **[65]**. Both AgNPs and Ag^+ show similar inhibition of biofilm formation and are able to reduce the cell viability in full-grown biofilms **[20]**.

2.2.2) Effect of AgNP properties on antimicrobial toxicity

The toxicity of AgNPs also depends on the properties of AgNPs, which are Ag^+ release, particle size, surface charge, and reactive species generation.

2.2.2.1) Effect of Ag^+ release

Ag^+ can be released from AgNPs by the following redox reaction **[96]**:

$$2Ag(s) + 1/2O_2 + 2H^+ \rightarrow 2Ag^+ + H_2O$$

The Ag^+ released provides more toxicity than the AgNPs. Park et al. **[35]** found that Ag^+ is more toxic to biofilms than AgNPs. In static conditions, AgNPs show less biofilm inactivation and biosorption than Ag^+ at the same concentration. However, the effect of AgNPs increases in dynamic conditions. The toxicity of AgNPs depends on biosorption whereas the toxicity of Ag^+ depends on the exposure time. Ag^+ is released more at the room temperature (25°C) than the higher temperature (37°C) **[26]**. Low AgNP concentrations allow for more Ag^+ release. The Ag^+ is slowly released from the AgNPs; therefore, the old age and long kept AgNPs are highly toxic because of high Ag^+ amount.

2.2.2.2) Effect of size

Gajjar et al. **[97]** found that size and AgNP aggregation play an important role to the AgNP toxicity. Smaller AgNPs will have less aggregation, leading to higher toxicity that the bulk Ag. Sotiriou and Pratsinis **[98]** also found that the smaller size of AgNPs has higher Ag^+ release, and the effect is mainly from the Ag^+. Also, small size AgNPs are able to generate more cellular ROS, resulting in more toxicity to metabolic activity, cell membrane integrity, inflammatory, and genotoxicity of cells **[99]**.

2.2.2.3) Effect of surface charge

A study on Gram-positive bacteria revealed that the toxicity of AgNPs is more related to the surface charges than the size **[24]**. The charge of AgNPs can induce or reduce the physical contact between the particles and the cells. More

positively-charged AgNPs show high toxicity to Gram-positive bacteria due to the attractive force between the positive charges and the negative cell membrane of bacteria, leading to more contact between the particles and the cells. However, the negatively-charged AgNPs can still interact with negative bacterial membrane and exhibit high toxicity against *E. coli* **[86]**. It is stated that when the net charge of the particles is non-zero, the particles have repulsion forces according to the same charges, which results in stability of the particles **[100]**. Therefore, positively- or negatively-charged AgNPs show higher toxicity when compared to more neutral charged AgNPs due to less aggregation of the particles. Samberg et al. **[25]** found that AgNPs with higher negative charges form stable dispersions in solution while lower negative charges result in more agglomeration of AgNPs.

2.2.2.4) Effect of reactive species

Generation of reactive species, such as hydroxyl radical (●OH) and ROS, is proposed to be an important mechanism of AgNP toxicity. In a study of the synergistic effect of AgNPs and antibiotics, AgNPs generated ●OH, which could play a role in the toxicity **[92]**. According to Hwang et al. **[90]**, AgNPs can produce superoxide radicals. The role of superoxide radicals was proven by the superoxide radical (*28xop*) gene expression and the reduced toxicity after adding an enzyme specific to the radical. Dimkpa et al. **[87]** found that Ag^+ release and H_2O_2 production contribute to the toxicity of AgNPs, but no ●OH production was found. ROS was highly generated from AgNPs at higher temperatures, and adding antioxidant and ROS scavenger was able to reduce the toxicity of AgNPs **[101]**. The aerobic conditions allow more toxicity from ROS than the anaerobic conditions.

2.2.3) AgNP toxicity on bacterial biofilms

AgNPs are able to inhibit biofilm formation and diminish the established biofilms. Martinez-Gutierrez et al. **[102]** showed that Gram-negative biofilms are more susceptible to AgNPs than Gram-positive biofilms. The effect of AgNPs on biofilms was also dose-dependent. Choi et al. **[37]** found that the biofilm cells are resistant to AgNPs more than planktonic cells, but the results are opposite in the case of Ag^+. This might be due to the aggregation of particles in extracellular matrix. AgNPs were able to penetrate into biofilms as deep as Ag^+. It was suggested that the biofilm resistance comes from the reduced diffusive transport of AgNPs into the biofilms since the aggregation was found in the biofilms.

The effects of AgNPs on natural marine biofilms include decreases in biomass, thickness, and volume of the biofilms **[103]**. The uptake of AgNPs into the marine biofilms increased with the dose. AgNPs could affect the community structure of biofilms. The impact of AgNPs and Ag^+ on biofilms is reduced in the presence of humic acid, which may be due to the effect of complexation between humic acid and AgNPs or Ag^+ **[104]**.

2.3) Biofilm formation

Biofilms are clusters of bacteria embedded in EPS. EPS are biosynthetic polymers produced by the bacteria and are localized at or outside the bacterial cell surface and consist of various high molecular weight organic macromolecules such as polysaccharides, proteins, nucleic acids along with other nonpolymeric constituents of low molecular weight **[105]**. Biofilms can be made up of single or multiple species of bacteria **[106]**. Jefferson **[107]** discussed that bacteria form biofilms because of four reasons: (1) Protection from harmful conditions or stresses, (2) Inhabitation due to

favorable conditions, (3) Benefit of community behavior, and (4) The default mode of growth.

Growth conditions can affect the biofilm formation. Increases in C/N availability and nutrients strongly influence the rate and amount of biofilm colonization and accumulation **[55]**. The temperature can affect the phenotypes and EPS production of biofilms **[108]**. Too acidic or basic in pH results in less biofilm formation **[109]**. The hydrophobicity and roughness of the surface also have an effect on biofilm formation: the most hydrophobic and rough surface induce more biofilm formation **[110]**.

Antibacterial agents can also influence the adhesion of bacteria and formation of biofilms. Hoffman et al. **[111]** observed increased cell number and biomass of *P. aeruginosa* and *E. coli* strains when adding aminoglycoside antibiotics. The degree of biofilm induction by antibiotics varies between bacterial species and types of antibiotics **[112]**. Another study conducted by Schreiber and Szewzyk **[113]** showed that the environmental-level concentrations of some pharmaceuticals (phenazone, amoxicillin, and erythromycin) influenced the adhesion of bacteria onto the surfaces. They also found that the initial adhesion of biofilms depends on the concentration of antibiotics and the adhesion surfaces.

In order to form biofilms, bacteria need to develop themselves through various steps. Watnick and Kolter **[43]** proposed the steps for biofilm formation. First, bacteria move to a surface via slow motility, then biofilm originates when the cells attached to the surface. In order to become a biofilm community, bacteria must repress their synthesis of the organelles used for motility, and produce 30xopolysaccharides to establish the biofilm structure. When biofilm is developed to

have high thickness, the growth rate may be slow due to limited area and high density of population. Occasionally, the biofilm bacteria detach from the biofilm matrix.

Similar to the stages of formation described above, Sauer et al. **[44]** characterized five stages of biofilm development. The first stage is reversible attachment, which involves attachment of flagella to the surface. The second stage is irreversible attachment, which occurs when cells begin their development and the mobility is stopped. The third stage, maturation-1, is characterized when cell clusters become layered, followed by maturation-2 in the fourth stage as the maximum thickness of biofilm is reached. The fifth stage is called dispersion and is observed when cell clusters undergo alterations in their structure due to the dispersion of bacteria from their interior portions.

The gene expression patterns change with time during biofilm development, which may be divided into 4 groups of functions **[114, 115]**:

(1) Switching from planktonic cells to attached cells. For example, *fliA* gene controls the flagella synthesis, which are important to initial attachment of bacteria on surface during the irreversible stage of biofilm formation **[116]**.

(2) Polysaccharide production. For example, in *Pseudomonas aeruginosa* PAO1, Psl and Pel exopolysaccharides are required for biofilm formation. The production is regulated by the *rsm* gene clusters, which are controlled by various systems responding to environmental conditions **[117]**.

(3) Stationary phase-cell characteristics. For example, RpoS, which is a sigma factor expressed during the stationary phase cells of *E. coli*, is also expressed during biofilm formation to form unimpaired biofilms **[118]**.

(4) Activation of stress-response pathways. This is because stress is developed within mature biofilms, so bacteria need to stabilize the biofilms by stress-response functions such as DNA repairing (RecO in *Listeria monocytogenes*) and oxidation stress response (SodB in *P. aeruginosa*) **[44, 119]**.

2.4) EPS of biofilms

EPS are divided into bound EPS and soluble EPS based on their physical state. The soluble EPS are actively secreted by bacteria and are biodegradable, while the bound EPS are inert biomass or are remnants resulting from cell lysis. Soluble EPS can be extracted by centrifugation alone, while the bound one requires additional methods **[120]**. Production of EPS by bacteria depends on various factors such as microbial species, phases of growth, nutritional status and the environmental conditions. Mostly, the production is induced by the environmental stressful conditions; however, biofilms can be developed in laboratory by controlling the nutrient status.

Variations of EPS components and characteristics depend on bacterial cells, shear forces, temperature, and nutrients **[121]**. Basically, biofilm EPS contain mostly polysaccharide **[122]**. The exopolysaccharides represent a major component of the macromolecules in EPS, which accounts for 40-95% of the microbial EPS **[123]**. They are differentiated as homo- and heteropolysaccharides. While the homopolysaccharides are neutral, the majority of the heteropolysaccharides are polyanionic due to the presence of either uronic acids (glucuronic acid, galacturonic acid and mannuronic acid) or ketal-linked pyruvate **[105]**.

EPS consists of not only polysaccharides but also proteins, glycoproteins, glycolipids, and in some cases extracellular DNA **[124]**. Different components of EPS

have different functions to biofilms as shown in Table 1. The composition of EPS can vary among the biofilms at different stages of maturity **[125]**. Instead of polysaccharides, proteins are also the major fraction of EPS in the biofilms of some bacteria **[126]**. Proteins are usually found in the inner layers of biofilm closed to bacteria cells; therefore, the measurement of exact amount of proteins can be affected by proteins from cell lysis during the extraction **[127]**. The function of proteins in biofilm matrix is primarily associated with the cell attachment and biofilm development. In addition, proteins are found as exoenzymes in the EPS of biofilm **[128]**.

Table 1 Functions of EPS of bacterial biofilms

Effect of EPS component	Type of EPS component	Role in biofilm
Constructive	Neutral polysaccharides	Aggregation of cells Structural component Protective barrier
	Amyloids	Structural component
Sorptive	Charged or hydrophobic polysaccharides	Ion exchange Sorption of inorganic ions
Active	Extracellular enzymes	Polymer degradation Enzymatic activity
Surface-active	Amphiphilic Membrane vesicles	Interface interactions Export from cell, sorption
Informative	Lectins Nucleic acids	Specificity, recognition Genetic information, structure
Redox active	Bacterial refractory polymers	Electron donor or acceptor
Nutritive	Various polymers	Source of C, N, P

*Summarized from Flemming and Wingender **[123]**, and Neu and Lawrence **[129]**.*

Other EPS constituents are in smaller quantities such as lipids, humic substances, and extracellular DNA. Extracellular DNA had been considered to be a remnant of lysed cells, but was found to be in high quantity and to play a part in biofilm structure **[124]**. Whitchurch et al. **[130]** studied the biofilm formation of *P. aeruginosa* and discovered that the majority of extracellular material was not 34xopolysaccharides but DNA. The addition of enzyme Dnase I to the culture medium could inhibit biofilm development. They concluded that extracellular DNA is required for the development of *P. aeruginosa* biofilms, and it may play a functional role in the biofilms.

Other roles of EPS include:

(1) EPS helps to initiate biofilm formation. According to the study by Schurr **[131]**, the initial stage of *P. aeruginosa* biofilm formation requires the production of polysaccharide components (Pel and Psl) while alginate is required in the later stages of biofilms.

(2) EPS contributes to the biofilm stability. Nilsson and Chiang **[132]** studied two novel putative exopolysaccharides gene clusters: *pea* and *peb*, which influence the biofilm stability. The results showed that the biofilms lacking one of these clusters have less biomass. The biofilm stability also decreased when treating with sodium dodecyl sulfate, which might be due to the loss of connecting components for the structure of biofilms; on the other hand, biofilm was able to withstand a washout when *pea* or *peb* cluster was expressed.

(3) EPS mitigates the effect of antibacterial agents. Some functional groups in the extracellular proteins of biofilms can bind to AgNPs, leading to the adsorption between the proteins and AgNPs, and the reduction in toxicity **[133]**.

2.5) Mechanisms of biofilm resistance

Biofilms are known for their resistance to toxic substances such as antibiotics, chlorine, and detergents **[134]**. Several mechanisms contribute to the resistance of biofilms including the physical barrier of the biomass, the chemical barrier of the EPS component, the activation of the stress-response, and the resistance of cells inside biofilms due to the limiting nutrients **[106]**.

2.5.1) Physical Barrier

The biofilm structure may reduce the penetration of antimicrobial agents by acting as a physical barrier **[31]**. The 35xopolysaccharides matrix has been found to be a partial barrier but not an impenetrable barrier to antimicrobial agents and other mechanisms should also be involved in the resistance **[106]**. Sheng and Liu **[38]** studied the effect of AgNPs on biofilms and proposed the physical protection as one of the possible mechanisms of biofilm tolerance to AgNPs.

2.5.2) EPS interactions

This mechanism includes the binding of antimicrobial agents by EPS components such as negatively charged phosphate, sulfate, and carboxylic acid groups **[135]**. In this way, the EPS of biofilms acts as an adsorbent or reactant, which reduces the amount of antimicrobial agents available to the inner cells **[31]**. Joshi et al. **[136]** investigated increased resistance of bacteria to AgNPs when EPS was present. The EPS overproducing bacteria showed higher survival against AgNPs. AgNPs are aggregated via EPS, resulting an increase in the hydrodynamic size. The aggregation of AgNPs via EPS is also shown by Choi et al. **[37]**. AgNPs aggregated within the matrix of biofilms, leading to their reduced transport and effect on biofilms.

2.5.3) Stress response mechanisms

Cell-to-cell signaling or quorum sensing has been demonstrated to play an important role in biofilm attachment, development, and resistance **[137-139]**. Quorum sensing may control important genes for increasing the resistance. As bacterial density increases, the quorum sensing is induced. Groups of *N*-acylated homoserine lactones (AHLs) are released in order to induce the transcription of specific genes, which may lead to the responsive activities to antimicrobial agents **[31]**. Hassett et al. **[138]** studied the quorum sensing in *P. aeruginosa* and found that it can control gene expression for producing catalases to reduce effects from hydrogen peroxide. Moreover, catalase activity that was not altered by quorum sensing in free cells had less resistance to hydrogen peroxide than biofilm cells. The central regulator for the stress response in biofilms was thought to be a sigma factor RpoS, which might also be related to quorum sensing as well **[106]**.

2.5.4) Resistance of biofilm cells

Bacteria in the substratum of biofilms are limited to nutrients, so they have slow growth rates or no growth **[48]**. The reduced growth and metabolic rates of bacteria inside biofilms make them less susceptible to antimicrobial agents **[31]**. These slow-growing biofilms have the mechanisms of antibiotic resistance similar to planktonic cells in stationary phase **[140]**. Also, a fraction of population in biofilms might be changed to persister cells **[141]**. In *E. coli* biofilms, the persister cells show no growth and exhibit multidrug tolerance **[142]**.

Chapter 3
Stage of Biofilm Maturity and Silver Nanoparticle Resistance

3.1) Introduction

The uses of AgNPs as an antibacterial agent pose a risk of widespread release to the environment and negative impact on beneficial bacteria in the ecosystems **[12]**. To determine the antibacterial effectiveness of AgNPs and consequences of their release, studying the effect of AgNPs on biofilms is important because bacteria are often present in biofilm communities. Compared to planktonic cells, biofilm cells have different phenotypes and genotypes, which leads to specific biological activities, metabolic pathways, and stress response **[143]**. The genes expressed in biofilms include functions related to surface attachment, transition to stationary phase-like cells, and EPS production **[115]**.

EPS of biofilms, which comprises polysaccharides, proteins, nucleic acids, and other macromolecules, can act as a supporting structure for bacterial adherence to surfaces and access to nutrients **[105]**. It also protects against antimicrobial agents **[144]**. However, AgNPs show an ability to eradicate bacterial biofilms. It was found that AgNPs are more toxic to phototrophic biofilms than Ag ions and are able to diminish biomass of the biofilms **[145]**. Smaller AgNPs can reduce more biomass and viability of biofilms due to better penetration into the EPS matrix **[146]**. The ability of AgNPs to inactivate biofilms also increases in dynamic conditions due to increased biosorption **[35]**. Still, mature biofilms have mechanisms to tolerate AgNPs by using EPS-mediated trapping, aggregation, and reduced diffusion of AgNPs **[36-38, 136]**.

During biofilm formation, biofilms develop themselves to different stages. There are at least four stages of biofilm formation: planktonic, attachment (reversible and irreversible), maturation (microcolonies and macrocolonies), and dispersion **[147]**. These stages occur dynamically during biofilm formation. The formation of various phenotypes related to each stage is regulated by different gene expressions. First, bacteria use organelles such as flagella to move onto the surface. To attach to surface, the flagella genes are repressed followed by the expressions of adhesion proteins such as curli, pilli, and type I fimbriae **[45, 114]**. After irreversibly attached to the surface, exopolysaccharides biosynthesis genes are expressed to produce EPS components such as capsule and alginate to construct mature biofilms **[45, 148]**. Since biofilms show different characteristics during maturation, biofilms in different stages may have different susceptibility to AgNPs.

Various studies have proven that biofilms in different stages show different levels of susceptibility to other antimicrobial agents. Tré-Hardy et al. **[49]** studied the co-administration of antibiotics on biofilms at different stages of maturation. They found that more mature biofilms were less susceptible to antibiotics. Other studies have shown that older biofilms are less susceptible to chlorhexidine and various sanitizers **[50, 51]**. However, the effect of biofilm maturity on their susceptibility to AgNPs has not yet been elucidated and should be studied in order to understand the adverse effect of AgNPs on environmental biofilms.

The objective of this part of the research is to determine the AgNPs resistance of *Pseudomonas putida* KT2440 biofilms at different stages of maturity. *P. putida* KT2440 was selected because it is an effective biofilm-producer found in soil and aquatic environments, and comprehensive physiological and genetic data are available

[149, 150]. Firstly, AgNPs were synthesized and determined for their characteristics. Secondly, biofilm maturation was observed in biofilms grown under static (96-well plate) and dynamic (Center for Disease Control and Prevention (CDC) biofilm reactor) conditions. Lastly, biofilms at different maturation stages were exposed to AgNPs and the effect on biofilm viability was determined. The framework of the experiments is shown in Figure 2.

3.2) Methodology

3.2.1) Synthesis and characterizations of AgNPs

AgNPs were synthesized according to the method by Choi et al. **[62]**, using sodium borohydride to reduce silver nitrate with 0.06% of polyvinyl alcohol (PVA) as a capping agent. The equation of the reaction is as follows:

$$AgNO_3 + NaBH_4 \rightarrow \frac{1}{2} H_2 + \frac{1}{2} B_2H_6 + NaNO_3 + \mathbf{Ag}\ (\text{nano})$$

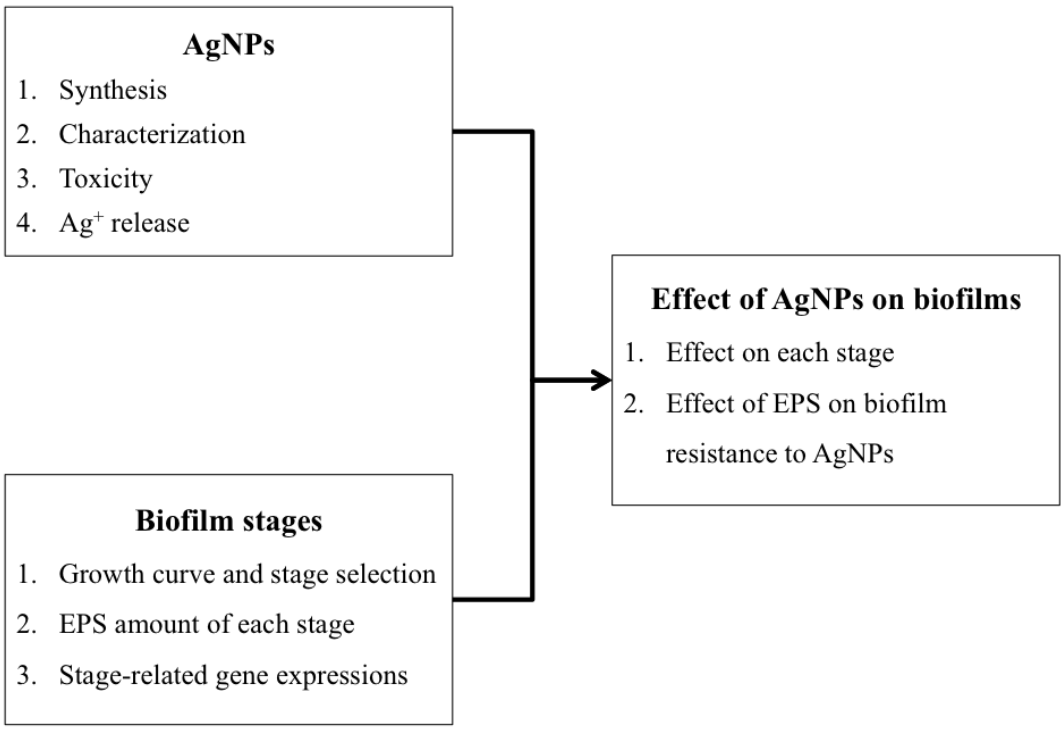

Figure 2 Experimental framework of part one of the research

The concentration of total Ag from the calculation was 26.3 mg/l. The formation of AgNPs was verified by scanning the absorbance of the solution between 250 and 700 nm with a UV-vis spectrophotometer **[151]**. The particles were characterized for size and zeta potential using a zetasizer (Malvern Instruments, Worcestershire, UK). To measure the amount of Ag ion, the AgNPs solution was centrifuged at 165,000× *g*, 4°C, for 1 h **[82]**. The supernatant was collected and dissolved with HNO_3 before measurement by inductively coupled plasma mass spectrometry (ICP-MS).

The toxicity of the synthesized AgNPs was tested from addition of the AgNPs to the 96-well plate with a bacterial culture before determining the biofilm formation at 24 h. The method for culture preparation, biofilm formation and determination of biofilm amount are described in the following subsections.

To observe the release of Ag^+ under experimental conditions, an experiment was performed using a polystyrene, flat-bottom, 6-well plate (Thermo Scientific). Each well contained 5 ml of and 50 µl of the *P. putida* KT2440 inoculum prepared according to the next subsection. The plate was incubated at room temperature (20°C) without shaking for 24 h to allow biofilm formation. After that, 4 ml of media was removed before adding 4 ml of AgNPs. The plate was incubated further at room temperature. After 48 h of exposure, the media was taken for total Ag and Ag^+ measurements by ICP-MS.

3.2.2) Bacterial strain and culture preparation

Before each experiment, *P. putida* KT2440 (ATCC 47054) was cultivated at 37°C overnight in Luria-Bertani (LB) medium. The suspension was centrifuged and the pellet was re-suspended in phosphate buffer saline (PBS). The optical density of

the culture, measured at 600 nm (OD_{600}), was adjusted to 0.4 with PBS (approximately 10^7 CFU/ml) before use as an inoculum in experiments.

3.2.3) Biofilm formation

A polystyrene, flat-bottom, 96-well microtiter plate (Greiner Bio-One, Frickenhausen, Germany) was used to support biofilm formation under static conditions. Each well contained 100 µl of 1X LB medium (final concentration = 0.5X), 95 µl of deionized (DI) water, and 5 µl of the prepared *P. putida* KT2440 inoculum. The plate was incubated at room temperature without shaking to allow biofilm formation.

A CDC biofilm reactor (Model 90-1, Biosurface Technologies, Bozeman, MT) was used to examine biofilm formation under dynamic conditions. The reactor is a one-liter glass vessel with a lid that can hold 8 polyethylene rods. Each rod holds three removable polycarbonate coupons serving as biofilm growth surfaces. The reactor and its components are shown in Figure A-1, Appendix. One milliliter of the *P. putida* KT2440 inoculum was pipetted into the reactor containing 500 ml of 0.5X LB medium. The reactor was operated in a batch mode (100 rpm stirring) and was kept at room temperature to allow biofilm formation.

3.2.4) Adenosine triphosphate (ATP) assay

An ATP based BacTiter-Glo™ microbial cell viability assay (Promega, Madison, WI) was used to monitor changes in bacterial activity during biofilm formation **[152]**. In 96-well plates, ATP concentration was measured every 3 h for the first 24 h and every 12 h between 24 and 72 h. Media was removed and the biofilm was rinsed twice with 200 µl of PBS. One hundred microliters of BacTiter-Glo™ reagent was added to the well and mixed briefly with the biofilm by pipetting. After

incubation at room temperature for 5 min, the bioluminescence was measured as relative light units (RLU) using a TD-20/20 luminometer (Turner Designs, Sunnyvale, CA).

Under CDC reactor conditions, the ATP concentration was measured every 12 h for 72 h. A rod was removed from the reactor and carefully dipped in two consecutive tubes containing 25 ml of PBS to remove the planktonic cells. The three coupons on each rod represented three replicates for the same time point. Each coupon was removed and put in a tube containing 2.5 ml of PBS. The biofilm was detached from the coupon by vortex mixing for 30 s. One hundred microliters of BacTiter-Glo^{TM} reagent was mixed with 100 µl of the cell suspension before measuring the bioluminescence as described above.

3.2.5) Biofilm amount

Two different methods were used for determination of biofilm amount in the 96-well plate and the CDC reactor. The biofilm amount in a 96-well plate was quantified by crystal violet (CV) staining according to the method by Sule et al. **[152]**. In the CDC reactor, the biofilm amount was determined from total carbohydrate by a phenol-sulfuric acid method modified from Masuko et al. **[153]**. The samples were prepared by the method described in the ATP assay subsection. A 1.5 ml aliquot of concentrated H_2SO_4 was added to 500 µl of the sample and incubated for 30 min. A 300 µl aliquot of 5% (w/v) phenol in water was added, and the sample was heated at 90°C in a water bath for 10 min. The sample was cooled at room temperature for 15 min before measuring the absorbance at 492 nm.

3.2.6) RNA extraction and qPCR

To extract RNA from the 96-well plate, media was removed and the biofilms were rinsed twice with PBS. One hundred microliters of PBS were added to each well and the biofilms were scraped with an inoculating needle. Disrupted biofilms were removed from the wells by a pipette. RNA was extracted from 500 µl of suspended biofilm using an Rneasy mini kit (Qiagen, Valencia, CA) in accordance with manufacturer's instructions. Genomic DNA contamination was removed by treatment with Dnase I (Qiagen).

Biofilms were collected from the CDC reactor by the sampling method described above for the ATP assay. To prepare a sample with an adequate number of cells, 20 ml of a cell suspension, prepared from 8 rods (24 coupons), was centrifuged and the pellet was re-suspended in 2.5 ml of PBS. RNA was extracted from 500 µl of the sample with an Rneasy Plus Micro kit according to the protocols provided by the manufacturer (Qiagen).

cDNA was synthesized using random primers (Promega) and Moloney Murine Leukemia Virus Reverse Transcriptase (MMLV-RT, Promega). The reverse transcription process was carried out at 37°C for 60 min followed by heating at 70°C for 10 min for enzyme inactivation. Samples without the reverse transcriptase were used as a negative control. Fragments of *csgA*, *alg8*, and 16S ribosomal RNA (rRNA; used to normalize expression) transcripts were amplified using a SYBR green qPCR approach according to the method by Horne and Prüß **[154]**. The fluorescence signal was monitored in an iQ5 thermocycler Real-Time PCR detection system (Biorad). Forward and reverse primers for *csgA* were 5'-ATA AAT CCA CCG TGT GGC AGG ACA-3' and 5'-AGG TCT GTT CGA TGA AAG CCT CGT-3', respectively.

Forward and reverse primers for *alg8* were 5'-GTG ACC TCG CCA GCT TTC AAC AAT-3' and 5'-TGA ACA GCA CAG CAA CGA AGA TGC-3', respectively. Forward and reverse primers for 16S rRNA were 5'-CCA GGG CTA CAC ACG TGT TA-3' and 5'-TCT CGC GAG GTC GCT TCT-3', respectively. Expression data were analyzed by the comparative C_t method ($\Delta\Delta C_t$), where C_t is the threshold cycle **[155]**.

3.2.7) Exposure of biofilms to AgNPs

For the 96-well plate, 150 µl of the media was removed before adding 150 µl of AgNPs solution (The concentration was approximately at 20 mg/l of total Ag). Biofilms were exposed to AgNPs for 48 h at room temperature. At 0, 3, 6, 9, 12, 24, and 48 h, the solution was removed; biofilms were rinsed twice in PBS before measuring the ATP concentration. Control experiments were carried out in a similar manner, with the exception that 150 µl of 0.06% PVA solution was used instead of the AgNPs solution. The effect of AgNPs on biofilms was determined by comparing the ATP concentration of treatment and control samples.

For CDC reactor experiments, the lid of the reactor containing the polyethylene rods was transferred to another reactor containing 400 ml of AgNPs solution and 100 ml of 1X LB medium. Control experiments were carried out in a similar manner, with the exception that 400 ml of 0.06% PVA solution was used instead of the AgNPs solution. The reactor was operated in a batch mode (100 rpm stirring) for 6 h at room temperature, and it was sampled after 0, 1, 3, and 6 h. During sampling, one rod was taken from the reactor and was replaced by a new rod to balance the fluid shear stress in the reactor. The ATP concentration in the biofilm was

determined as described earlier. Biofilms also were examined using a conventional plate count method **[156]**.

3.2.8) Effect of EPS on biofilm resistance to AgNPs

Experiments to examine the effect of EPS on biofilm susceptibility to AgNPs were conducted in a 96-well plate with biofilms grown for 6, 12, and 48 h. At each time point, media was removed, the biofilm was rinsed twice with PBS, and part of EPS was removed using 200 µl of 2% (w/v) ethylenediaminetetraacetic acid (EDTA) **[157]**. The reduction of biofilm amount was observed by the CV assay. Control experiments were carried out using DI water instead of EDTA. Treatment and control plates were incubated at 4°C for 3 h before rinsing the biofilms with PBS and treating with 200 µl of AgNPs solution at 4°C for 2 h. The effect was determined by comparing the ATP concentration of treatment and control samples as described earlier.

3.2.9) Statistical analysis

Experimental data were statistically analyzed using GraphPad Prism® software version 6.01 (GraphPad Software, La Jolla, CA). In every experiment, the standard deviation of the triplicate data was calculated and presented as error bars. The multiple *t*-test was used to analyze the statistical differences between two interested groups of compared data. To correct the errors from multiple comparisons of *t*-test, the Holm-Sidak method was used over the *t*-test at 5% significance level.

3.3) Results and discussion

3.3.1) Characteristics and toxicity of AgNPs

AgNPs showed the characteristic absorbance at 395 nm similar to a previous report **[28]**. The particle size range was 40 to 60 nm, and a zeta potential range of –2

to –6 mV indicated a nearly neutral charge. The concentration of synthesized AgNPs was 25.86 mg of total Ag/l from the measurement by ICP-MS (26.3 mg/l from calculation). At the concentrations from 1.4 to 6.8 mg/l of total Ag, both AgNPs with and without PVA showed high toxicity to *P. putida* KT2440 and were able to inhibit the biofilm formation within 24 h of exposure (Figure 3). The inhibition was higher when the total Ag concentration was increased. The data also showed that the synthesized AgNPs with PVA as a capping agent had higher toxicity than the bare particles (without PVA).

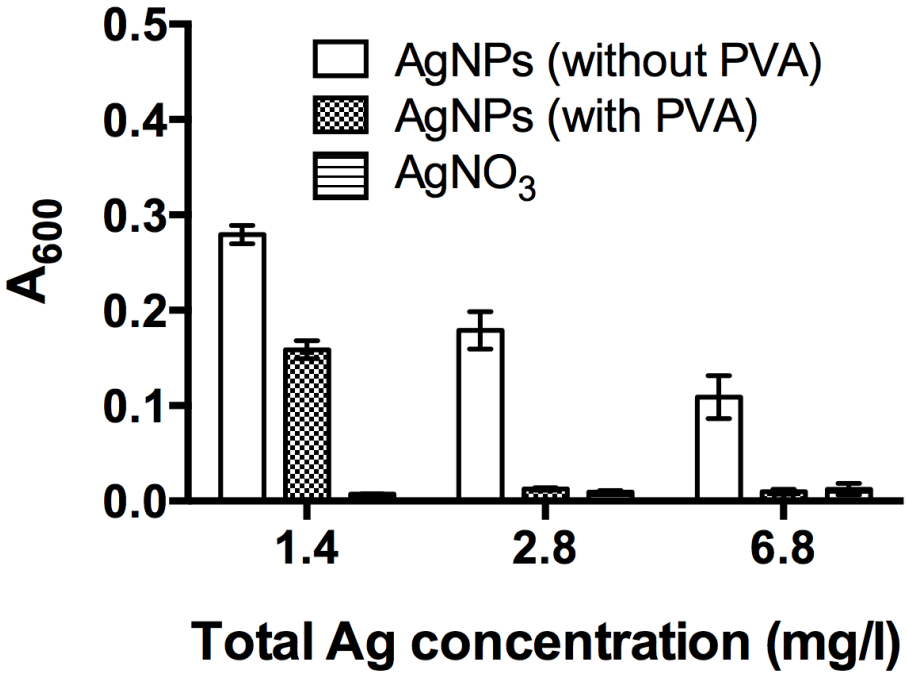

Figure 3 AgNP toxicity to *P. putida* KT2440. Y-axis shows the amount of biofilms determined by CV staining presented as the absorbance at 600 nm (A_{600}). X-axis shows three concentrations of Ag used. The means and standard deviations are based on 3 different biofilm samples.

The synthesized AgNPs released 1.24 mg/l of Ag^+, which was 4.8% of total Ag. The 6-well plate experiment showed the reduction in total Ag from 20.61 to 17.94 mg/l after 48 h of exposure, suggesting the transport of AgNPs into biofilms. After 48 h, the AgNPs released more Ag^+ at 1.76 mg/l, which was 9.8% of the total Ag. Therefore, the synthesized AgNPs should have the mechanisms of toxicity through both AgNPs and Ag^+.

3.3.2) Stages of *P. putida* biofilm maturation

Figure 4 presents ATP levels for *P. putida* over a 72 h period under static (96 well plate) and dynamic (CDC reactor) conditions. A similar temporal pattern of ATP activity was observed in biofilms grown under both conditions, with the exception that ATP activity for dynamic conditions was not detectable before 12 h and peak activity was not observed until 30 h. Three stages of biofilm development were identified from these ATP activity data. The first stage (stage 1) represents early development, when metabolic activity is increasing (6 and 12 h under static and dynamic conditions, respectively). The second stage (stage 2) represents a biofilm at peak metabolic activity (12 and 30 h under static and dynamic conditions, respectively). The third stage (stage 3) represents the stable, lower metabolic activity of a mature biofilm (48 h under both static and dynamic conditions).

The biofilm amount should increase with maturity of the biofilms as EPS is produced for cell adhesion to surfaces and protection from environmental stresses **[158]**. Therefore, the amount of biofilms at selected stages was determined for maturity under static and dynamic growth conditions using the CV and total carbohydrate assays, respectively (Figure 5). Under static conditions, the amounts of biofilms at stage 2 (12 h) and stage 3 (48 h) were 6 and 5 times higher than at stage 1

(6 h) (p = 0.016 for 6 h vs. 12 h; p = 0.006 for 6 h vs. 48 h). Similarly, under dynamic conditions, the amounts of biofilms at stage 2 (30 h) and stage 3 (48 h) were 2 and 3 times higher, respectively, than at stage 1 (12 h) (p = 0.019 for 12 vs. 30 h; p = 0.008 for 12 vs. 48 h).

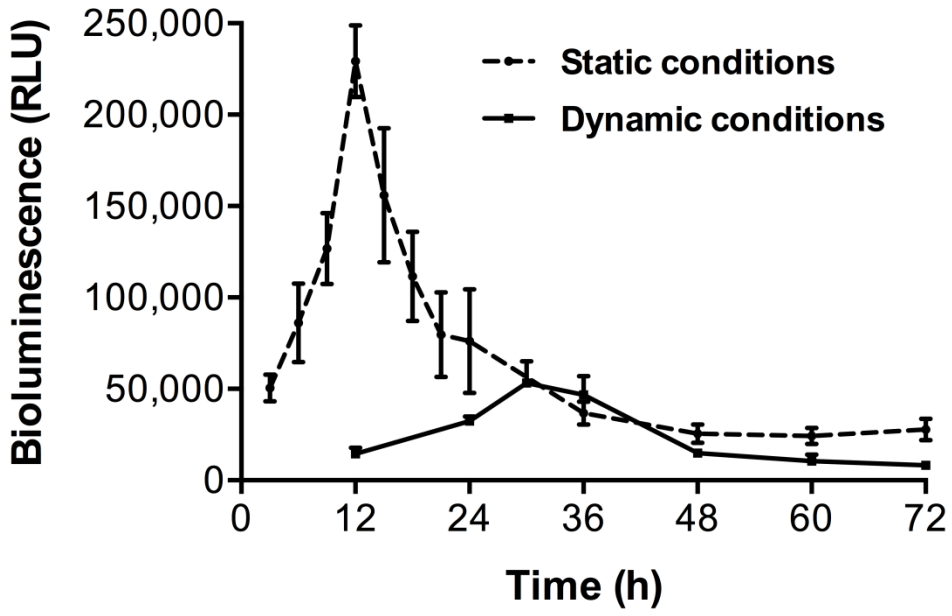

Figure 4 Time course of ATP amount of *P. putida* KT2440 biofilm. The time period is on x-axis, and the ATP amount is presented as the bioluminescence in relative light units (RLU) on y-axis. The means and standard deviations are based on 3 different biofilm samples.

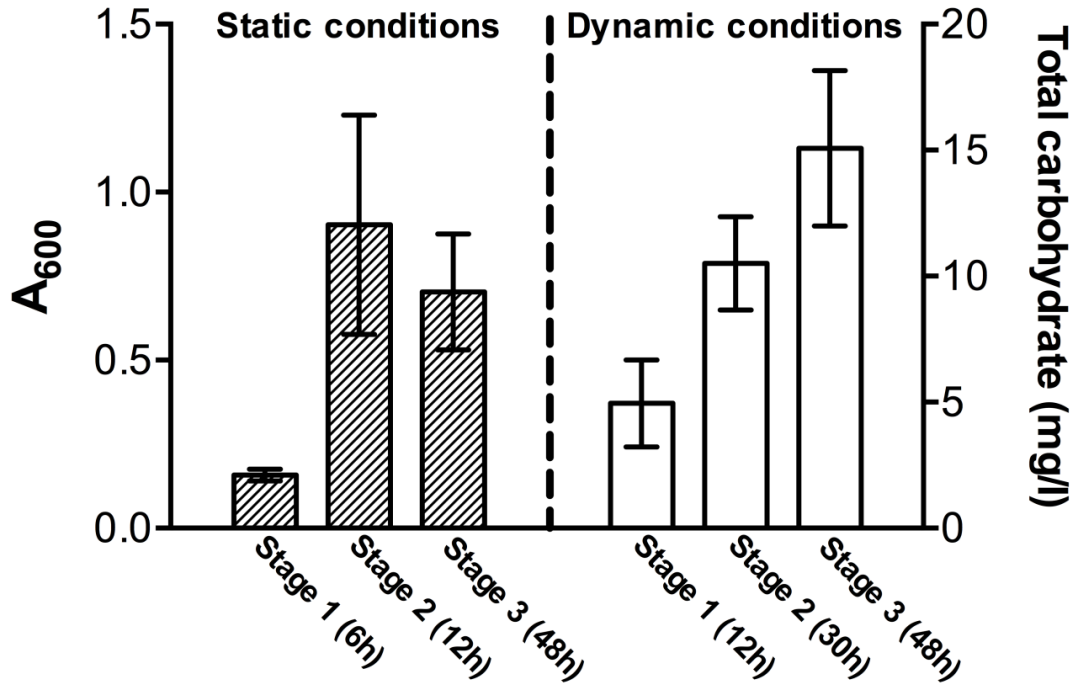

Figure 5 Biofilm amount of *P. putida* KT2440 biofilms at different stages. The left y-axis shows the absorbance at 600 nm (A_{600}) from the CV assay measured in the 96-well plate experiments (static conditions). The right y-axis describes the total carbohydrate measured in the CDC reactor experiments (dynamic conditions) with the unit of mg/l by using D-glucose as a standard. The means and standard deviations are based on 3 different biofilm samples.

Under static conditions, it appeared that biofilms at stage 2 had a higher amount of biomass than at stage 3, while it was the opposite under dynamic conditions. This might be due to the different methods used in different experiments. In the total carbohydrate assay used under dynamic conditions, only carbohydrate from the EPS of biofilms was measured whereas under static conditions the total biomass from live cells, dead cells, and EPS was measured in the CV assay. According to the activity of biofilms under static conditions (Figure 4), stage 2 biofilms should have much higher cell numbers than in stage 3, which was likely to give more CV staining as shown in Figure 5. However, there was no statistical difference between the amount of biofilms in stage 2 and 3 under both conditions (p = 0.401 and p = 0.093 under static and dynamic conditions, respectively).

As biofilms mature, they do not only produce more extracellular matrix but also different components. Among various components, curli is a protein component used for bacterial adhesion to surface **[159]**. Six proteins encoded by the *csgBA* and *csgDEFG* operons contribute to the formation of curli fiber **[160]**. In *Pseudomonas putida* KT2440, *csgA* gene is present for encoding a major subunit of curli. During the irreversible attachment phase, *csgA* gene should be highly expressed **[45]**. A polysaccharide component of EPS, alginate, also contributes to the development, structure, and resistance of biofilms **[161]**. *Alg8* gene encodes alginate biosynthesis protein in *P. putida* KT2440. As biofilms produce polysaccharides to form the structure of biofilms, the expression of *alg8* should increase in mature biofilm. Since bacteria had to adhere to the surface (expression of *csgA* gene) before they could form the structure of biofilms by producing polysaccharide components such as alginate

(expression of *alg8*), it was hypothesized that *csgA* gene would be highly expressed before *alg8* gene in biofilm maturation.

Figure 6 shows that, analogous to EPS levels, expression of *csgA* and *alg8* was higher in biofilms at later stages. The earlier increase in *csgA* expression relative to *alg8* supported our hypothesis. *csgA* expression increased significantly between stage 1 and stage 2 (p = 0.001 and p = 0.013 under static and dynamic conditions, respectively) and again between stage 2 and stage 3 (p = 0.024 and p = 0.030 under static and dynamic conditions, respectively). *Alg8* expression did not differ between stages 1 and 2, but increased significantly between stages 2 and 3 (p = 0.002 and p = 0.002 under static and dynamic conditions, respectively). Collectively, the EPS and gene expression data support the conclusion that biofilm development stages identified from ATP activity data represent stages of increasing maturation. The next subsection examined the effect of AgNPs on biofilms at different stages of maturity.

3.3.3) Effect of stages of maturity on the AgNP resistance of biofilms

The effect of AgNPs on biofilms was measured as a reduction in ATP activity relative to that in a non-treated control. A plate count was used in addition to ATP activity for biofilms grown under dynamic conditions. Figure 7 shows that the least mature biofilms (stage 1) were most susceptible to AgNPs, with greater than 90% reduction in ATP activity and plate count. ATP was not reduced in the more mature stage 2 and stage 3 biofilms under static conditions, and small reductions in ATP and plate count were observed in stage 2 and stage 3 biofilms grown under dynamic conditions. The effect of AgNPs on mature biofilms in dynamic conditions was higher

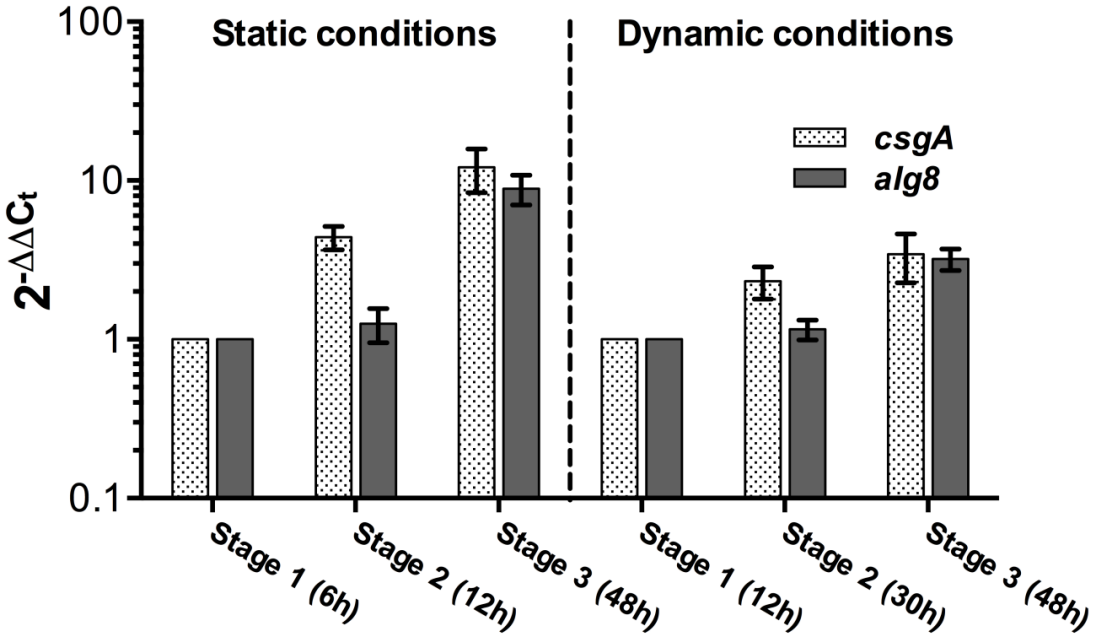

Figure 6 Expressions of *csgA* and *alg8* genes of biofilms at different stages. Y-axis illustrates the level of gene expression in a log scale. X-axis shows different stages of biofilms for static and dynamic conditions. The means and standard deviations are based on 3 different experiments. The expression levels for stage 1 biofilms are equal to 1 because they were used as calibrators; therefore, the error bars are not shown.

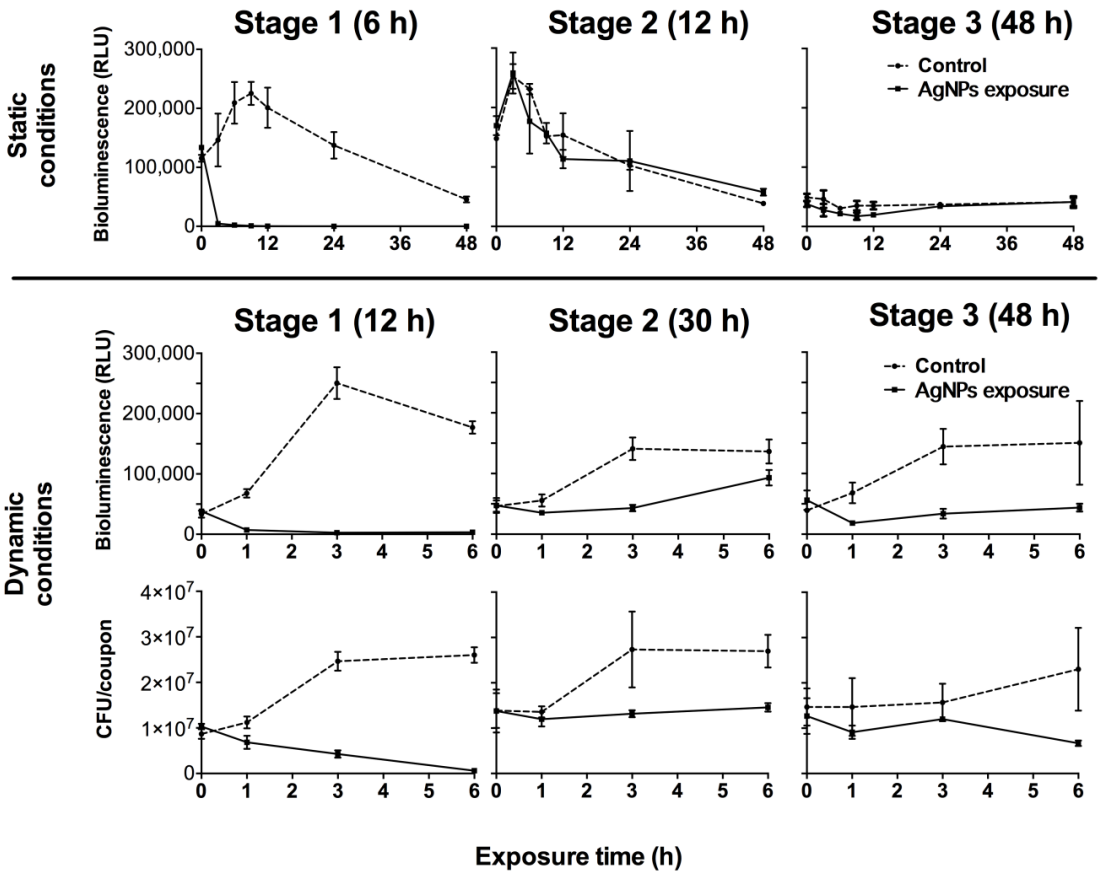

Figure 7 Effect of AgNPs on biofilms at different stages. The effect of AgNPs is shown as ATP reduction (static and dynamic conditions) and cell number reduction (dynamic conditions) on y-axis. The exposure time is illustrated on x-axis. The means and standard deviations are based on 3 different biofilm samples.

than that in static conditions, which can be observed by the gap between the control and the exposure samples. This increased effect might be due to the effect of stirring, which could increase biosorption of AgNPs by biofilms and lead to more inactivation by AgNPs **[35]**.

Several factors may explain the increased resistance of mature biofilms to AgNPs. Firstly, bacterial cells in mature biofilms are likely to be in the stationary growth phase and, therefore, less susceptible to antimicrobial agents **[162]**. To prove this, the exposure experiment was conducted on planktonic cells at different stages (Figure 8). With the same starting cell number, after 3 h of exposure to 20 mg/l of AgNPs, the log-phase cells (6 h) of *P. putida* KT2440 were not observed by the plate count method while the stationary-phase cells (16 h) were still at 10^5 CFU/well, showing more tolerance to AgNPs. Secondly, cells that die in the outer layers of mature biofilms could provide nutrients that enhance the growth of cells in deeper layers **[48]**. A previous study on the effects of single-walled carbon nanotubes on *E. coli* biofilm showed that dead bacterial cells could cause aggregation of the nanotubes and at the same time release intracellular substances to serve as nutrients for other cells **[163]**. Also, the high thickness or high amount of EPS in mature biofilms may have a role in transport limitations of AgNPs through biofilms.

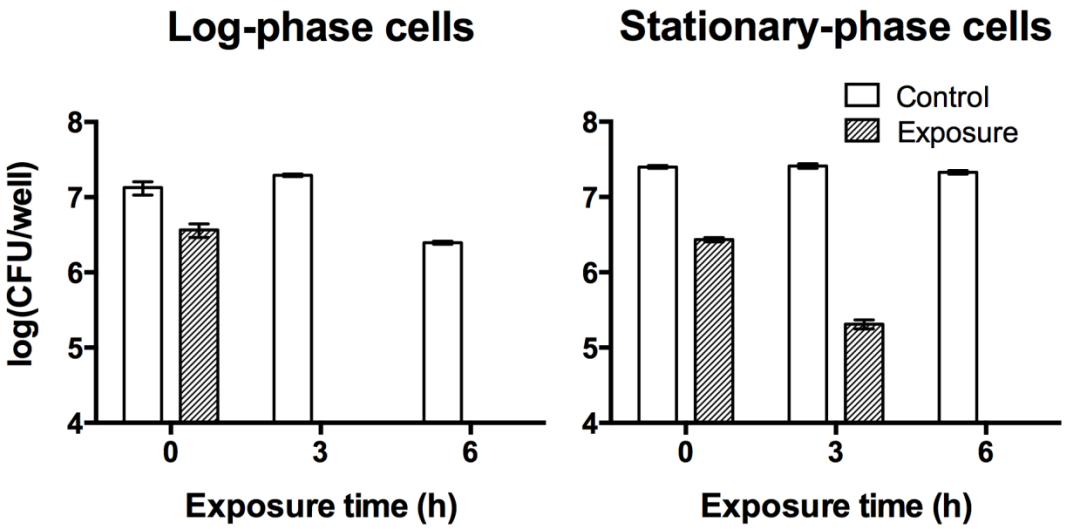

Figure 8 Effect of AgNPs on planktonic cells of *P. putida* KT2440 at different growth phases. The effect is shown as cell number reduction (y-axis). The exposure times were 0, 3, and 6 h (x-axis). The means and standard deviations are based on 3 different samples.

3.3.4) Role of EPS in biofilm resistance to AgNPs

To determine how EPS affects biofilm susceptibility to AgNPs, EPS of biofilms was partly removed by EDTA **[164]**. Figure 9 shows the reduction of ATP activity and biofilm amount after 3 h of EDTA treatment. All stages of biofilms showed a statistically significant reduction of ATP activity (6 h: $p = 0.008$, 12 h: $p = 0.0005$, 48 h: $p = 0.009$). The EDTA treatment could reduce the biomass of more mature biofilms (48 h: $p = 0.003$) while it did not reduce the biomass of 6 h biofilms. After EPS stripping by EDTA treatment, the biofilms were exposed to AgNPs and the effect was measured by reduction in ATP activity (Figure 10). The results showed the critical role of EPS in the protection of biofilm communities from AgNPs. The EPS-stripped biofilms in all three stages showed significantly higher reduction in ATP than biofilms with intact EPS (control) at every time point of exposure ($p < 0.05$).

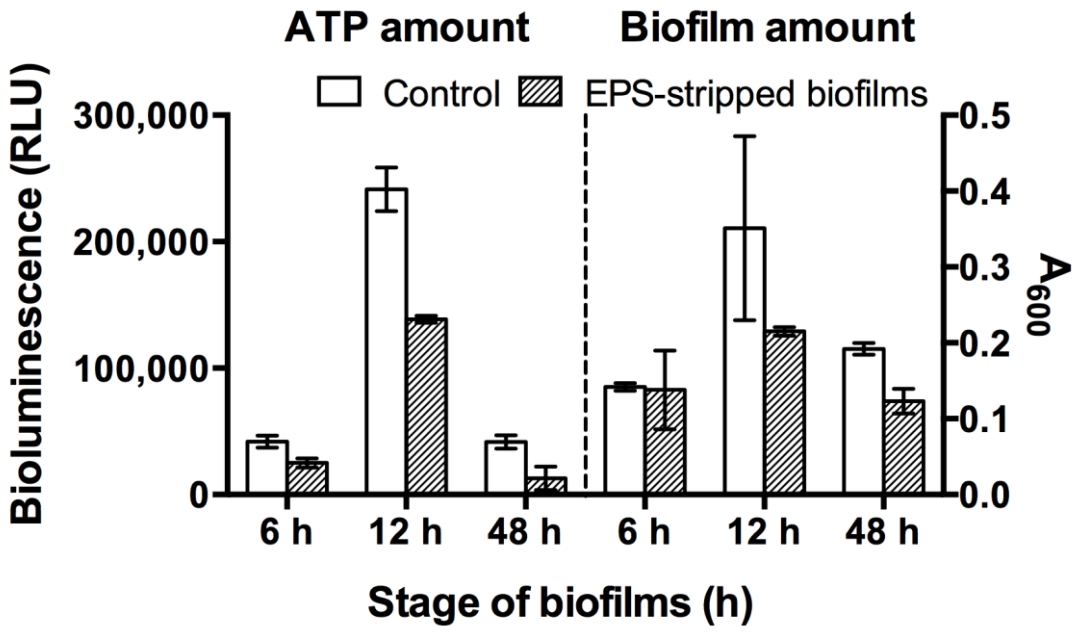

Figure 9 Removal of biofilms by EDTA treatment. Different stages of biofilms before and after EDTA treatment are illustrated on x-axis. The ATP amount is presented as the bioluminescence in relative light units (RLU) on the left y-axis. The biofilm amount measured from the CV is shown as the absorbance at 600 nm (A_{600}) on the right y-axis. The means and standard deviations are based on 3 different biofilm samples.

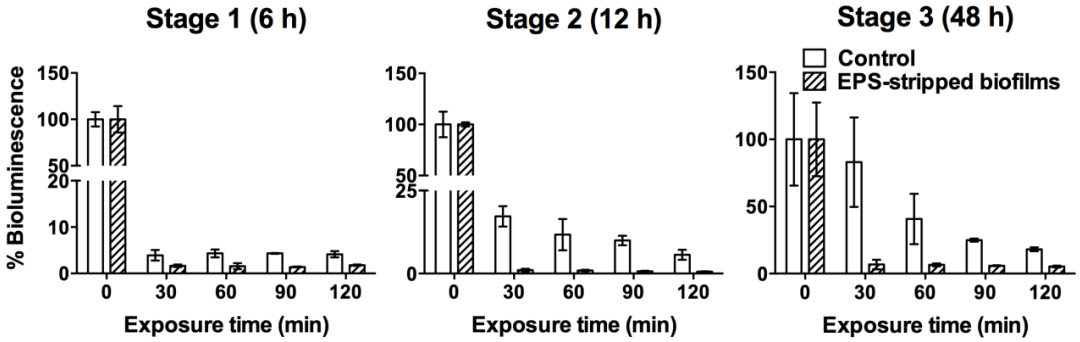

Figure 10 Effect of EPS on biofilm susceptibility to AgNPs. The effect of AgNPs is shown on y-axis as percentage bioluminescence normalized to the sample at 0 h of exposure. X-axis shows the exposure time. The means and standard deviations are based on 3 different biofilm samples.

It should be noted that EDTA did not make the cells of *P. putida* KT2440 more susceptible to AgNPs. To demonstrate this, the susceptibility of planktonic cells to AgNPs was tested after 3 h of EDTA treatment (Figure 11). Between cells with EDTA treatment and without EDTA treatment, there was no significant difference of ATP percentage after 1 h of AgNP exposure ($p = 0.971$). However, after 2 h of AgNP exposure, cells without EDTA treatment even showed less susceptibility to AgNPs than cells treated with EDTA ($p = 0.031$). From these results, it can be concluded that EDTA did not increase the susceptibility of cells to AgNPs. Therefore, the reduction in ATP of biofilms after EPS stripping should be from the EPS removal. Similarly, in a study on effects of AgNPs on wastewater biofilms, greater bacterial reductions were achieved after loosely-bound EPS was removed **[38]**. This is consistent with the findings by Peulen and Wilkinson that EPS density reduces the diffusion of AgNPs into biofilms **[36]**.

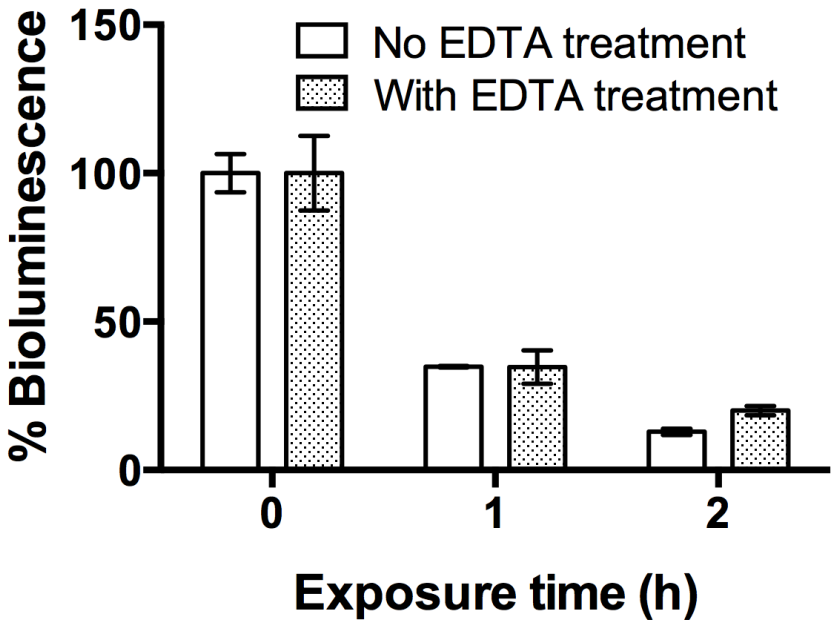

Figure 11 Effect of AgNPs on planktonic cells with/without EDTA treatment. The effect of AgNPs was measured in reduction of ATP activity (% bioluminescence) as described in y-axis. X-axis shows the exposure time.

The mechanisms of AgNP resistance in biofilms at different stage of maturity are summarized in Figure 12. Even though the mature biofilms are less active (more dead cells than live cells in stage 3), they have higher biomass compared with less-mature biofilms (stage 1). When biofilms are exposed to AgNPs, the biomass acts as a barrier for protection from AgNPs. The AgNPs are not able to diffuse into mature biofilms with higher biomass, leading to less impact of AgNPs.

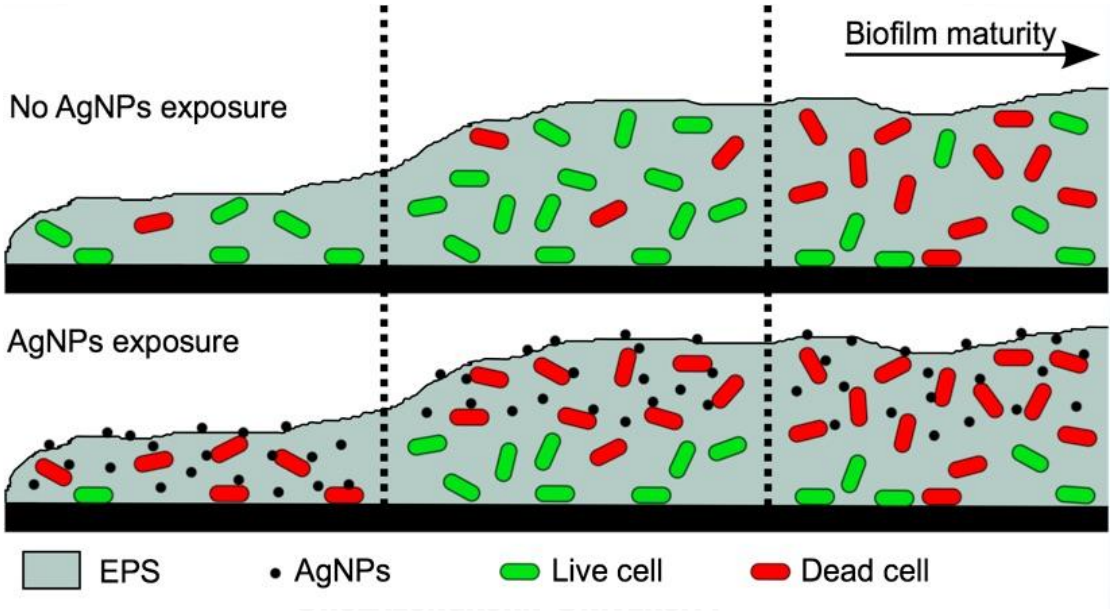

Figure 12 AgNP resistance of biofilms at different stage of maturity. Three stages of biofilm maturity proceed from left to right.

3.4) Summary

The effect of AgNPs on *P. putida* KT2440 biofilms at different stages of maturity was determined. Three biofilm stages (1-3, representing early to late stages of development) were identified from bacterial ATP activity under static (96-well plate) and dynamic conditions (CDC biofilm reactor). The EPS levels, measured using CV and total carbohydrate assays, and expression of the EPS-associated genes, *csgA* and *alg8*, supported the conclusion that biofilms at later stages were older than those at earlier stages. More mature biofilms (stages 2 and 3) showed little to no reduction in ATP activity following exposure to AgNPs. In contrast, the same treatment reduced ATP activity by more than 90% in the less mature stage 1 biofilms. Regardless of maturity, biofilms stripped of their EPS were more susceptible to AgNPs than controls with intact EPS, demonstrating that EPS is critical for biofilm tolerance of AgNPs. The findings from this study show that stage of maturity is an important factor to consider when studying effect of AgNPs on biofilms.

Chapter 4
Biofilm Physical Characteristics and Silver Nanoparticle Resistance

4.1) Introduction

Biofilms are the form of bacteria living on surface by assembling themselves within the EPS. In natural water systems, bacteria form biofilms to facilitate nutrients for growth, to survive in diverse conditions, or to protect themselves from harmful substances **[31, 33, 107]**. Compared to free-floating cells, biofilms are more resistant to antimicrobial agents including antibiotics, sanitizers, and nanoparticles **[37, 48, 51]**. AgNPs are one of the metal nanoparticles largely applied into various products and can be released into wastewater and natural water systems **[165, 166]**. AgNPs have high antimicrobial toxicity that can affect environmental biofilms include inhibition of biofilm formation, inactivation of metabolic activity, and eradication of biofilms **[4, 35, 146]**. Biofilms show some resistance to AgNPs due to the EPS of biofilms **[38, 136]**; however, the mechanisms of AgNP resistance in biofilms have not been elucidated.

In the previous chapter, it is shown that the stage of maturity plays a role in the AgNP resistance of biofilms. Biofilms develop high AgNP resistance when they are in more mature stages. However, in different growth conditions, mature biofilms can have different physical characteristics, which may lead to different resistance. Factors contributing to the physical characteristics of biofilms include nutrient type, nutrient level, and temperature. Growth rate and cell density of biofilms are high in carbohydrate- and humic-type carbon sources **[167]**. When organic carbon concentration increases, the rate of biomass production in biofilms also increases,

leading to more EPS production and higher thickness in biofilms **[55, 168]**. Also, biofilm formation depends on the metabolic activity of bacteria, which is influenced by temperature **[57]**. For example, *Pseudomonas fluorescens* biofilms tend form less and have lower metabolic activity when increasing the temperature from 4 to 30°C **[169]**. Biofilms grown under different conditions can exhibit different physical characteristics such as thickness, volume, or diffusion coefficient. *Pseudomonas* biofilms forming in glucose or methanol as a carbon source show more thickness and less porous volume than biofilms forming in acetate or ethanol, which show higher diffusion distance in biofilms **[54]**. The physical characteristics or biofilm structure can help provide the resistance to antibiotics by limiting the penetration of antibiotics into biofilms **[31, 52, 170, 171]**. Therefore, it is important to determine the effect of physical characteristics of mature biofilms on the biofilm resistance to AgNPs.

The objective of the research described in this chapter is to determine AgNP resistance of *P. putida* KT2440 biofilms with different physical characteristics. Biofilms were grown under different carbon sources, carbon concentrations, and temperatures. The mature biofilms from these conditions were analyzed for their EPS amount and component, and physical characteristics. They were exposed to AgNPs and the effect of AgNPs on biofilm viability was determined. Lastly, the effect of biofilm characteristics on the AgNP resistance was elucidated. The research framework is shown in Figure 13.

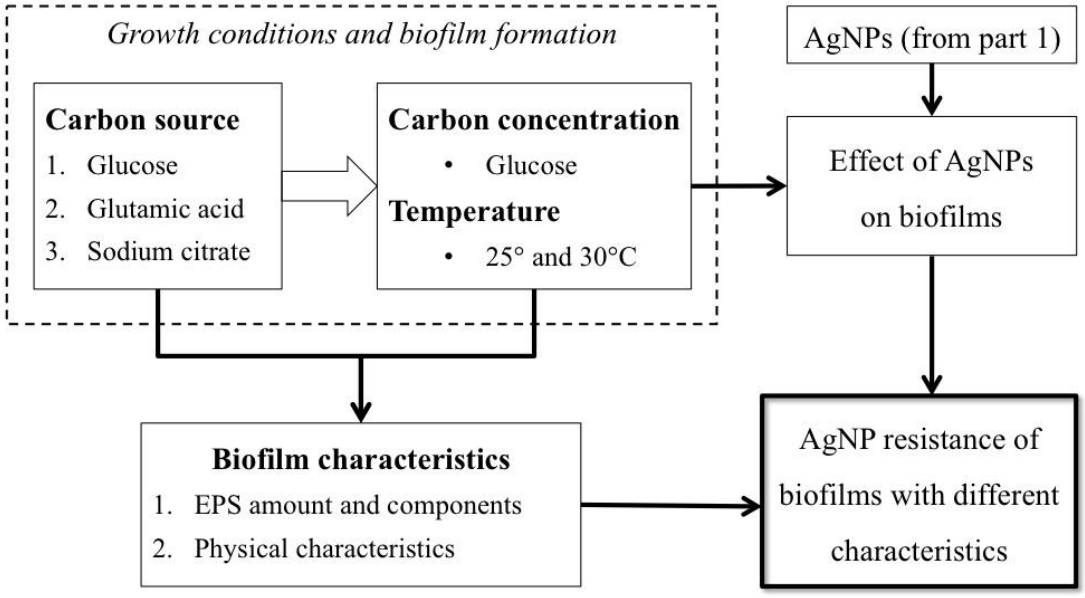

Figure 13 Experimental framework of part two of the research

4.2) Methodology

4.2.1) Synthesis of AgNPs

The synthesis of AgNPs was conducted according to section 3.2.1.

4.2.2) Bacterial strain and culture preparation

P. putida KT2440 was used and the preparation of the culture was done in the same method as section 3.2.2.

4.2.3) Biofilm experiments

Biofilm formation was conducted in a polystyrene, flat-bottom, 96-well microplate (Nunc™, cell-culture treated, Thermo Scientific™). Each well (200 µl) contained M9 minimal medium (48 mM Na_2HPO_4, 9 mM NaCl, 22 mM KH_2PO_4, 19 mM NH_4Cl, 2 mM $MgSO_4$, and 100 µM $CaCl_2$), 2% (v/v) of the prepared inoculum, and a carbon source. The plate was incubated at a controlled temperature without shaking to allow biofilm formation under static conditions. To study the effect of different growth conditions (in 96-well plates), biofilms were cultivated in three

carbon sources (10 mM of glucose, glutamic acid, and citrate), three carbon source concentrations (5, 10, and 50 mM of glucose), and two temperatures (25 and 30°C).

4.2.4) ATP assay

The metabolic activity of biofilms forming in the 96-well plate was measured by the ATP assay according to section 3.2.4.

4.2.5) CV staining

The amount of biofilms in the 96-well plate was measured from CV staining as described in section 3.2.5.

4.2.6) Drop plate method

The cell number in biofilms was determined by the drop plate method **[172]**. The method is similar to the conventional plate count method. The difference is that after the serial dilution, a drop of sample is dispensed onto the agar instead of spreading. After 24 h of incubation, the colonies are counts and the cell number is determined by CFU.

4.2.7) EPS components of biofilms

To obtain enough volume for EPS analyses, biofilm formation was conducted in flat-bottom, 6-well multidishes (Nunc™, cell-culture treated, Thermo Scientific™) with 5 ml of the media and growth conditions identical to the 96-well plate. After the biofilm formation, the media was removed and the biofilms were rinsed twice with 0.85% NaCl. Biofilms were removed from the well by pipette mixing with 5 ml of 0.85% NaCl. The suspension was centrifuged at 20,000× *g*, 4°C, for 20 min. The supernatant was stored at -18°C before EPS analyses.

For the conditions with different carbon sources, the whole biofilms were analyzed for different EPS components by Fourier transform infrared spectroscopy

(FTIR) (Spectrum One, PerkinElmer). The sample was scanned for different functional groups of EPS between 4000 cm^{-1} and 650 cm^{-1}.

Total carbohydrate was measured by the phenol-sulfuric method as described in the section 3.2.5. Total protein was measured by Lowry's method **[173]** with bovine serum albumin (BSA) as a standard. The method relies on the reaction between peptide bonds and copper ion under alkaline conditions, followed by the Folin–Ciocalteau reaction. The absorbance of the solution was measured at 750 nm.

4.2.8) Effect of AgNPs on biofilms forming in different growth conditions

The exposure of biofilms to AgNPs was conducted in the 96-well plate according to section 3.2.7. After rinsing twice, the biofilms were re-suspended with 0.85% NaCl before determining the cell number by the drop plate method. The effect of AgNPs on biofilms was determined by comparing the cell number of the treatment samples with that of the control samples.

4.2.9) Confocal laser scanning microscopy and image analysis

For microscopic observation, biofilms were cultivated in a chambered coverslip (μ-Slide 8 well, Ibidi) instead of the 96-well plate. The biofilms were stained with FilmTracer™ LIVE/DEAD® Biofilm Viability Kit (Invitrogen, Life Technologies) according to the manufacturer's protocol. The kit contains SYTO 9 (green) and propidium iodide (PI) (red) for staining of the DNA of bacteria. Biofilms were observed under a confocal laser scanning microscope (CLSM) (Nikon, D-Eclipse C1) with the excitation/emission wavelengths: 482/500 nm for SYTO 9 and 490/635 for PI. The z-stack images from the green fluorescent signal were analyzed with the COMSTAT software **[174]** to calculate the physical characteristics and structure of the biofilms.

4.2.10) Effect of biofilm structure on AgNP resistance of biofilms

Biofilms were cultivated in the 96-well plate with two glucose concentrations (5 and 50 mM) and two temperatures (25 and 30°C). To change the structure of the biofilms, the EDTA treatment was used to partially strip EPS similar to section 3.2.8 except that the concentration of EDTA was reduced to 0.25% (w/v) to avoid complete eradication of biofilms. The CV staining was used to confirm the stripping process. The EPS-stripped biofilms were observed under CLSM and analyzed for the structure as described above. After the EPS stripping, the biofilms were exposed to 20 mg/l of AgNPs and the effect was determined by the drop plate method.

4.2.11) Statistical analysis

In every experiment, the standard deviation of the triplicate data was calculated and presented as error bars. The multiple *t*-test was used to determine the statistical differences between total carbohydrate and total protein for biofilms forming in different carbon sources. The analysis was also used for the statistical differences of physical characteristics (thickness, biomass volume, surface to volume ratio, and roughness) among biofilms different carbon sources, carbon concentrations, and temperatures.

4.3) Results and discussion

4.3.1) *P. putida* KT2440 biofilm formation under different carbon sources

For *Pseudomonas* biofilms, when glucose and citrate are used as different carbon sources, the microcolonies in biofilms exhibit different structure **[175]**. Also, the types of carbon sources, which are carbohydrate, humic acids, and amino acids, affect the growth and density of biofilms **[167]**. In this experiment, biofilm formation of *P. putida* KT2440 was conducted by using 10 mM of glucose, glutamic acid, and citrate. Three biofilms showed similar ATP activity trends over 48 h of formation (Figure 14(a)). Despite the variations, the ATP activity of all biofilms increased in the first 15 to 18 h and tended to stabilize or decrease after that. Similar trends were observed for cell number (Figure 14(b)) and biomass of the biofilms (Figure 14(c)). Therefore, 15 h was selected as a time point for mature biofilms. The EPS of mature biofilms was extracted and analyzed for total carbohydrate and total protein. Figure 15(a) shows the total carbohydrate and total protein contents of biofilms forming in glucose, glutamic acid, and citrate. The amount of carbohydrate (10 – 15 mg/well as determined from the 6-well plate experiments) is 100 times higher than that of protein (0.5 – 0.15 mg/well), suggesting that carbohydrate is a major constituent of *P. putida* KT2440 biofilms **[128]**. While the amount of total carbohydrate was similar among three biofilms (No statistical differences as shown in Table A-1, Appendix), the amount of total protein was highest in glucose biofilms (0.15 mg/well), followed by glutamic acid (0.10 mg/well) and citrate biofilms (0.05 mg/well) ($p < 0.05$ as shown in Table A-1, Appendix), respectively. The analysis of EPS by FTIR (Figure 15(b)) shows peaks of carbohydrate, protein, and lipid **[176, 177]**.

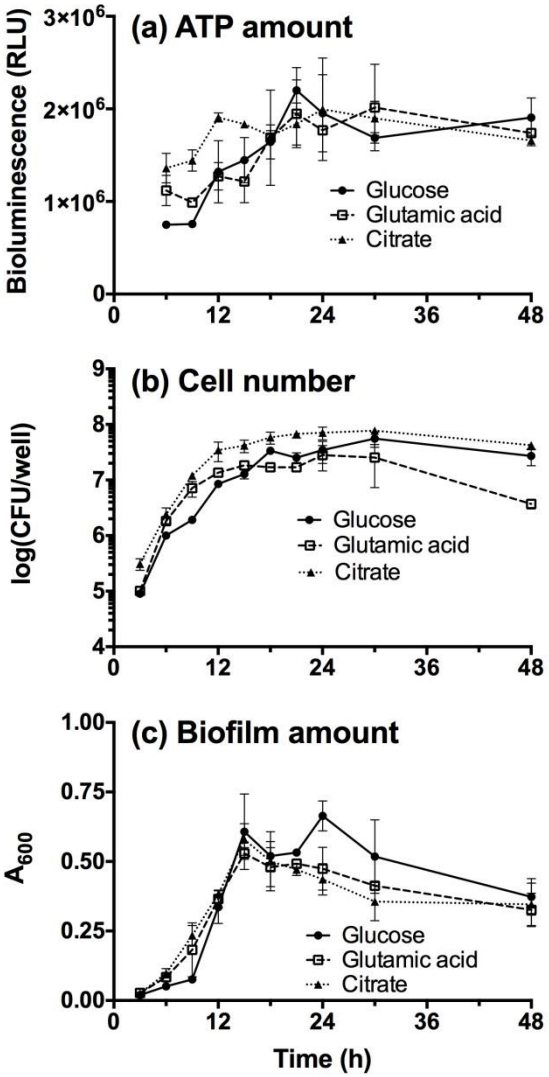

Figure 14 Time courses of *P. putida* KT2440 biofilms forming in glucose, glutamic acid, and citrate: (a) ATP amount, (b) cell number, (c) biofilm amount. The time period is on x-axis. The ATP amount is presented as the bioluminescence in RLU. The cell number is presented as CFU/well. The amount of biofilms is presented as A_{600}. The means and standard deviations are based on 3 different biofilm samples.

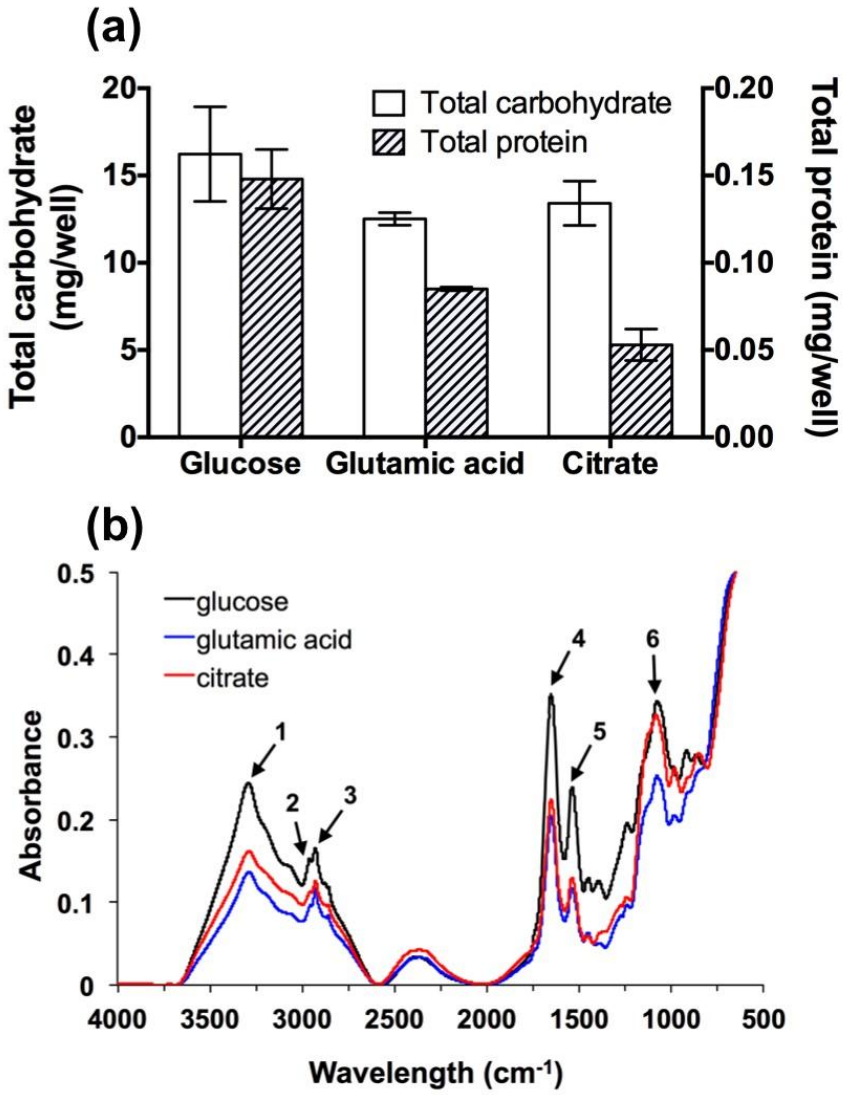

Figure 15 EPS component of biofilms forming in glucose, glutamic acid, and citrate: (a) total carbohydrate and protein data, (b) FTIR spectra. The total carbohydrate and total protein are shown in the unit of mg/well on the left and right y-axis, respectively. The means and standard deviations are based on 3 different biofilm samples. Band assignments for the FTIR spectra: 1, 6 (carbohydrates); 4, 5 (proteins); and 2, 3 (lipids).

The almost-identical wavelengths of the peaks (Table A-2, Appendix) suggest that the EPS of three biofilms had similar functional groups and compositions. Miqueleto et al. **[168]** also observed similar EPS compositions of biofilms forming in various carbon sources while the EPS amounts were different. According to FTIR data, glucose biofilms had the highest amount of each component, which can be observed by the height of the absorbance peaks (Figure 15(b)). It can be seen that, when the EPS was analyzed by FTIR, the amount of protein was high according to the peak absorbance, and the lipid content was also detected. This might be due to the limitations of protein detection from the Lowry's method by the interference from many substances such as sugars, which may result in lower amount of protein **[178]**.

It can be seen that different methods for measurement can give different amounts of EPS. Three mature biofilms (15 h) showed no difference in overall biomass when measured by CV staining (Figure 14(c)), but they had different EPS in terms of compositions when measured by more advanced method such as FTIR (Figure 15(b)). However, the methods used in these experiments only determine the difference in chemical components of biofilms while the biofilms forming in glucose, glutamic acid, and citrate may not only have different chemical characteristics but also physical characteristics. Therefore, the biofilms were stained and observed under CLSM to determine biofilm structure or physical characteristics.

Biofilms forming in three different carbon sources were observed for their physical characteristics. The images of biofilms under CLSM are shown in Figure 16 (the COMSTAT processed images are shown in Figure A-2, Appendix). Four parameters were calculated (Table 2): (1) Thickness of biofilms; (2) Biomass volume of biofilms; (3) surface to volume ratio, which is the ratio between surface area of the

top layer of biofilms and the biomass volume; and (4) roughness coefficient, which shows the roughness of biofilm surface. From the results, glucose biofilms had significantly higher biofilm thickness (p = 0.006 vs. glutamic acid; p = 0.0003 vs. citrate) and volume (p = 0.19 vs. glutamic acid; p = 0.01 vs. citrate). Glutamic biofilms also show higher thickness and volume than citrate biofilms even though statistically the thickness of these two biofilms were not different (see Table A-3, Appendix for statistical differences). The higher thickness of glucose biofilms than citrate biofilms was also observed by Klausen et al. **[175]**. The surface/volume ratio was similar in three biofilms while glucose biofilms had slightly higher roughness than the other two biofilms (no statistical differences).

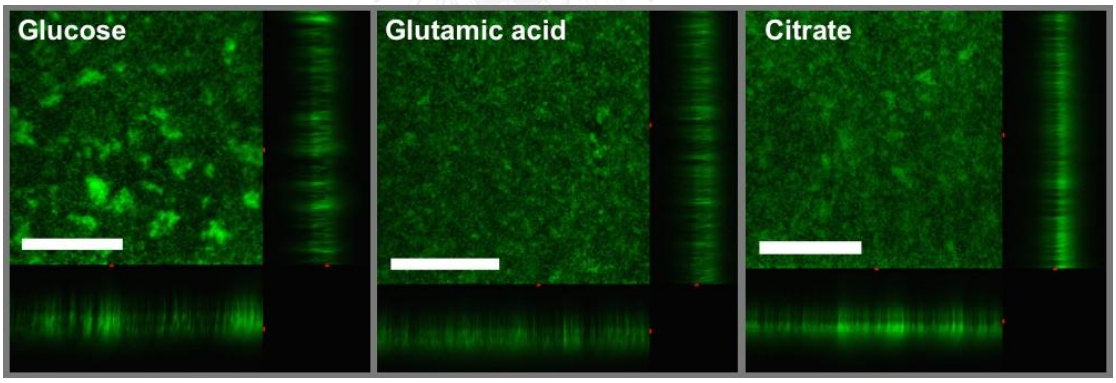

Figure 16 *P. putida* KT2440 biofilms at stage 2 (15 h) forming in glucose, glutamic acid, and citrate. Green color shows the viability of biofilm cells. The thickness of biofilms is shown under and on the right of the top view image. The white bar indicates 50 µm in scale.

Table 2 Characteristics of *P. putida* KT2440 biofilms forming in glucose, glutamic acid, and citrate.

Biofilm characteristics	Carbon source		
	Glucose	Glutamic acid	Citrate
Thickness (μm)	39.89 ± 1.14	33.90 ± 1.60	29.83 ± 0.95
Biomass volume ($\mu m^3/ \mu m^2$)	25.73 ± 2.02	22.82 ± 2.50	19.13 ± 1.66
Surface to volume ratio ($\mu m^2/ \mu m^3$)	0.216 ± 0.011	0.217 ± 0.025	0.230 ± 0.015
Roughness coefficient	0.034 ± 0.001	0.025 ± 0.002	0.026 ± 0.02

According to the results, when glucose was used as a carbon source, the biofilms not only had different EPS components but also different structures or physical characteristics compared to when glutamic acid and citrate were used. This possibly leads to different AgNP resistance among three biofilms. Therefore, the effect of AgNPs on biofilms forming in different carbon sources is determined in the next experiment.

4.3.2) Effect of AgNPs on biofilms forming under different carbon sources

Mature biofilms forming in three carbon sources were exposed to 20 mg/l of AgNPs for 24 h, and the reduction in cell number was observed (Figure 17). As the growth media in part two was different from part one (LB media), the effect of AgNPs on pre-mature biofilms (9 h) was also determined to confirm the findings from part one of the research. Likewise, biofilms at mature stage still exhibited higher resistance to AgNPs than the pre-mature biofilms. When compared among three carbon sources, the AgNP resistance in mature biofilms forming in glucose (< 1 order of magnitude in cell number reduction) was similar to glutamic acid (around 1 order of magnitude in cell number reduction), which was higher than biofilms forming in citrate (2 orders of magnitude in cell number reduction).

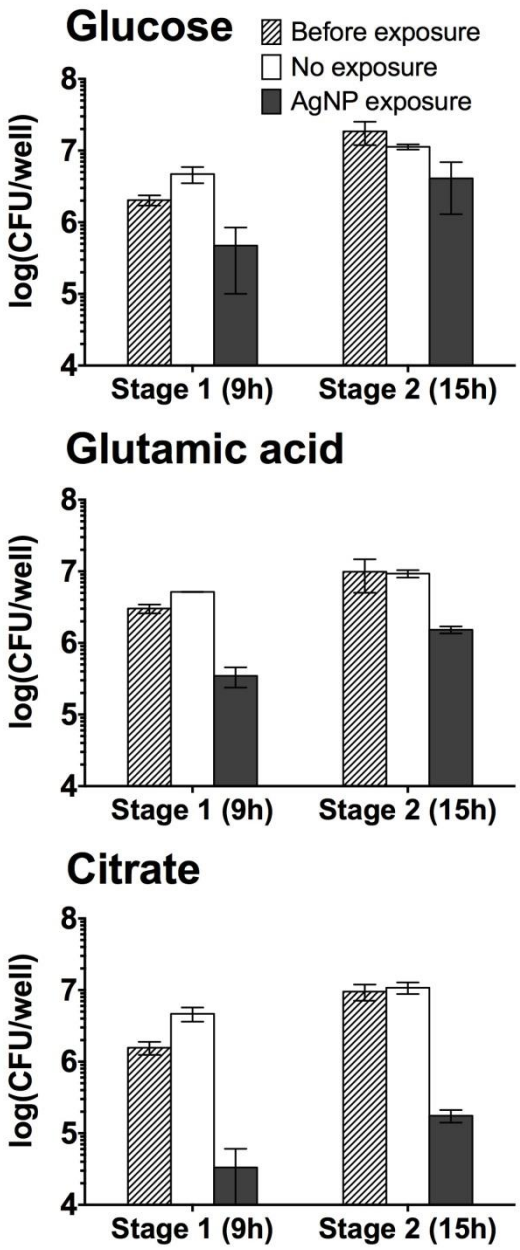

Figure 17 Effect of AgNPs on biofilms forming in glucose, glutamic acid, and citrate after 24 h of exposure. The effect is shown as the reduction in cell number of biofilms on y-axis. The means and standard deviations are based on 3 different biofilm samples.

Some factors can play a role in the AgNP resistance of biofilms forming in different carbon sources. First, the carbohydrate and protein are the EPS components that can mitigate the effect of AgNPs by causing aggregation in AgNPs, therefore reducing the toxicity **[133, 179]**. The highest amounts of carbohydrate and protein were observed in glucose biofilms (Figure 15(a)), which had the highest AgNP resistance. Second, it is possible that different carbon sources could change the cell resistance to AgNPs. This was proven by the exposure of planktonic cells of *P. putida* KT2440 at stationary phase to AgNPs at the same concentration (Figure 18). After 6 h of exposure, cells grown in glutamic acid exhibited highest resistance to AgNPs as the cell number reduced 4 orders of magnitude while the cell numbers in glucose and citrate were zero (no colonies were observed). This may be the reason for similar AgNP resistance between glucose and glutamic biofilms even though the EPS components of glutamic biofilms were lower.

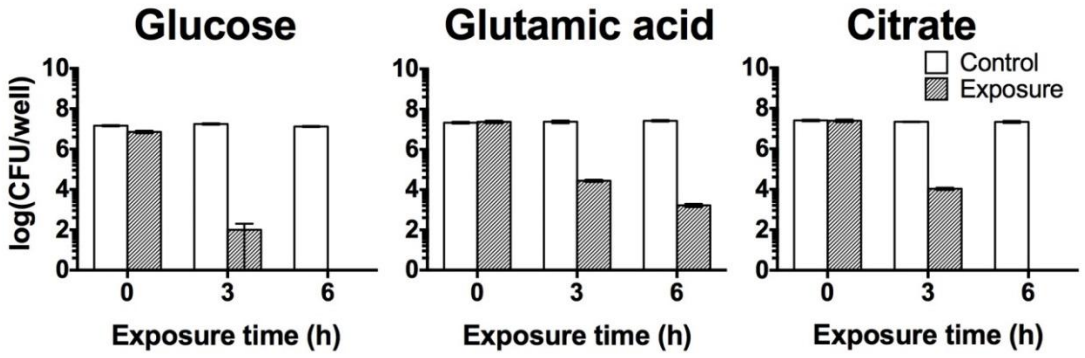

Figure 18 Effect of AgNPs on planktonic cells grown in glucose, glutamic acid, and citrate. The cells were harvested from the stationary phase and exposed to 0 and 20 mg/l of AgNPs. The effect is shown as the reductions in ATP and cell number. The means and standard deviations are based on 3 different biofilm samples.

Another factor for biofilm resistance is the biofilm structure, which can help limiting the diffusion of AgNP into biofilms **[180]**. According to the physical characteristics of biofilms (Table 2), glucose and glutamic acid biofilms exhibited much higher thickness and volume than citrate biofilms. This could mean that those two biofilms had better structure in terms of protection from AgNPs. Therefore, the AgNP resistances in glucose and glutamic biofilms were higher than that of citrate biofilms.

According to the results, the AgNP resistance of biofilms could be contributed by the difference in both chemical and physical characteristics of biofilms. The next experiment tried to focus more on the physical characteristics and minimize the effect from different EPS component (chemical characteristics); therefore, glucose was used as a sole carbon source for biofilm formation.

4.3.3) *P. putida* KT2440 biofilm formation under different glucose concentrations and temperatures

Pseudomonas biofilms have different physical characteristics when forming under different nutrient concentrations and temperatures **[181]**. In this experiment, biofilms were cultivated in different glucose concentrations (5, 10, and 50 mM) and two temperatures (25 and 30° C), and the growth curves of biofilm formation over 48 h are shown in Figure 19. Increasing the temperature from 25 to 30°C seemed to increase the ATP activity of all biofilms while increasing the glucose concentration could increase both activity and biomass of biofilms. The effect of both glucose concentration and temperature on biomass of biofilms can be clearly observed in Figure 20, in which the biomass was determined from mature biofilms at 24 h selected from the growth curve.

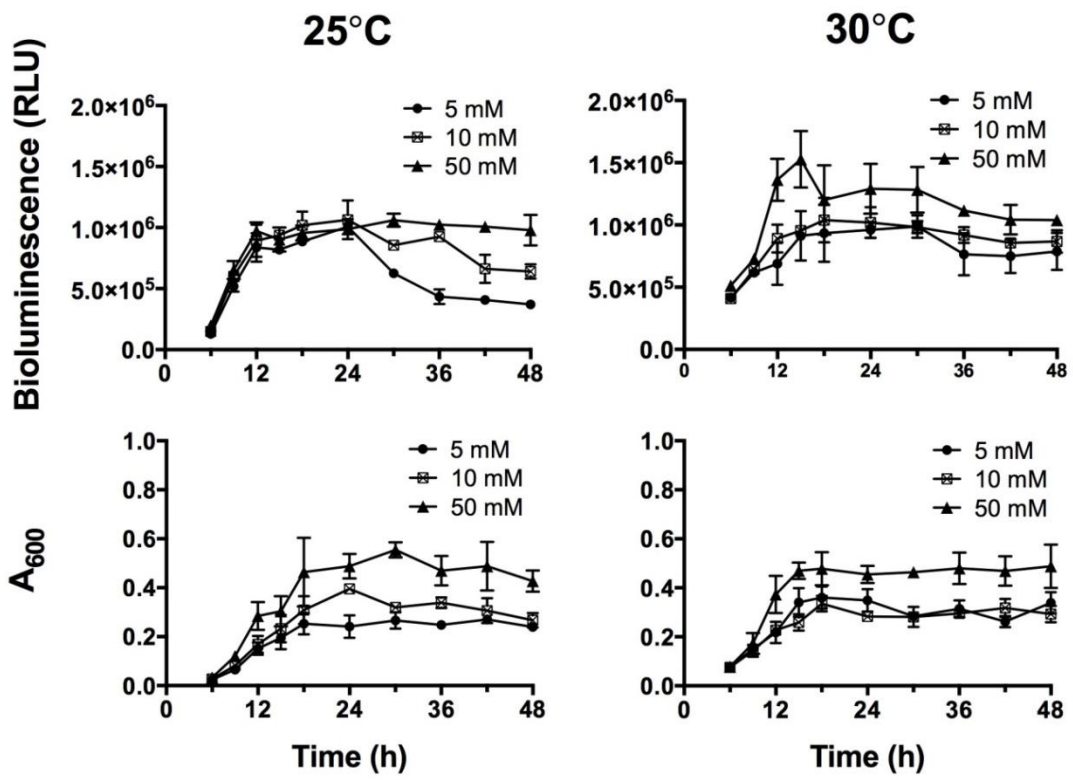

Figure 19 Time courses of *P. putida* KT2440 biofilm formation under different glucose concentrations (5, 10, and 50 mM) and temperatures (25 and 30°C). The time period is on x-axis. The ATP amount and biomass of biofilms are presented on y-axis as the bioluminescence in RLU and A_{600}, respectively. The means and standard deviations are based on 3 different biofilm samples.

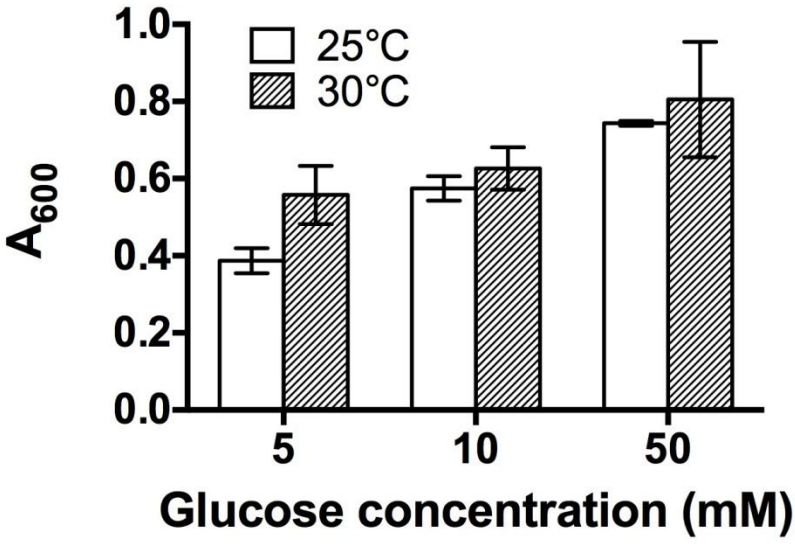

Figure 20 Biomass of mature biofilms forming under different glucose concentrations and temperatures. The biomass of biofilms is presented as A_{600} on y-axis. The means and standard deviations are based on 3 different biofilm samples.

Increasing glucose concentration from 5 mM to 50 mM doubled the biomass of biofilms in both temperatures; however, at the same glucose concentration, changing temperature from 25 to 30°C increased the biomass of biofilms only when glucose was at 5 mM. This might be due to the increased metabolic activity of *P. putida* KT2440 at the optimal growth temperature (30°C), leading to more production of biomass **[182]**. Since only glucose was used as a sole carbon source, the difference in EPS composition was not observed. The biofilms forming in two glucose concentrations (5 and 50 mM) and temperatures (25 and 30°C) were determined for their physical characteristics under CLSM (Figure 21; The COMSTAT processed images can be found in Figure A-3, Appendix). The physical characteristics, which are biofilm thickness, biomass volume, surface per volume ratio, and roughness coefficient, were calculated (Table 3). The carbon concentration and temperature were

able to provide more distinct physical characteristics of biofilms than different carbon source in previous experiment especially the surface to volume ratio and roughness coefficient. Both glucose concentration and temperature affected biofilm physical characteristics (see Table A-4 and A-5 for the statistical differences between any pair of data). For example, when the temperature was fixed at 25°C and the glucose concentration increased from 5 to 50 mM, the thickness of biofilms increased from 20.81 μm to 23.47 μm; the biomass volume increased from 7.04 to 17.56 $\mu m^3/\mu m^2$; the surface to volume ratio decreased from 0.978 to 0.428 $\mu m^2/\mu m^3$; and the roughness coefficient decreased from 0.11 to 0.07. Similarly, when the glucose concentration was fixed at 5 mM and the temperature increased from 25 to 30°C, the thickness of biofilms increased from 20.81 μm to 31.50 μm; the biomass volume increased from 7.04 to 15.76 $\mu m^3/\mu m^2$; the surface to volume ratio decreased from 0.978 to 0.450 $\mu m^2/\mu m^3$; and the roughness coefficient decreased from 0.11 to 0.03. Among four biofilms, the biofilms forming at 50 mM of glucose and 30°C seemed to have weakest structure than other biofilms (lowest thickness and volume; highest surface to volume and roughness). This is contradicted to the biomass data when determined by the CV staining (Figure 20), in which the 50 mM biofilms at 30°C had high biomass similar to the 50 mM biofilms at 25°C. This could be due to the combined effect from growth conditions, different measurements, and different experiments. First, under the conditions of high carbon availability (50 mM) and preferable growth temperature (30°C), it can lead to less biofilm formation or dispersion of biofilms **[56, 183]**. Second, the CV stained all biomass of biofilms including EPS, live cells, and dead cells whereas

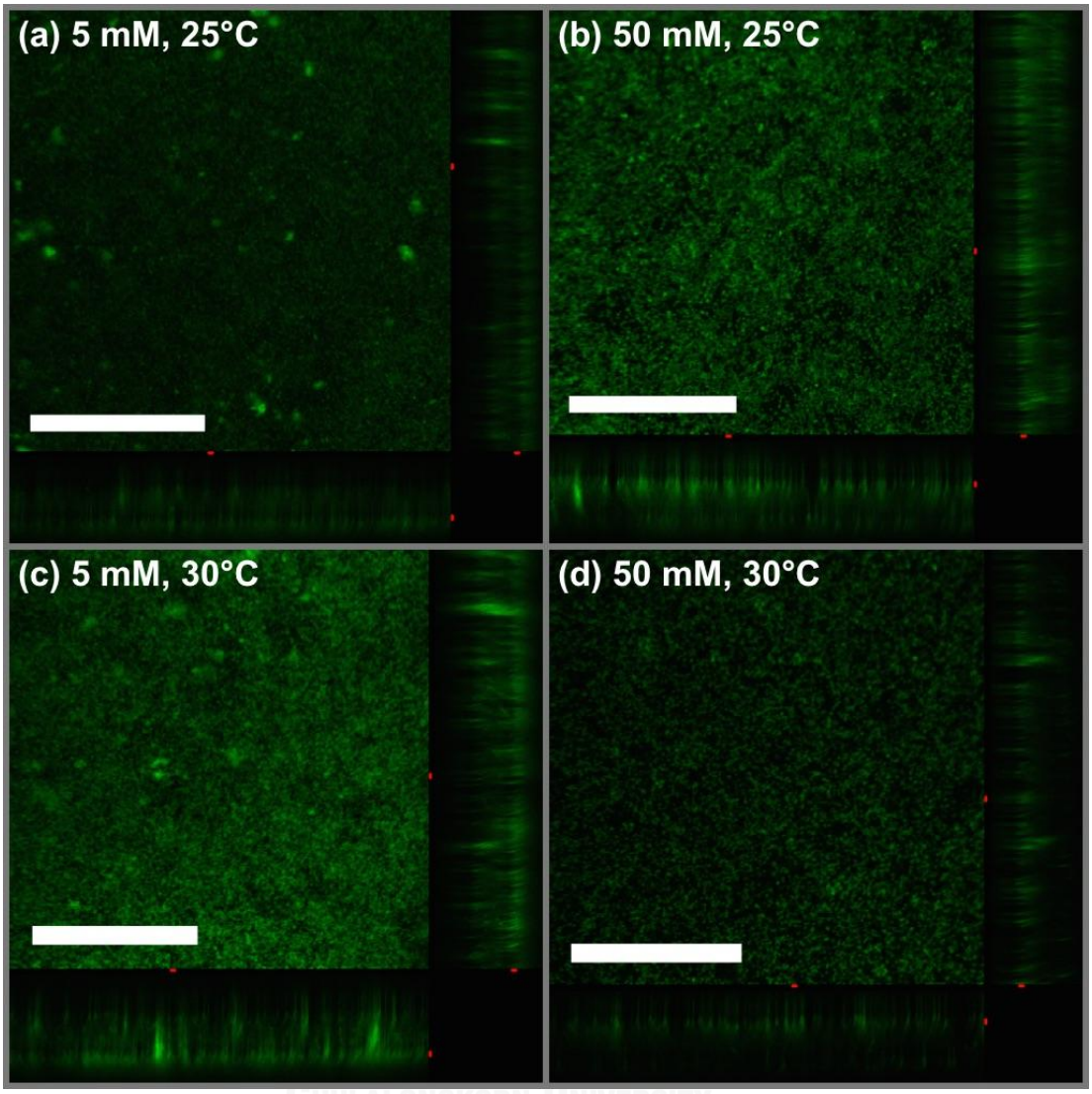

Figure 21 *P. putida* KT2440 biofilms forming in different glucose concentration and temperature: (a) 5 mM at 25°C, (b) 50 mM at 25°C, (c) 5 mM at 30°C, and (d) 50 mM at 30°C. Green color shows the viability of biofilm cells. The thickness of biofilms is shown under and on the right of the top view image. The white bar indicates 50 μm in scale.

Table 3 Characteristics of *P. putida* KT2440 biofilms forming in different glucose concentration and temperature.

Biofilm characteristics	5 mM glucose		50 mM glucose	
	25°C	30°C	25°C	30°C
Thickness (μm)	20.81 ± 3.11	31.50 ± 2.86	23.47 ± 2.93	15.37 ± 0.91
Biomass volume ($\mu m^3/ \mu m^2$)	7.04 ± 4.82	15.76 ± 3.63	17.56 ± 1.85	6.97 ± 1.53
Surface to volume ratio ($\mu m^2/ \mu m^3$)	0.978 ± 0.292	0.450 ± 0.235	0.428 ± 0.136	1.247 ± 0.369
Roughness coefficient	0.11 ± 0.07	0.03 ± 0.01	0.07 ± 0.04	0.35 ± 0.20

the COMSTAT software calculated the physical characteristics only from the green fluorescent signal of live cells **[174]**. This could result in more measurement of biomass from the CV assay. Also, different surface materials can allow different amount of biofilm attachment **[110]**. For the CV assay, biofilms were grown on the polystyrene surface in the 96-well plate whereas for the CLSM observation, biofilms were grown on the treated glass surface of Ibidi slide.

According to the results, biofilms forming under different glucose concentrations and temperatures exhibit different physical characteristics leading to different AgNP resistance levels. Therefore, the effect of AgNPs on the biofilms was observed in the next experiment.

4.3.4) Effect of AgNPs on biofilms forming under different glucose concentrations and temperatures

The mature biofilms were exposed to 5 and 20 mg/l of AgNPs for 24 h before determining the effect of AgNPs by reduction in cell number (Figure 22). The adverse effect of AgNPs increased with AgNP concentration in every biofilm sample. The AgNP resistance of biofilms is related to both biomass amount (Figure 20) and physical characteristics (Table 3). At 25°C, biofilms forming at higher glucose concentrations exhibited higher AgNP resistance, which is shown by the change from

3-log reduction in 5 mM biofilms to less than 1-log reduction in 50 mM biofilms. This is because biofilms produced more biomass amount in higher glucose concentration. Similarly, when the temperature was increased from 25 to 30°C in 5 mM biofilms, the biofilms produced more amount of biomass, resulting in higher AgNP resistance than at 25°C (from 3 log reduction at 25°C to 1 log reduction at 30°C).

When the total amounts of two biofilms were similar, the AgNP resistance depended on the structure or physical characteristics of biofilms. For example, the biofilms forming in 50 mM of glucose at 25 and 30°C showed similar amount of biomass (Figure 20) but different AgNP resistance (Figure 4.10; less than 1-log reduction at 25°C and 2-log reduction at 30°C). Compared to 50 mM biofilms at 25°C, the 50 mM biofilms at 30°C showed lower thickness, lower volume, higher surface to volume ratio, and higher roughness. This trend of physical characteristics was observed for the biofilms with less AgNP resistance when comparing any pair of biofilms, suggesting the relationship between the physical characteristics and the AgNP resistance of biofilms (Table 3 and Figure 22). Biofilms with less thickness and volume may allow more diffusion of AgNPs into biofilms **[184]**. The surface to volume ratio and roughness coefficient were negatively related to the biofilm resistance, which is similar to the study by Xue et al. **[180]**. More roughness of biofilms provides more area for AgNP biosorption whereas high surface to volume ratio means more surface area for biosorption or less biomass volume for AgNP diffusion, all of which result in more effect of AgNPs on biofilms **[35, 36]**.

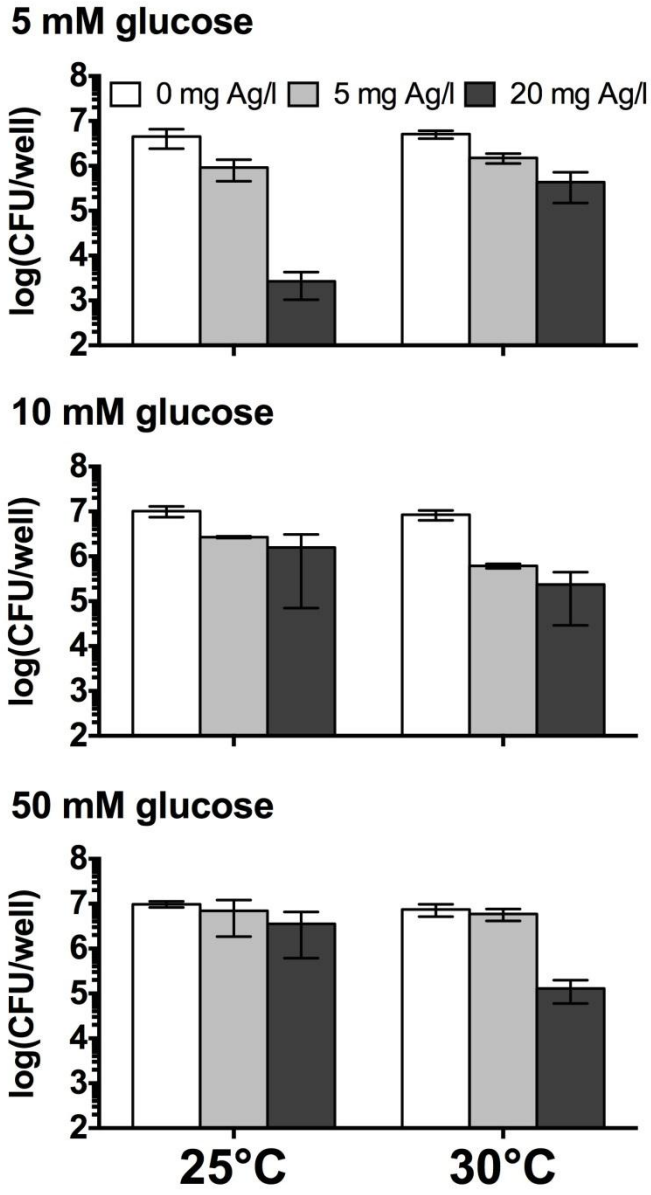

Figure 22 Effect of AgNPs on biofilms forming under different glucose concentrations and temperatures. The concentrations of AgNPs were 5 and 20 mg/l. The exposure time was 24 h. The effect is shown as the reduction in cell number after 24 h exposure on y-axis. The means and standard deviations are based on 3 different biofilm samples.

As the thickness, volume, surface to volume ratio, and roughness of biofilms are related to their AgNP resistance, changing these parameters could result in reduced AgNP resistance of biofilms. In the next experiment, EPS of biofilms forming in 5 and 50 mM of glucose and at 25 and 30°C were partly removed to change the structure of the biofilms before determination of the effect of AgNPs on biofilms.

4.3.5) Physical characteristics and AgNP resistance of biofilms

As shown in Chapter 3, when the biomass of biofilms was partly removed by EDTA treatment, the AgNP resistance of biofilms decreased, which could be from less EPS to protect cells from AgNPs. In other words, the biofilms that have their EPS partly removed could have their physical characteristics changed, leading to reduction in AgNP resistance. In this experiment, the biofilms forming in different glucose concentrations and temperatures were treated with 0.25% EDTA to strip some of the EPS and change the structure of the biofilms (Figure 23). The biomass of biofilms decreased after EDTA treatment compared to the control samples, which were treated by DI (Figure 24). Not only was the biomass of all biofilms reduced after EDTA treatment, but also the structures of biofilms were significantly altered (Table 4, with all p values < 0.05 except for the 50 mM biofilms at 30°C; see Table A-6, Appendix for all statistical differences). After EPS stripping, biofilms lost some of their thickness and biomass volume while their surface to volume ratio and roughness were increased. This shows that EDTA treatment could change the structure of biofilms, which might be due to the breaking of the link between EPS molecules **[185]**.

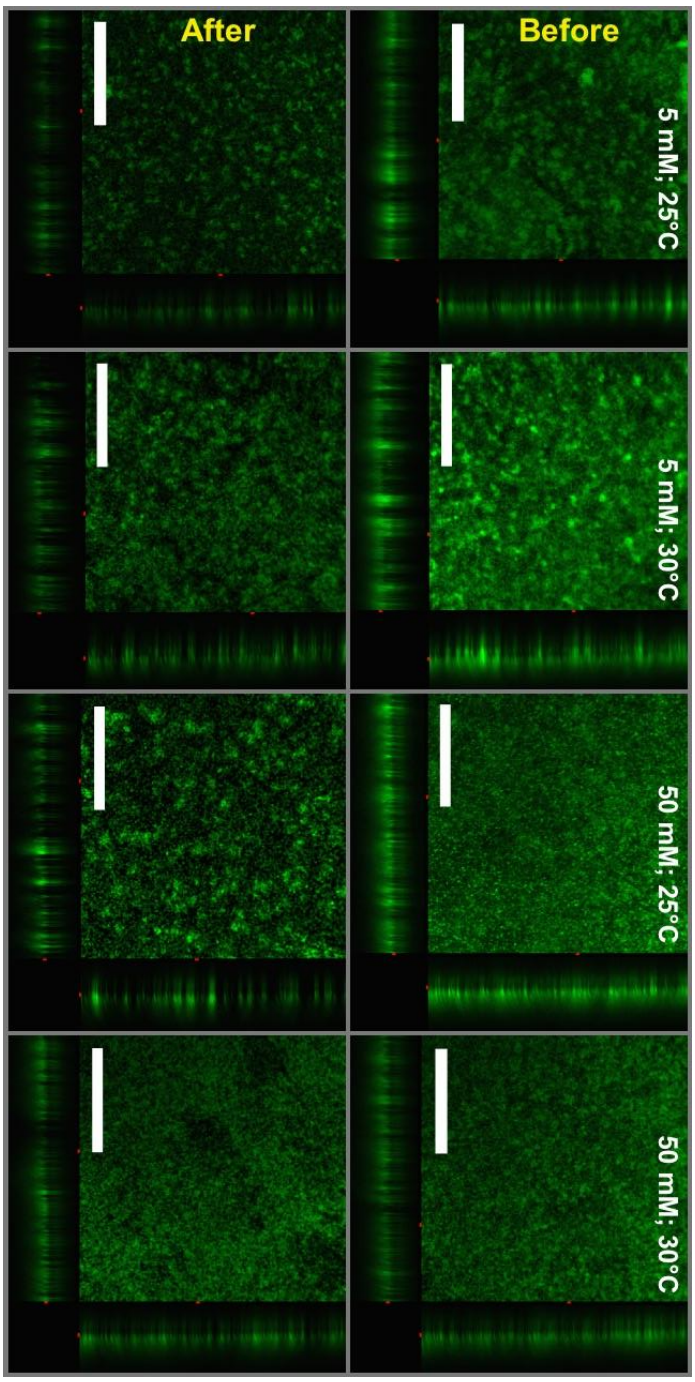

Figure 23 *P. putida* KT2440 biofilms before and after EDTA treatment. Green color shows the viability of biofilm cells. The thickness of biofilms is shown under and on the right of the top view image. The white bar indicates 50 μm in scale.

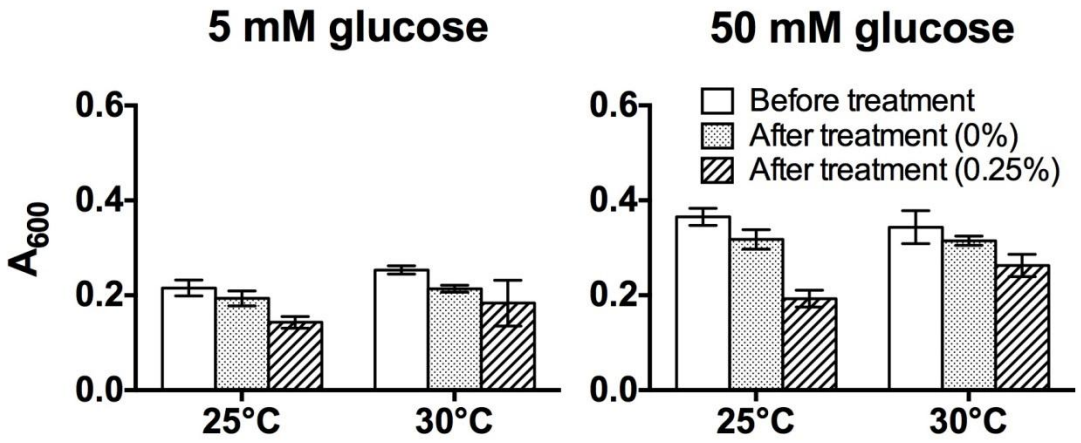

Figure 24 Biomass reduction by EDTA treatment of biofilms forming under different glucose concentrations and temperatures. The biomass is based on the CV assay and shown as A_{600} on y-axis. The means and standard deviations are based on 3 different biofilm samples.

Table 4 Change of biofilm characteristics by EDTA treatment

Biofilm characteristics	5 mM glucose		50 mM glucose	
	Before	After	Before	After
25°C				
Thickness (μm)	31.74 ± 0.39	22.17 ± 2.68	34.60 ± 0.69	23.48 ± 1.19
Biomass volume ($\mu m^3/ \mu m^2$)	22.30 ± 1.37	9.59 ± 3.82	28.25 ± 0.23	9.59 ± 3.95
Surface to volume ratio ($\mu m^2/ \mu m^3$)	0.191 ± 0.018	0.623 ± 0.155	0.302 ± 0.004	0.632 ± 0.078
Roughness coefficient	0.042 ± 0.002	0.108 ± 0.039	0.040 ± 0.005	0.117 ± 0.029
30°C				
Thickness (μm)	35.25 ± 2.58	28.17 ± 3.54	30.27 ± 1.24	26.38 ± 1.45
Biomass volume ($\mu m^3/ \mu m^2$)	27.46 ± 0.78	18.67 ± 2.92	25.74 ± 6.87	19.91 ± 1.67
Surface to volume ratio ($\mu m^2/ \mu m^3$)	0.195 ± 0.005	0.351 ± 0.043	0.254 ± 0.090	0.244 ± 0.053
Roughness coefficient	0.037 ± 0.009	0.067 ± 0.009	0.046 ± 0.008	0.038 ± 0.014

The EPS-stripped (0.25% EDTA treated) and control (0% of EDTA treated) biofilms were exposed to 20 mg/l of AgNPs, and the reduction in cell number was measured (Figure 25). Surprisingly, not all EPS-stripped biofilms showed reduction in the AgNP resistance. At 50 mM of glucose, the EPS-stripped biofilms show similar or equal resistance to the control biofilms at both 25 and 30°C (3-log reduction in both EPS-stripped and control biofilms). This may be explained by several reasons. First, biofilms at 50 mM of glucose had high biomass (Figure 20). The EPS-stripping process might not remove enough biomass or change the structure for the AgNP resistance to decrease. Second, the control biofilms treated by DI also lost some of their biomass (Figure 24) and probably their structure, giving less difference between the effects of AgNPs on the EPS-stripped and control biofilms. Lastly, there could be an error for relating the change in physical characteristics (Table 4) to the change in AgNP resistance of biofilms (Figure 25). As described earlier, the biofilms were grown in Ibidi glass surface for microscopic observation while they were grown in polystyrene surface for exposure experiments. This might provide the different attachment and characteristics of biofilms between the two experiments.

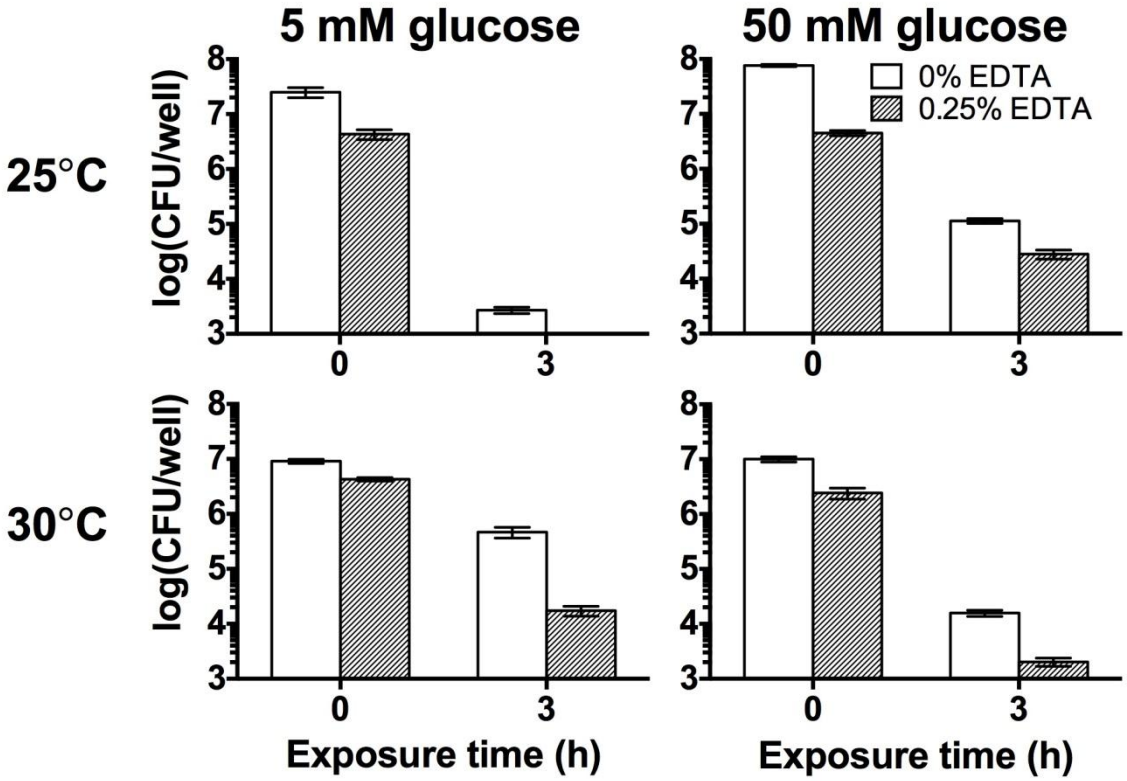

Figure 25 Effect of AgNPs on biofilms forming under different glucose concentrations and temperatures after the EPS-stripping by EDTA treatment. Biofilms were exposed to 20 mg/l of AgNPs for 24 h. The effect is shown on y-axis as the reduction in cell number. The cell number for the biofilm samples at 5 mM of glucose and 25°C could not be observed after 3 h of exposure (no colony), and the bar is not shown on the figure.

From the results, it is highly possible that physical characteristics are related to the AgNP resistance of biofilms. By having better structure including more thickness, more biomass volume, less surface to volume ratio, and less roughness, biofilms are more resistant to AgNPs by various mechanisms (Figure 26). Less surface area and roughness allowed less adsorption of AgNPs on biofilms **[35, 180]**. High thickness and biomass volume limit the AgNP diffusion into biofilms **[184]**. Due to various chemical components and charges of EPS, AgNPs will likely agglomerate on surface or in biomass of biofilms **[186]**. Also, the EPS components can interact or adsorb on the surface of AgNPs **[133, 136, 179]**. All of these processes lead to reduction in the effect of AgNPs on biofilms.

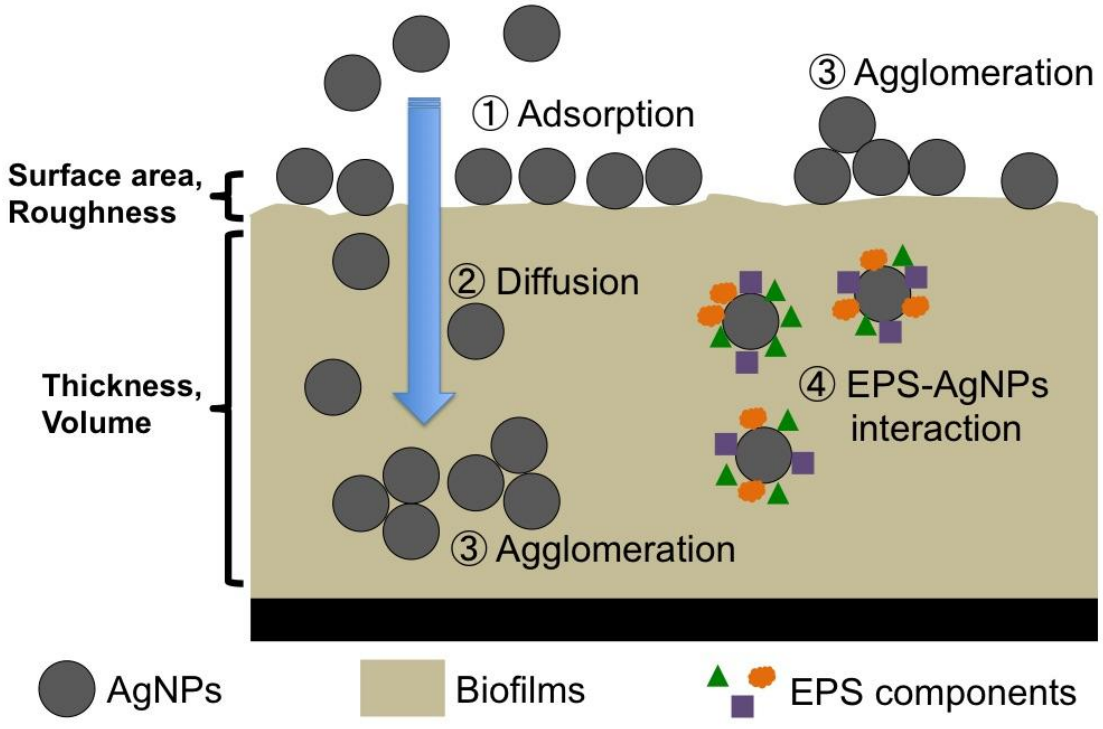

Figure 26 Mechanisms of AgNP resistance in biofilms due to the physical characteristics

4.4) Summary

Under diverse environmental conditions, mature biofilms can have different characteristics leading to the question whether they will have the same resistance to AgNPs. In this part, the AgNP resistance of *P. putida* KT2440 biofilms was determined by focusing on the effect of physical characteristics, which are thickness, biomass volume, surface to volume ratio, and roughness. Mature biofilms forming in different carbon sources (glucose, glutamic acid, and citrate), glucose concentrations (5 and 50 mM), and temperatures (25 and 30°C) showed different physical characteristics, which were related to the AgNP resistance of biofilms. The biofilms with lower thickness, lower volume, higher surface to volume ratio, and higher roughness coefficient were more resistant to AgNPs. While the surface/volume ratio and roughness coefficient were similar among three biofilms in three carbon sources, the thickness and biomass volume of glucose and glutamic acid biofilms were higher than citrate biofilms. Comparably, the AgNP resistance of biofilms forming in glucose (< 1 order of magnitude in cell number reduction) was similar to glutamic acid (around 1 order of magnitude in cell number reduction), which was higher than citrate (2 orders of magnitude in cell number reduction). Higher glucose concentrations and temperatures seemed to increase the thickness and biomass volume of biofilms while decreasing the surface to volume ratio and roughness coefficient, which increased the AgNP resistance of biofilms. At 25°C, biofilms forming at higher glucose concentrations exhibited higher AgNP resistance (3-log reduction in 5 mM and less than 1-log reduction in 50 mM). Similarly, when the temperature was increased in 5 mM biofilms, the biofilms had higher AgNP resistance (3 log reduction at 25°C and 1 log reduction at 30°C). When some of the

EPS was stripped of the biofilms (0.25% EDTA treatment), the thickness and biomass volume decreased while the surface to volume ratio and roughness increased. This leads to the reduction in AgNP resistance. According to the results, it is shown that physical characteristics can contribute to the AgNP resistance of biofilms. In environment where different growth conditions are found, the biofilm resistance to AgNPs can vary although they are mature, which should be taken into account for evaluating the impact of AgNPs on biofilms.

Chapter 5
Silver Nanoparticle Properties Influencing Toxicity to Biofilms

5.1) Introduction

AgNPs have been commonly used in consumer products. There are concerns of AgNP release and its impact on the environment **[187, 188]**. AgNPs released from products can travel to natural water systems where they can harm environmental bacteria **[166, 189]**. The strong antibacterial activity of AgNPs including cell wall and membrane damage, DNA and protein damage, and oxidative stress, can affect natural beneficial bacteria such as elemental cycle regulators and contaminant degraders leading to deterioration of natural water systems **[19, 22, 86, 92, 190, 191]**. However, environmental bacteria generally form biofilms, which are more resistant to AgNPs than free cells **[35, 37]**. Therefore, understanding the biofilm resistance to AgNPs is important to determine the impact of AgNPs on environmental bacteria.

The biofilm resistance to AgNPs may depend on the physical protection by EPS production, the slow growth rate of bacteria inside biofilms, and the hydrophobicity of cells **[38, 52, 88, 136]**. The previous chapters show that stage of maturity and physical characteristics of biofilms play a role in the AgNP resistance of biofilms. Biofilms develop high AgNP resistance when they are in more mature stages. Also, the biofilms with lower thickness, lower volume, higher surface to volume ratio, and higher roughness were more resistant to AgNPs. Therefore, both of stages and physical characteristics must be considered when determining the effect of AgNPs on environmental biofilms.

Under the environmental conditions that biofilms are mature and have better characteristics for protection, it does not mean low impact of AgNPs on biofilms. AgNPs that persist in the environment gradually increase their toxicity by various mechanisms due to their properties. Because AgNPs slowly release Ag^+, and many studies found that Ag^+ is more toxic than AgNPs; therefore, dissolution of Ag^+ from AgNPs is an important mechanism of toxicity **[26, 192-194]**. The effect of AgNPs increased when the fraction of Ag^+ is higher, and the toxicity from Ag^+ release can be equal to or even higher than AgNPs **[29, 82]**. Smaller AgNPs are more toxic because they are able to penetrate deeper into biofilms, resist to agglomeration, and release more reactive species **[25, 36, 99]**. Apart from the size, the toxicity is also dependent on the surface charge of AgNPs **[195]**. In the case of AgNPs, AgNPs with high negative charge are more stable and dispersed while AgNPs with high positive charge are attracted to bacterial cells, both of which increase the toxicity of AgNPs **[24, 25]**.

In this chapter, the research objective is to determine the biofilm resistance to AgNPs with different properties. AgNPs were synthesized by varying BH_4^-/Ag^+ ratio and characterized for different Ag^+ release, particle size, and surface charge. Biofilms were grown in different glucose concentrations and temperatures according to the previous chapter to obtain biofilms with different physical characteristics. Finally, the effect of different AgNPs on biofilms was observed.

5.2) Methodology

5.2.1) Synthesis of AgNPs with different properties

AgNPs were synthesized and characterized for size, zeta potential, and Ag^+ according to the method described in section 3.2.1. To obtain AgNPs with different properties, the concentration of $AgNO_3$ was fixed (0.25 mM) while the concentration

of $NaBH_4$ was varied **[22]**. The BH_4^-/Ag^+ ratios used in the synthesis were at 1, 0.5, and 0.1 based on the $NaBH_4$ concentrations of 10, 5, and 1 mM.

5.2.2) Culture preparation and biofilm experiments

P. putida KT2440 was used and the preparation of the culture was done in the same way as described in section 3.2.2. The biofilm formation was conducted in the 96-well plate according to section 4.2.3.

5.2.3) Effect of Ag^+ release on biofilms

The effect of Ag^+ release on biofilms was determined from the 96-well plate experiments described in section 4.2.8. The amounts of Ag^+ release were taken from the results of the experiment determining Ag^+ release in section 3.2.1. The effect of Ag^+ on biofilms was determined by using $AgNO_3$ (in 0.06% PVA) at the concentration equal to the release.

5.2.4) Effect of AgNPs with different properties on planktonic cells

The culture of *P. putida* KT2440 was grown in 50 mM of glucose in M9 media at 30°C to the stationary phase. The cells were harvested and re-suspended in 0.85% NaCl ($OD_{540} \approx 0.2$). The AgNPs solution was added to the cell suspension to the final concentrations of 5 and 20 mg/l, and the mixture was shaken at 150 rpm and 30°C. At 0, 3, and 6 h of exposure time, the effect of AgNPs was determined by taking 100 μl of the solution and analyzing the cell number by the drop plate method (section 4.2.6).

5.2.5) Effect of AgNPs with different properties on biofilms with different physical characteristics

Biofilms with different physical characteristics were grown from two glucose concentrations (5 and 50 mM) and temperatures (25 and 30°C) as presented in

Chapter 4. The biofilms were exposed to AgNPs with different properties, and the effect of AgNPs on biofilms was determined from the 96-well plate experiments as described in section 4.2.8.

5.2.6) Confocal laser scanning microscopy

The effect of AgNPs was also observed using CLSM. Biofilms were cultivated in a chambered coverslip (μ-Slide 8 well, Ibidi) before exposure to AgNPs with different properties. Biofilm staining and microscopic observation were performed as described in section 4.2.9.

5.2.7) Statistical analysis

In every experiment, the standard deviation of the triplicate data was calculated and presented as error bars. The statistical differences between two interested data groups of AgNP properties (average size, percentage of Ag^+, and zeta potential) were analyzed as described in section 3.2.9. The statistical differences between the effects of AgNPs on two interested biofilms were also analyzed.

5.3) Results and discussion

5.3.1) Effect of Ag^+ release on *P. putida* biofilms

Ag^+ release is one of the important mechanisms of antimicrobial toxicity of AgNPs, and many studies found that Ag^+ is more toxic to bacteria than AgNPs **[29, 193, 196, 197]**. As a result, it is important to determine whether the toxicity in this study is from AgNPs or Ag^+ release, which will lead to a better understanding on how biofilms resist AgNPs. According to the 6-well plate experiment in Chapter 3, the synthesized AgNPs used in previous experiments released around 5% of Ag^+, and it was increased to 7 and 10% after 24 and 48 h of exposure time, respectively. Therefore, the experiment was conducted to determine the toxicity from Ag^+ release

by using $AgNO_3$ at the concentrations equal to the minimum and maximum levels of Ag^+ release.

Biofilms forming in 5 and 50 mM of glucose at 25 and 30°C were exposed to $AgNO_3$ equal to 5% and 10% of AgNPs (Figure 27). Two concentrations of AgNPs were 5 and 20 mg/l, resulting in 0.25 and 1 mg/l of $AgNO_3$ for 5% release, and 0.5 and 2 mg/l of $AgNO_3$ for 10% release, respectively. At 5 mg/l of total Ag (Figure 27(a)), both AgNPs and released Ag^+ showed low to no toxicity to biofilms (less than 1-log reduction or no reduction in cell number), but the toxicity increased when the total Ag concentration was increased to 20 mg/l (Figure 27(b)). Similar toxicity was observed between AgNPs and 10% released Ag^+ in the biofilms at 5 mM and 50 mM of glucose at 30°C (1 to 2-log reduction). However, for the biofilms at 5 mM and 25°C, the toxicity from AgNPs (3 to 4-log reduction) was much higher than that from released Ag^+ (less than 1-log reduction). From these results, it can be inferred that the toxicity of AgNPs in this study should be mostly from the nanosized AgNPs, combining with some toxicity from the released Ag^+.

The released Ag^+ although small contributed to the AgNP toxicity. Therefore, when AgNPs can release more Ag^+, the toxicity should be higher. In the next experiment, different AgNPs were synthesized and tested for their toxicity whether they are related to the Ag^+ release.

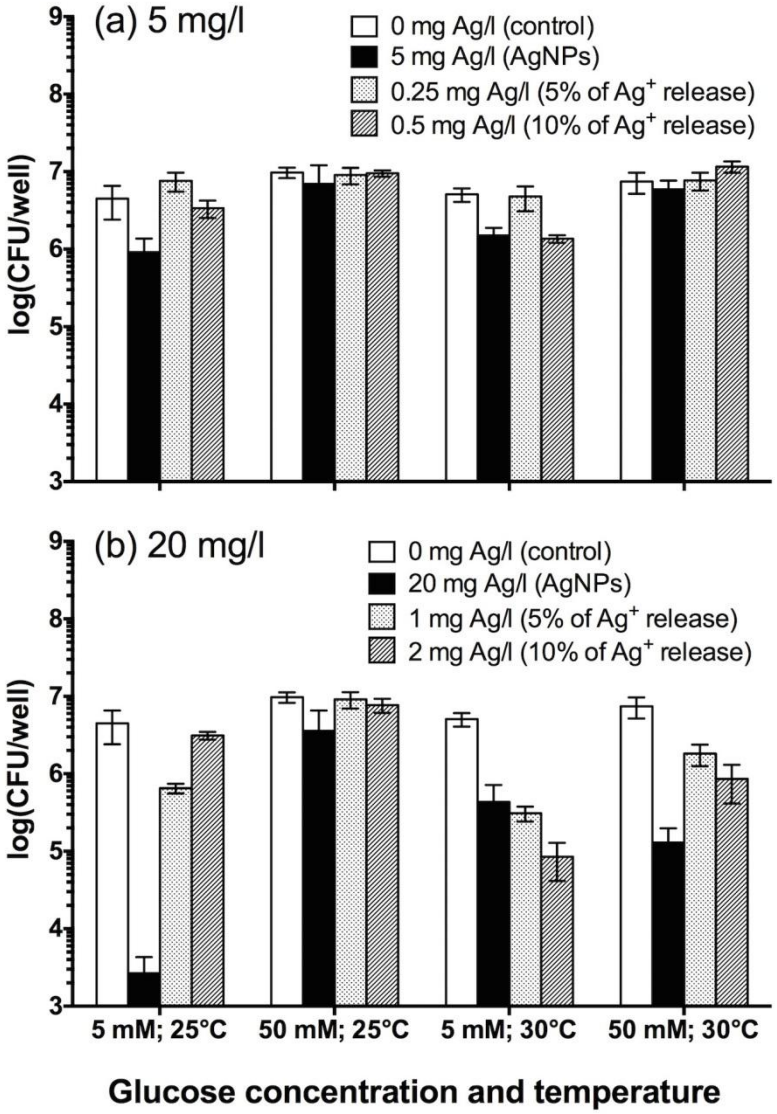

Figure 27 Effect of AgNPs and Ag^+ release on biofilms growing in different conditions. Biofilms were exposed to AgNPs and $AgNO_3$ for 24 h. Two concentrations of total Ag were used: (a) 5 mg/l; and (b) 20 mg/l. The effect is shown as reduction in cell number on y-axis. The means and standard deviations are based on 3 different biofilm samples.

5.3.2) Properties of AgNPs and toxicity to planktonic cells

Table 5 shows the properties three different AgNPs synthesized from the BH_4^- /Ag^+ ratios of 1, 0.5, and 0.1, which are listed as AgNPs#1, AgNPs#2, and AgNPs#3, respectively. AgNPs#1 are the same AgNPs used in previous chapters. The UV-vis spectra with similar peaks at 395 to 400 nm (Figure 28) suggest the formation of AgNPs. The sizes of the AgNPs were similar between AgNPs#1 (47 nm) and AgNPs#3 (42 nm), which were slightly smaller than AgNPs#2 (67 nm). Three AgNPs released different amounts of Ag^+, which were 5.3% for AgNPs#1, 7.7% for AgNPs#2, and 9.1% for AgNPs#3. For the zeta potential or surface charge, all AgNPs exhibited nearly neutral charge. However, the highly negative and positive charges were observed in AgNPs#3 (the distribution curve for zeta potential is provided in Figure A-4, Appendix), which resulted in the average neutral charge. The mechanisms for the formation of two types of surface charge are now known in this study. However, it is speculated to be from BH_4^- used in the synthesis. Because the BH_4^- amount applied to reduce Ag^+ was fairly low (1 mM compared to 10 mM in AgNPs#1), the incomplete reaction may cause AgNPs#3 to be different from other AgNPs **[22]**.

Table 5 Properties of AgNPs

Properties	AgNPs#1	AgNPs#2	AgNPs#3
Molar ratio of BH_4^-/Ag^+	1	0.5	0.1
Average size (nm)	47 ± 4	67 ± 2	42 ± 2
Surface plasmon peak (nm)	395	400	400
Percentage of Ag^+ (%)	5.33 ± 0.01	7.73 ± 0.07	9.10 ± 0.06
Zeta potential (mV)	-1.4 ± 0.2	-5.5 ± 0.7	-2.4 ± 0.3*

*According to the data from the zeta potential distribution curve (Figure A-4, Appendix), the measurement of intensity showed that around 70% of the particles were highly negative charged (-60 to -95 mV) while around 30% were highly positive (+140 mV).

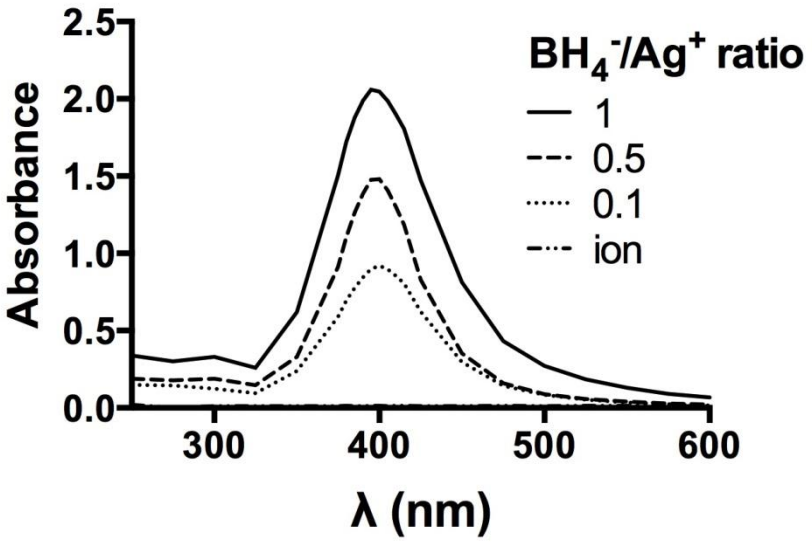

Figure 28 UV-vis spectra of AgNPs synthesized from different molar ratios of BH_4^-/Ag^+. The Ag^+ shows almost no absorbance in the wavelength range tested.

The free cells of *P. putida* KT2440 were exposed to 5 and 20 mg/l of three AgNPs, and the toxicity was determined by reduction in cell number (Figure 29). The cells were also exposed to $AgNO_3$ for comparison of the toxicity between Ag^+ and AgNPs. At 5 mg/l of total Ag, the cell number was reduced after 6 h of exposure to AgNPs and Ag^+ (1 to 2-log reduction in cell number). AgNPs#3 showed highest toxicity while AgNPs#1, AgNPs#2, and Ag^+ showed similar toxicity. When the Ag concentration was increased to 20 mg/l, the toxicity of AgNPs#1, AgNPs#2, and Ag^+ increased similarly (2 to 3-log reduction in cell number) whereas AgNPs#3 could completely kill the cells at 6 h, showing the highest toxicity among three AgNPs.

The highest toxicity in AgNPs#3 could be contributed by the Ag^+ release. AgNPs#3 released 9% of Ag^+ compared to 5% release from AgNPs#1. However, AgNPs#2 also show almost 8% release but the toxicity is similar to AgNPs#1 and $AgNO_3$, in which the amount of Ag^+ can be considered as 100% release. Beer et al. **[82]** also observed high toxicity of AgNPs when the released Ag^+ was more than 5% of total Ag. As described in the previous section, Ag^+ release in this study contributed to the toxicity of AgNPs but should not be the main mechanism of the toxicity. Therefore, the higher toxicity of AgNPs#3 should not be only from the Ag^+ release. Another possible mechanism of toxicity is the charge of AgNPs. AgNPs#3 is the only one that exhibits the highly positive and negative charges. The positively-charged AgNPs could be more attracted to the negatively-charged bacterial membrane, leading to more toxicity of AgNPs **[24]**. Even though the negatively-charged AgNPs may be less attracted to bacteria, they can still show high toxicity due to high stability and low aggregation,

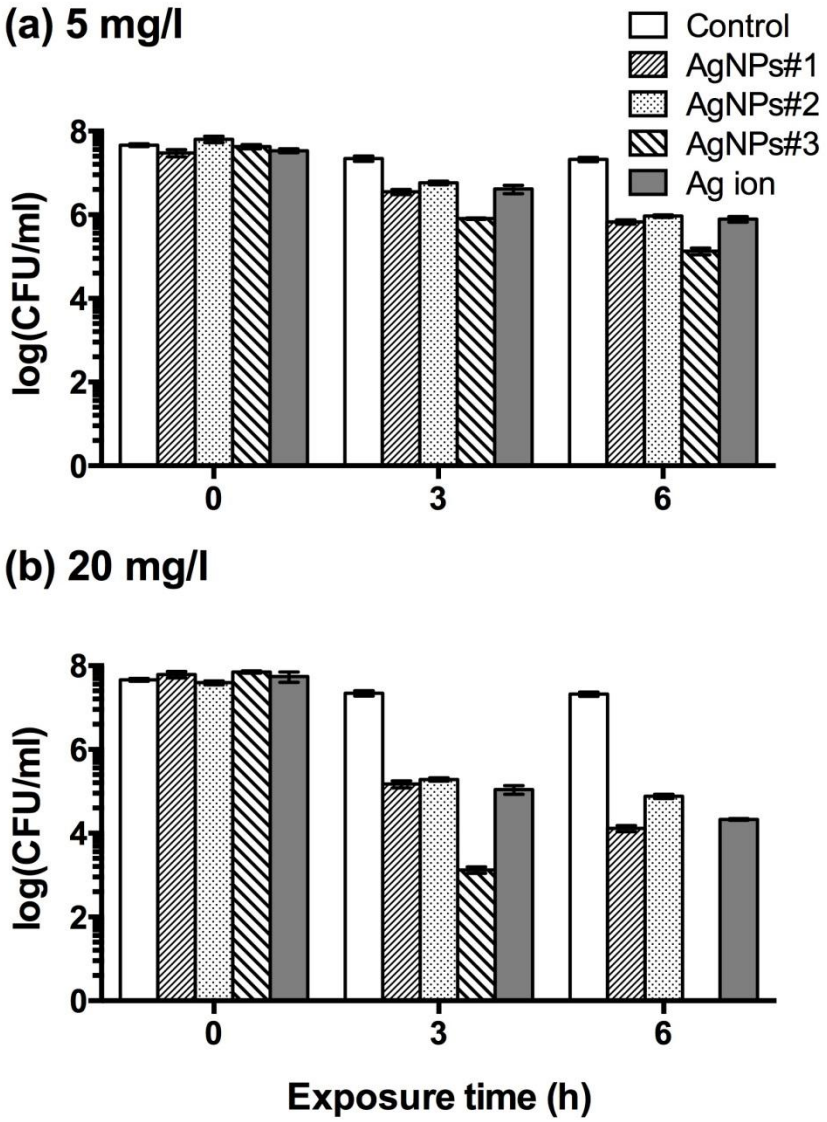

Figure 29 Toxicity of different AgNPs to planktonic cells at the concentrations of: (a) 5 mg/l; and (b) 20 mg/l. Planktonic cells in stationary phase were grown in 50 mM of glucose before the cells were harvested for the exposure. The effect is shown as reduction in cell number on y-axis. The means and standard deviations are based on 3 different samples.

Which is from the repulsive force between the charges **[25, 86, 100]**. Therefore, AgNPs#3 that consists of two types of charges showed more toxicity than AgNPs#1 and AgNPs#2, which have nearly neutral charge.

The results show that Ag^+ release and surface charge of AgNPs are important to the toxicity of AgNPs. This leads to the question whether these properties of AgNPs can affect the toxicity to biofilms. Therefore, the effect of different AgNPs on biofilms was determined in the next experiment.

5.3.3) Effect of AgNPs with different properties on *P. putida* biofilms

From the data in Chapter 4, biofilms with higher biomass and favorable physical characteristics (more thickness and volume; less surface/volume ratio and roughness) are more resistant to AgNPs. However, if there are more Ag^+ release and more negative or positive charges, the effect of AgNPs on biofilms tends to increased. In this experiment, Biofilms forming at different glucose concentrations (5 and 50 mM) and temperatures (25 and 30°C) were exposed to three AgNPs from the previous experiment, and the effect was determined by live/dead staining observed under CLSM (Figure 30) and reduction in cell number (Figure 31). The CLSM images show more live cells (green) in the biofilms exposed AgNPs#1 than other AgNPs (Figure 30). This was supported by the reductions in cell number data (Figure 31), which show the lowest effect on biofilms by AgNPs#1 (1 to 2-log reduction versus 3-log reduction by AgNPs#2 and AgNPs#3). The effect of AgNPs on biofilms also increased when the concentration was increased from 5 to 20 mg/l.

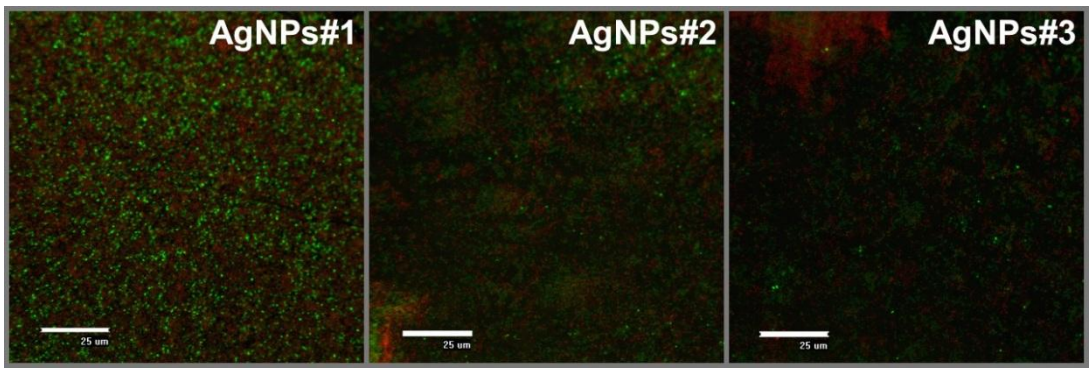

Figure 30 Biofilms after exposed to different AgNPs for 24 h. The concentration of AgNPs was 20 mg/l. Green and red colors show the live and dead cells, respectively. The bar indicates 25 μm in scale.

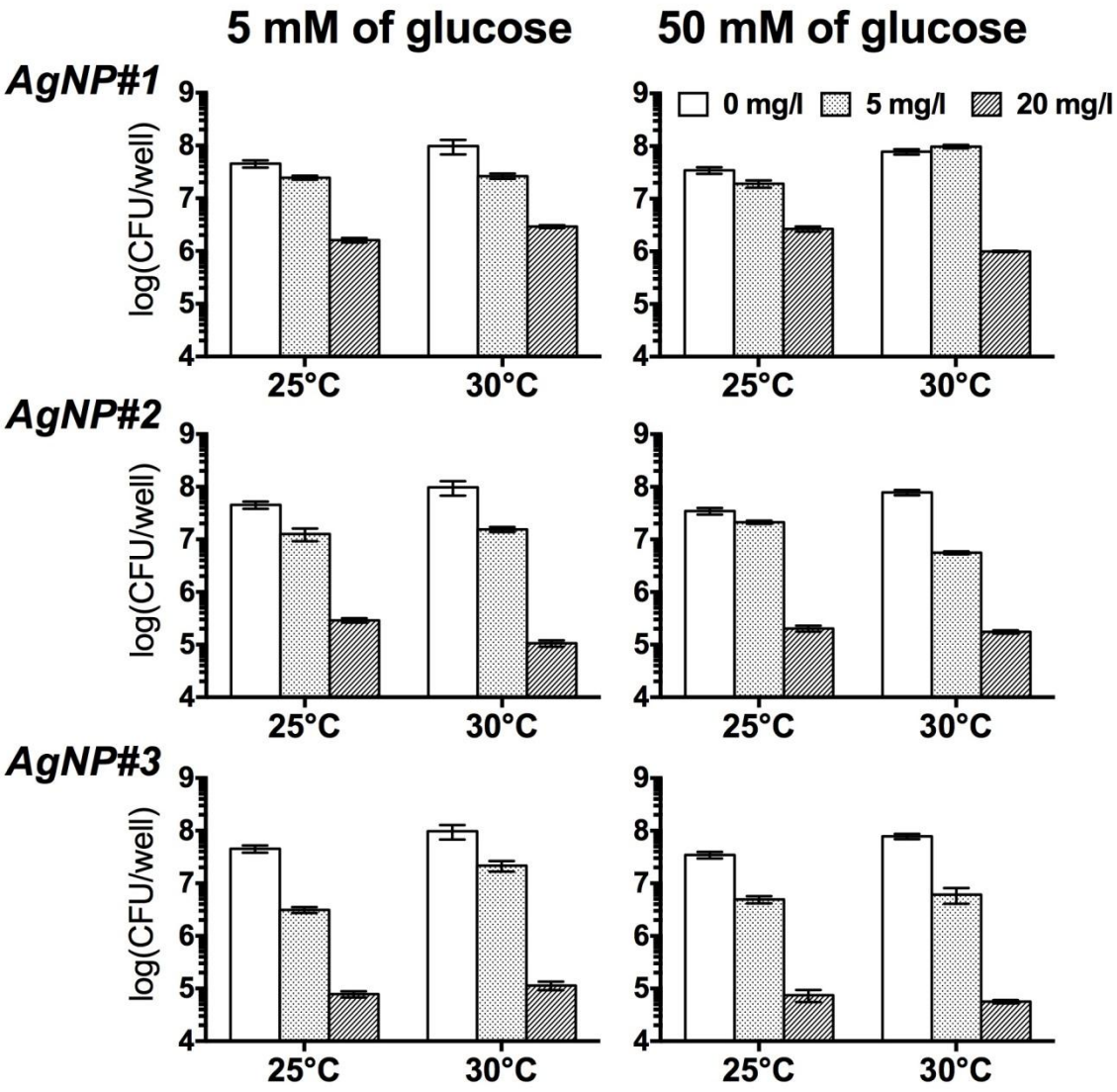

Figure 31 Effect of different AgNPs on biofilms forming under different glucose concentration (5 and 50 mM) and temperature (25 and 30°C). The exposure time was 24 h. The effect is shown as reduction in cell number on y-axis. The means and standard deviations are based on 3 different biofilm samples.

The AgNPs#3 still showed highest toxicity to biofilms similar to the results in planktonic cells (Figure 29). However, the toxicity of AgNPs#3 to biofilms was only slightly higher than that of AgNPs#2, which is different from the toxicity to planktonic cells where AgNPs#3 was much more toxic than AgNPs#2. This might be due to the difference in the exposure time between planktonic and biofilm experiments. Because biofilms showed higher AgNP resistance than planktonic cells **[37]**, the exposure time for biofilms was increased to 24 h, which may be long enough for AgNPs#2 to produce greater effect than that observed in planktonic cells.

The different toxicity of AgNPs is also supported by the Ag^+ release data. After 24 h exposure of biofilms to AgNPs, the released Ag^+ increased from 8 to 13% in AgNPs#2, and from 9 to 12% in AgNPs#3 whereas it only increased from 5 to 7% in AgNPs#1. Therefore, the higher Ag^+ amount in AgNPs#2 and AgNPs#3 possibly increased the effect of AgNPs on biofilms. González et al. **[145]** found more accumulation of Ag^+ than AgNPs in biofilms, which may explain the increased effect of AgNPs with higher Ag^+ release. Other mechanisms may also contribute to the effect on biofilms. Choi et al. **[22]** suggested that the effect of AgNPs is correlated with the fraction of AgNPs smaller than 5 nm. Also, the amount of ROS generated from AgNPs can increase the toxicity **[23, 63, 101]**. Unfortunately, both of these properties of AgNPs were not measured in this experiment, so it is still inconclusive whether they contributed to the effect observed in this study.

In Chapter 4, it was found that biofilms growing in 5 and 50 mM of glucose and at 25 and 30°C showed different resistance to AgNPs due to their biomass and physical characteristics. However, when they were exposed to AgNPs#3, which had more Ag^+ release and highly positive and negative charges, they showed similar

AgNP resistance regardless of their growing conditions. Also, the resistance to AgNPs#3 was much lower than the resistance to AgNPs#1 used in the previous chapters. This shows that the effect of AgNPs on biofilms can be increased if AgNPs are able to release more Ag^+ and are highly deviated from neutral charge. The mechanisms of increased toxicity in AgNPs with more Ag^+ release and less neutral charges are proposed in Figure 32. AgNPs with highly positive charges are subject to more adsorption onto biofilms with negative charges of EPS **[36]**. Both negatively- and positively-charged AgNPs are more stable and can release more Ag^+ **[16]**.

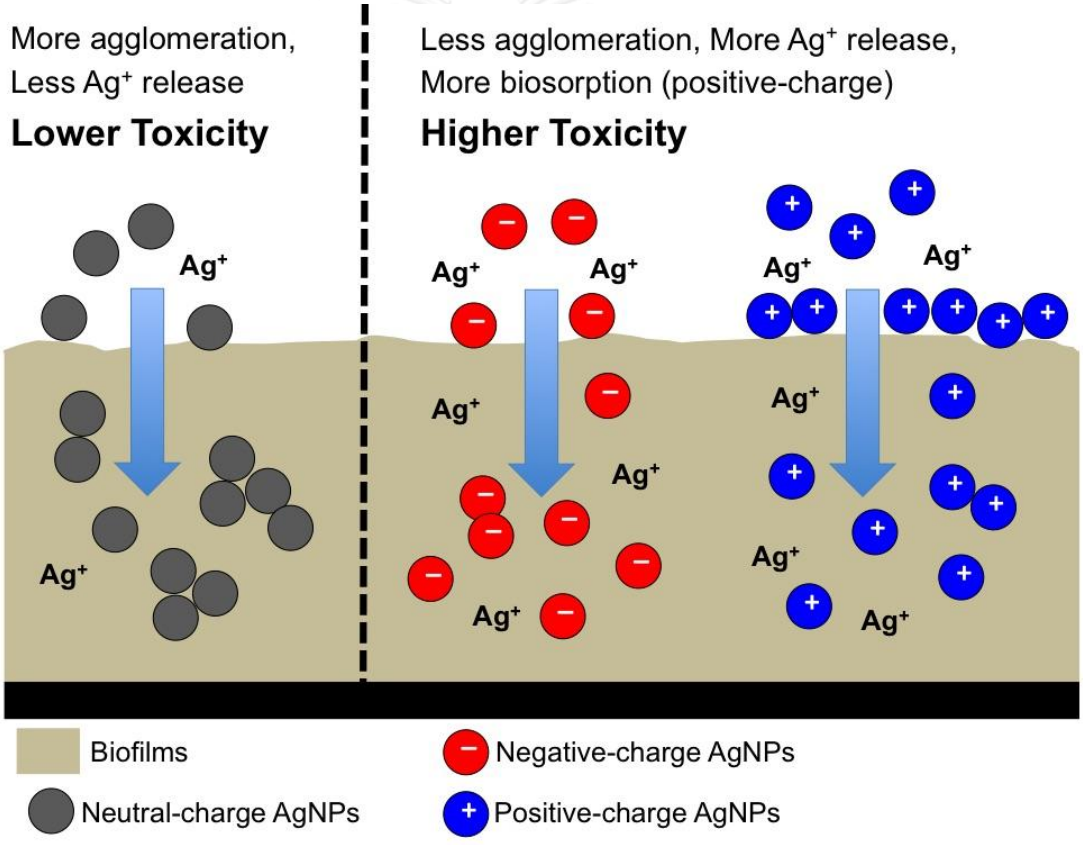

Figure 32 Mechanisms of toxicity of different AgNPs to biofilms

5.4) Summary

The degree of AgNP toxicity to biofilms can depend on the Ag^+ dissolution from AgNPs and surface charge of AgNPs. The toxicity from Ag^+ release was determined by exposing biofilms to $AgNO_3$ at the concentrations equal to the minimum (5%) and maximum levels (10%) of release. The released Ag^+ showed some toxicity to biofilms (less than 1-log reduction) even though it was less than that of AgNPs (3 to 4-log reduction). Since the AgNP toxicity is partly from Ag^+ release, the AgNP toxicity should increase when AgNPs can dissolute more Ag^+. Three AgNPs were synthesized to have different Ag^+ release by using the BH_4^-/Ag^+ ratio of 1, 0.5, and 0.1. While having similar sizes, three AgNPs released different amounts of Ag^+ (5.3% for AgNPs#1; 7.7% for AgNPs#2; and 9.1% for AgNPs#3). For the zeta potential or surface charge, all AgNPs exhibited nearly neutral charge; however, the highly negative (-60 to -95 mV) and positive charges (+140 mV) were observed in AgNPs#3, which resulted in the average neutral charge. The effect of AgNPs on biofilms was increased when AgNPs have more Ag^+ release and highly negative or positive charges. The AgNPs#3 exhibited highest toxicity to biofilms (3-log reduction) whereas AgNPs#1 showed least toxicity (1 to 2-log reduction). From the results, the properties of AgNPs and the factors affecting them must be carefully considered when assessing the toxicity of AgNPs to environment. Even though the effect of AgNPs on environmental biofilms appears to be low due to the biofilm resistance, it can gradually increase due to the stability of AgNPs and increased Ag^+ release.

Chapter 6
Conclusions, Implications, and Suggestions for Future Research

6.1) Conclusions

The goal of this research is to elucidate the effect of AgNPs on bacteria in the environment. In order to achieve this goal, it is important to understand the mechanisms of AgNP resistance in biofilms, because they are abundant in the environment and likely to be affected by AgNPs. By using *P. putida* KT2440 as a model of environmental biofilms, the obtained results contribute to the understandings of AgNP resistance in biofilms by adding the importance of biofilm stage and physical characteristics. Biofilms need to be in mature stage to resist AgNPs as they can produce enough EPS for protection from the adverse effect of AgNPs. However, a presence of mature biofilms is not a guarantee for high AgNP resistance. Under various growth conditions, mature biofilms can have different structures or physical characteristics, which leads to different levels of AgNP resistance. High AgNP resistance can be found in biofilms with high thickness, high biomass volume, low surface to volume ratio, and low roughness. Furthermore, even though biofilms already exhibit AgNP resistance through the mature stage and physical characteristics, the adverse effect of AgNPs is still possible if AgNPs have high Ag^{+} release and highly negative or positive charges. In conclusion, biofilm maturity, physical characteristics, and AgNP properties must be considered together when evaluating the impact of AgNPs on environmental biofilms.

6.2) Environmental implications

The findings from the research have important implications in environmental management for both wastewater treatment systems and natural water systems. In wastewater treatment plants, different effects of AgNPs are expected at different phases of operation. AgNPs will be less toxic in steady-state systems with mature biofilms, but systems during start-up, when biofilms are becoming established, will be vulnerable to AgNPs. Biofilms with high biomass, thickness, and volume in the system are less vulnerable to AgNPs and may be able to remove AgNPs by biosorption.

In different environmental systems, there are different conditions provided for biofilm formation. Therefore, biofilms may not only have different stages of maturity but also have different characteristics, which lead to different AgNP resistance. When biofilms have more thickness and biomass volume, the AgNP resistance should be high, which means less adverse effect of AgNPs. Regardless of the thickness and volume of biofilms, AgNPs with more stability and Ag^+ release may exhibit severe toxicity in certain environmental conditions such as oligotrophic, where there are less environmental constituents for AgNP transformation to reduce the impact.

6.3) Suggestions for future research

It should be noted that this study only focused on the effect of AgNPs on single-species biofilms grown in batch conditions. In natural and engineered systems, various species of bacteria are present as a community under the dynamic conditions. It is possible that the stage of maturity and characteristics of biofilms will be different from the results in this study, leading to different effects of AgNPs on biofilms. Therefore, the continuous conditions and multi-species biofilms should be considered

for further studies in order to better understand the effect of AgNPs on biofilms at different stages of maturity and biofilms with different characteristics.

Moreover, this research uses only artificial conditions such as batch conditions and enriched media, which may not represent the environmental conditions. The future research should consider environmental conditions to study the biofilm stage and characteristics, and their AgNP resistance. The presence of other constituents in natural water or wastewater systems such as S^{2-} could be augmented to simulate the actual conditions that biofilms are exposed to AgNPs.

REFERENCES

1. Mijnendonckx, K., Leys, N., Mahillon, J., Silver, S., and Van Houdt, R., *Antimicrobial silver: uses, toxicity and potential for resistance.* BioMetals, 2013. **26**(4): p. 609-621.
2. Gangadharan, D., Harshvardan, K., Gnanasekar, G., Dixit, D., Popat, K. M., and Anand, P. S., *Polymeric microspheres containing silver nanoparticles as a bactericidal agent for water disinfection.* Water Research, 2010. **44**(18): p. 5481-5487.
3. Pollini, M., Paladini, F., Catalano, M., Taurino, A., Licciulli, A., Maffezzoli, A., and Sannino, A., *Antibacterial coatings on haemodialysis catheters by photochemical deposition of silver nanoparticles.* Journal of Materials Science: Materials in Medicine, 2011. **22**(9): p. 2005-2012.
4. Monteiro, D. R., Gorup, L. F., Takamiya, A. S., Ruvollo-Filho, A. C., Camargo, E. R. d., and Barbosa, D. B., *The growing importance of materials that prevent microbial adhesion: antimicrobial effect of medical devices containing silver.* International Journal of Antimicrobial Agents, 2009. **34**(2): p. 103-110.
5. Mirjalili, M., Yaghmaei, N., and Mirjalili, M., *Antibacterial properties of nano silver finish cellulose fabric.* Journal of Nanostructure in Chemistry, 2013. **3**(1): p. 1-5.
6. Tian, J., Wong, K. K. Y., Ho, C.-M., Lok, C.-N., Yu, W.-Y., Che, C.-M., Chiu, J.-F., and Tam, P. K. H., *Topical delivery of silver nanoparticles promotes wound healing.* ChemMedChem, 2007. **2**(1): p. 129-136.
7. Bystrzejewska-Piotrowska, G., Golimowski, J., and Urban, P. L., *Nanoparticles: their potential toxicity, waste and environmental management.* Waste Management, 2009. **29**(9): p. 2587-2595.
8. Lorenz, C., Windler, L., von Goetz, N., Lehmann, R. P., Schuppler, M., Hungerbühler, K., Heuberger, M., and Nowack, B., *Characterization of silver release from commercially available functional (nano)textiles.* Chemosphere, 2012. **89**(7): p. 817-824.
9. Pasricha, A., Jangra, S. L., Singh, N., Dilbaghi, N., Sood, K. N., Arora, K., and Pasricha, R., *Comparative study of leaching of silver nanoparticles from fabric and effective effluent treatment.* Journal of Environmental Sciences, 2012. **24**(5): p. 852-859.
10. Kaegi, R., Voegelin, A., Sinnet, B., Zuleeg, S., Hagendorfer, H., Burkhardt, M., and Siegrist, H., *Behavior of metallic silver nanoparticles in a pilot wastewater treatment plant.* Environmental Science and Technology, 2011. **45**(9): p. 3902-3908.
11. Kaegi, R., Voegelin, A., Ort, C., Sinnet, B., Thalmann, B., Krismer, J., Hagendorfer, H., Elumelu, M., and Mueller, E., *Fate and transformation of silver nanoparticles in urban wastewater systems.* Water Research, 2013. **47**(12): p. 3866-3877.
12. Dobias, J. and Bernier-Latmani, R., *Silver release from silver nanoparticles in natural waters.* Environmental Science and Technology, 2013. **47**(9): p. 4140-4146.

13. Reinsch, B. C., Levard, C., Li, Z., Ma, R., Wise, A., Gregory, K. B., Brown, J., G. E., and Lowry, G. V., *Sulfidation of silver nanoparticles decreases Escherichia coli growth inhibition.* Environmental Science and Technology, 2012. **46**: p. 6992-7000.
14. Chambers, B. A., Afrooz, A. R. M. N., Bae, S., Aich, N., Katz, L., Saleh, N. B., and Kirisits, M. J., *Effects of chloride and ionic strength on physical morphology, dissolution, and bacterial toxicity of silver nanoparticles.* Environmental Science and Technology, 2013. **48**(1): p. 761-769.
15. Gao, J., Powers, K., Wang, Y., Zhou, H., Roberts, S. M., Moudgil, B. M., Koopman, B., and Barber, D. S., *Influence of Suwannee River humic acid on particle properties and toxicity of silver nanoparticles.* Chemosphere, 2012. **89**(1): p. 96-101.
16. Levard, C., Hotze, E. M., Colman, B. P., Dale, A. L., Truong, L., Yang, X. Y., Bone, A. J., Brown, G. E., Tanguay, R. L., Di Giulio, R. T., Bernhardt, E. S., Meyer, J. N., Wiesner, M. R., and Lowry, G. V., *Sulfidation of silver nanoparticles: Natural antidote to their toxicity.* Environmental Science and Technology, 2013. **47**(23): p. 13440-13448.
17. Schacht, V. J., Neumann, L. V., Sandhi, S. K., Chen, L., Henning, T., Klar, P. J., Theophel, K., Schnell, S., and Bunge, M., *Effects of silver nanoparticles on microbial growth dynamics.* Journal of Applied Microbiology, 2013. **114**(1): p. 25-35.
18. García, A., Delgado, L., Torà, J. A., Casals, E., González, E., Puntes, V., Font, X., Carrera, J., and Sánchez, A., *Effect of cerium dioxide, titanium dioxide, silver, and gold nanoparticles on the activity of microbial communities intended in wastewater treatment.* Journal of Hazardous Materials, 2012. **199–200**(0): p. 64-72.
19. Morones, J. R., Elechiguerra, J. L., Camacho, A., Holt, K., Kouri, J. B., Ramírez, J. T., and Yacaman, M. J., *The bactericidal effect of silver nanoparticles.* Nanotechnology, 2005. **16**(10): p. 2346-2353.
20. Radzig, M. A., Nadtochenko, V. A., Koksharova, O. A., Kiwi, J., Lipasova, V. A., and Khmel, I. A., *Antibacterial effects of silver nanoparticles on gram-negative bacteria: Influence on the growth and biofilms formation, mechanisms of action.* Colloids and Surfaces B: Biointerfaces, 2013. **102**(0): p. 300-306.
21. Rai, M. K., Deshmukh, S. D., Ingle, A. P., and Gade, A. K., *Silver nanoparticles: the powerful nanoweapon against multidrug-resistant bacteria.* Journal of Applied Microbiology, 2012. **112**(5): p. 841-852.
22. Choi, O. K. and Hu, Z. Q., *Size dependent and reactive oxygen species related nanosilver toxicity to nitrifying bacteria.* Environmental Science and Technology, 2008. **42**(12): p. 4583-4588.
23. Carlson, C., Hussain, S. M., Schrand, A. M., K. Braydich-Stolle, L., Hess, K. L., Jones, R. L., and Schlager, J. J., *Unique cellular interaction of silver nanoparticles: Size-dependent generation of reactive oxygen species.* The Journal of Physical Chemistry B, 2008. **112**(43): p. 13608-13619.
24. El Badawy, A. M., Silva, R. G., Morris, B., Scheckel, K. G., Suidan, M. T., and Tolaymat, T. M., *Surface charge-dependent toxicity of silver*

nanoparticles. Environmental Science and Technology, 2011. **45**(1): p. 283-287.
25. Samberg, M. E., Orndorff, P. E., and Monteiro-Riviere, N. A., *Antibacterial efficacy of silver nanoparticles of different sizes, surface conditions and synthesis methods.* Nanotoxicology, 2011. **5**(2): p. 244-253.
26. Kittler, S., Greulich, C., Diendorf, J., Köller, M., and Epple, M., *Toxicity of silver nanoparticles increases during storage because of slow dissolution under release of silver ions.* Chemistry of Materials, 2010. **22**(16): p. 4548-4554.
27. Liang, Z., Das, A., and Hu, Z., *Bacterial response to a shock load of nanosilver in an activated sludge treatment system.* Water Research, 2010. **44**(18): p. 5432-5438.
28. Yuan, Z., Li, J., Cui, L., Xu, B., Zhang, H., and Yu, C.-P., *Interaction of silver nanoparticles with pure nitrifying bacteria.* Chemosphere, 2013. **90**(4): p. 1404-1411.
29. Yang, Y., Wang, J., Xiu, Z., and Alvarez, P. J. J., *Impacts of silver nanoparticles on cellular and transcriptional activity of nitrogen-cycling bacteria.* Environmental Toxicology and Chemistry, 2013. **32**(7): p. 1488-1494.
30. Das, P., Williams, C. J., Fulthorpe, R. R., Hoque, M. E., Metcalfe, C. D., and Xenopoulos, M. A., *Changes in bacterial community structure after exposure to silver nanoparticles in natural waters.* Environmental Science and Technology, 2012. **46**(16): p. 9120-9128.
31. Davies, D., *Understanding biofilm resistance to antibacterial agents.* Nature Reviews Drug Discovery, 2003. **2**(2): p. 114-122.
32. Allison, D. G., *The biofilm matrix.* Biofouling: The Journal of Bioadhesion and Biofilm Research, 2003. **19**(2): p. 139 - 150.
33. Hall-Stoodley, L., Costerton, J. W., and Stoodley, P., *Bacterial biofilms: from the natural environment to infectious diseases.* Nature Reviews Microbiology, 2004. **2**(2): p. 95-108.
34. Velázquez-Velázquez, J. L., Santos-Flores, A., Araujo-Meléndez, J., Sánchez-Sánchez, R., Velasquillo, C., González, C., Martínez-Castañon, G., and Martinez-Gutierrez, F., *Anti-biofilm and cytotoxicity activity of impregnated dressings with silver nanoparticles.* Materials Science and Engineering: C, 2015. **49**(0): p. 604-611.
35. Park, H.-J., Park, S., Roh, J., Kim, S., Choi, K., Yi, J., Kim, Y., and Yoon, J., *Biofilm-inactivating activity of silver nanoparticles: A comparison with silver ions.* Journal of Industrial and Engineering Chemistry, 2013. **19**(2): p. 614-619.
36. Peulen, T.-O. and Wilkinson, K. J., *Diffusion of nanoparticles in a biofilm.* Environmental Science and Technology, 2011. **45**(8): p. 3367-3373.
37. Choi, O., Yu, C.-P., Fernández, G. E., and Hu, Z., *Interactions of nanosilver with Escherichia coli cells in planktonic and biofilm cultures.* Water Research, 2010. **44**(20): p. 6095-6103.
38. Sheng, Z. and Liu, Y., *Effects of silver nanoparticles on wastewater biofilms.* Water Research, 2011. **45**(18): p. 6039-6050.

39. Oliveira, M., Nunes, S. F., Carneiro, C., Bexiga, R., Bernardo, F., and Vilela, C. L., *Time course of biofilm formation by Staphylococcus aureus and Staphylococcus epidermidis mastitis isolates.* Veterinary Microbiology, 2007. **124**(1–2): p. 187-191.
40. Nett, J. E., Lepak, A. J., Marchillo, K., and Andes, D. R., *Time course global gene expression analysis of an in vivo Candida biofilm.* Journal of Infectious Diseases, 2009. **200**(2): p. 307-313.
41. Gupta, K., Marques, C. N. H., Petrova, O. E., and Sauer, K., *Antimicrobial tolerance of Pseudomonas aeruginosa biofilms is activated during an early developmental stage and requires the two-component hybrid SagS.* Journal of Bacteriology, 2013. **195**(21): p. 4975-4987.
42. Lee, J.-W., Nam, J.-H., Kim, Y.-H., Lee, K.-H., and Lee, D.-H., *Bacterial communities in the initial stage of marine biofilm formation on artificial surfaces.* The Journal of Microbiology, 2008. **46**(2): p. 174-182.
43. Watnick, P. I. and Kolter, R., *Biofilm, city of microbes.* Journal of Bacteriology, 2000. **182**(10): p. 2675-2679.
44. Sauer, K., Camper, A. K., Ehrlich, G. D., Costerton, J. W., and Davies, D. G., *Pseudomonas aeruginosa displays multiple phenotypes during development as a biofilm.* Journal of Bacteriology, 2002. **184**(4): p. 1140-1154.
45. Prüß, B. M., Besemann, C., Denton, A., and Wolfe, A. J., *A complex transcription network controls the early stages of biofilm development by Escherichia coli.* Journal of Bacteriology, 2006. **188**(11): p. 3731-3739.
46. Williams, D., Woodbury, K., Haymond, B., Parker, A., and Bloebaum, R., *A modified CDC biofilm reactor to produce mature biofilms on the surface of PEEK membranes for an in vivo animal model application.* Current Microbiology, 2011. **62**(6): p. 1657-1663.
47. Yeater, K. M., Chandra, J., Cheng, G., Mukherjee, P. K., Zhao, X., Rodriguez-Zas, S. L., Kwast, K. E., Ghannoum, M. A., and Hoyer, L. L., *Temporal analysis of Candida albicans gene expression during biofilm development.* Microbiology, 2007. **153**(8): p. 2373-2385.
48. Ito, A., Taniuchi, A., May, T., Kawata, K., and Okabe, S., *Increased antibiotic resistance of Escherichia coli in mature biofilms.* Applied and Environmental Microbiology, 2009. **75**(12): p. 4093-4100.
49. Tré-Hardy, M., Macé, C., El Manssouri, N., Vanderbist, F., Traore, H., and Devleeschouwer, M. J., *Effect of antibiotic co-administration on young and mature biofilms of cystic fibrosis clinical isolates: the importance of the biofilm model.* International Journal of Antimicrobial Agents, 2009. **33**(1): p. 40-45.
50. Shen, Y., Stojicic, S., and Haapasalo, M., *Antimicrobial efficacy of chlorhexidine against bacteria in biofilms at different stages of development.* Journal of Endodontics, 2011. **37**(5): p. 657-661.
51. Beauchamp, C. S., Dourou, D., Geornaras, I., Yoon, Y., Scanga, J. A., Belk, K. E., Smith, G. C., Nychas, G. J. E., and Sofos, J. N., *Sanitizer efficacy against Escherichia coli O157:H7 biofilms on inadequately cleaned meat-contact surface materials.* Biblographic citation: Food Protection Trends, 2012. **32**(4): p. 173-182.

52. Kirby, A. E., Garner, K., and Levin, B. R., *The relative contributions of physical structure and cell density to the antibiotic susceptibility of bacteria in biofilms.* Antimicrobial Agents and Chemotherapy, 2012. **56**(6): p. 2967-2975.
53. Drenkard, E. and Ausubel, F. M., *Pseudomonas biofilm formation and antibiotic resistance are linked to phenotypic variation.* Nature, 2002. **416**: p. 740-713.
54. Srinandan, C. S., D'souza, G., Srivastava, N., Nayak, B. B., and Nerurkar, A. S., *Carbon sources influence the nitrate removal activity, community structure and biofilm architecture.* Bioresource Technology, 2012. **117**(0): p. 292-299.
55. Rochex, A. and Lebeault, J. M., *Effects of nutrients on biofilm formation and detachment of a Pseudomonas putida strain isolated from a paper machine.* Water Research, 2007. **41**(13): p. 2885-2892.
56. Bester, E., Kroukamp, O., Hausner, M., Edwards, E. A., and Wolfaardt, G. M., *Biofilm form and function: carbon availability affects biofilm architecture, metabolic activity and planktonic cell yield.* Journal of Applied Microbiology 2010. **110**: p. 387-398.
57. Uhlich, G. A., Chen, C.-Y., Cottrell, B. J., and Nguyen, L.-H., *Growth media and temperature effects on biofilm formation by serotype O157:H7 and non-O157 Shiga toxin-producing Escherichia coli.* FEMS Microbiology Letters, 2014. **354**(2): p. 133-141.
58. Castelijn, G. A. A., Veen, S. v. d., Zwietering, M. H., Moezelaar, R., and Abee, T., *Diversity in biofilm formation and production of curli fimbriae and cellulose of Salmonella Typhimurium strains of different origin in high and low nutrient medium.* Biofouling, 2012. **28**(1): p. 51-63.
59. Schluesener, J. and Schluesener, H., *Nanosilver: application and novel aspects of toxicology.* Archives of Toxicology, 2013. **87**(4): p. 569-576.
60. Shahverdi, A. R., Fakhimi, A., Shahverdi, H. R., and Minaian, S., *Synthesis and effects of silver nanoparticles on the antibacterial activity of different antibiotics against Staphylococcus aureus and Escherichia coli.* Nanomedicine, 2007. **18**: p. 103-112.
61. Pal, S., Tak, Y. K., and Song, J. M., *Does the antibacterial activity of silver nanoparticles depend on the shape of the nanoparticle? A study of the gram-negative bacterium Escherichia coli.* Applied and Environmental Microbiology, 2007. **73**(6): p. 1712-1720.
62. Choi, O. K., Deng, K. K., Kim, N.-J., Ross Jr, L., Surampalli, R. Y., and Hu, Z. Q., *The inhibitory effects of silver nanoparticles, silver ions, and silver chloride colloids on microbial growth.* Water Research, 2008. **42**(12): p. 3066-3074.
63. Choi, O. K. and Hu, Z. Q., *Role of reactive oxygen species in determining nitrification inhibition by metallic/oxide nanoparticles.* Journal of Environmental Engineering, 2009. **135**(12): p. 1365-1370.
64. Guzman, M., Dille, J., and Godet, S., *Synthesis and antibacterial activity of silver nanoparticles against gram-positive and gram-negative bacteria.* Nanomedicine: Nanotechnology, Biology and Medicine, 2012. **8**(1): p. 37-45.
65. Kora, A. and Arunachalam, J., *Assessment of antibacterial activity of silver nanoparticles on Pseudomonas aeruginosa and its mechanism of action.*

World Journal of Microbiology and Biotechnology, 2011. **27**(5): p. 1209-1216.

66. El-Rafie, M. H., Mohamed, A. A., Shaheen, T. I., and Hebeish, A., *Antimicrobial effect of silver nanoparticles produced by fungal process on cotton fabrics.* Carbohydrate Polymers, 2010. **80**(3): p. 779-782.
67. Song, H. Y., Ko, K. K., Oh, I. H., and Lee, B. T., *Fabrication of silver nanoparticles and their antimicrobial mechanisms.* European Cells and Materials, 2006. **11**: p. 58.
68. Rai, M., Yadav, A., and Gade, A., *Silver nanoparticles as a new generation of antimicrobials.* Biotechnology Advances, 2009. **27**(1): p. 76-83.
69. Rivero, P. J., Urrutia, A., Goicoechea, J., Rodríguez, Y., Corres, J. M., Arregui, F. J., and Matías, I. R., *An antibacterial submicron fiber mat with in situ synthesized silver nanoparticles.* Journal of Applied Polymer Science, 2012. **126**(4): p. 1228-1235.
70. Roe, D., Karandikar, B., Bonn-Savage, N., Gibbins, B., and Roullet, J.-B., *Antimicrobial surface functionalization of plastic catheters by silver nanoparticles.* Journal of Antimicrobial Chemotherapy, 2008. **61**(4): p. 869-876.
71. Kostenko, V., Lyczak, J., Turner, K., and Martinuzzi, R. J., *Impact of silver-containing wound dressings on bacterial biofilm viability and susceptibility to antibiotics during prolonged treatment.* Antimicrobial Agents and Chemotherapy, 2010. **54**(12): p. 5120-5131.
72. Fayaz, A. M., Balaji, K., Girilal, M., Yadav, R., Kalaichelvan, P. T., and Venketesan, R., *Biogenic synthesis of silver nanoparticles and their synergistic effect with antibiotics: a study against gram-positive and gram-negative bacteria.* Nanomedicine : nanotechnology, biology, and medicine, 2010. **6**(1): p. 103-109.
73. Dankovich, T. A. and Gray, D. G., *Bactericidal paper impregnated with silver nanoparticles for point-of-use water treatment.* Environmental Science & Technology, 2011. **45**: p. 1992-1998.
74. Benn, T. M. and Werterhoff, P., *Nanoparticle silver released into water from commercially available sock fabrics.* Environmental Science and Technology, 2008. **42**: p. 4133-4139.
75. Geranio, L., Heuberger, M., and Nowack, B., *The behavior of silver nanotextiles during washing.* Environmental Science and Technology, 2009. **43**(21): p. 8113-8118.
76. Lanzano, T., Bertram, M., De Palo, M., Wagner, C., Zyla, K., and Graedel, T. E., *The contemporary European silver cycle.* Resources, Conservation and Recycling, 2006. **46**: p. 27-43.
77. Blaser, S. A., Scheringer, M., MacLeod, M., and Hungerbühler, K., *Estimation of cumulative aquatic exposure and risk due to silver: Contribution of nano-functionalized plastics and textiles.* Science of The Total Environment, 2008. **390**(2-3): p. 396-409.
78. Wang, Y., Westerhoff, P., and Hristovski, K. D., *Fate and biological effects of silver, titanium dioxide, and C_{60} (fullerene) nanomaterials during simulated wastewater treatment processes.* Journal of Hazardous Materials, 2012. **201–202**(0): p. 16-22.

79. Kim, B., Park, C.-S., Murayama, M., and Hochella, M. F., *Discovery and characterization of silver sulfide nanoparticles in final sewage sludge products.* Environmental Science and Technology, 2010. **44**(19): p. 7509-7514.
80. Levard, C., Hotze, E. M., Lowry, G. V., and Brown, G. E., *Environmental transformations of silver nanoparticles: Impact on stability and toxicity.* Environmental Science and Technology, 2012. **46**(13): p. 6900-6914.
81. Gaiser, B. K., Fernandes, T. F., Jepson, M. A., Lead, J. R., Tyler, C. R., Baalousha, M., Biswas, A., Britton, G. J., Cole, P. A., Johnston, B. D., Ju-Nam, Y., Rosenkranz, P., Scown, T. M., and Stone, V., *Interspecies comparisons on the uptake and toxicity of silver and cerium dioxide nanoparticles.* Environmental Toxicology and Chemistry, 2012. **31**(1): p. 144-154.
82. Beer, C., Foldbjerg, R., Hayashi, Y., Sutherland, D. S., and Autrup, H., *Toxicity of silver nanoparticles—Nanoparticle or silver ion?* Toxicology Letters, 2012. **208**(3): p. 286-292.
83. Asghari, S., Johari, S. A., Lee, J. H., Kim, Y. S., Jeon, Y. B., Choi, H. J., Moon, M. C., and Yu, I. J., *Toxicity of various silver nanoparticles compared to silver ions in Daphnia magna.* Journal of nanobiotechnology, 2012. **10**: p. 14.
84. Wang, Z., Chen, J., Li, X., Shao, J., and Peijnenburg, W. J. G. M., *Aquatic toxicity of nanosilver colloids to different trophic organisms: Contributions of particles and free silver ion.* Environmental Toxicology and Chemistry, 2012. **31**(10): p. 2408-2413.
85. Khan, S., Mukherjee, A., and Chandrasekaran, N., *Silver nanoparticles tolerant bacteria from sewage environment.* Journal of Environmental Sciences, 2011. **23**(2): p. 346-352.
86. Sondi, I. and Salopek-Sondi, B., *Silver nanoparticles as antimicrobial agent: a case study on E. coli as a model for Gram-negative bacteria.* Journal of Colloid and Interface Science, 2004. **275**(1): p. 177-182.
87. Dimkpa, C. O., Calder, A., Gajjar, P., Merugu, S., Huang, W., Britt, D. W., McLean, J. E., Johnson, W. P., and Anderson, A. J., *Interaction of silver nanoparticles with an environmentally beneficial bacterium, Pseudomonas chlororaphis.* Journal of Hazardous Materials, 2011. **188**(1-3): p. 428-435.
88. Habimana, O., Steenkeste, K., Fontaine-Aupart, M.-P., Bellon-Fontaine, M.-N., Kulakauskas, S., and Briandet, R., *Diffusion of nanoparticles in biofilms is altered by bacterial cell wall hydrophobicity.* Applied and Environmental Microbiology, 2011. **77**(1): p. 367-368.
89. Vahdati, A. and Sadeghi, B., *A study on the assessment of DNA strand-breaking activity by silver and silica nanoparticles.* Journal of Nanostructure in Chemistry, 2013. **3**(1): p. 1-3.
90. Hwang, E. T., Lee, J. H., Chae, Y. J., Kim, Y. S., Kim, B. C., Sang, B.-I., and Gu, M. B., *Analysis of the toxic mode of action of silver nanoparticles using stress-specific bioluminescent bacteria.* Small, 2008. **4**(6): p. 746-750.
91. Das, P., Xenopoulos, M. A., Williams, C. J., Hoque, M. E., and Metcalfe, C. D., *Effects of silver nanoparticles on bacterial activity in natural waters.* Environmental Toxicology and Chemistry, 2012. **31**(1): p. 122-130.

92. Hwang, I.-S., Hwang, J. H., Choi, H., Kim, K.-J., and Lee, D. G., *Synergistic effects between silver nanoparticles and antibiotics and the mechanisms involved.* Journal of Medical Microbiology, 2012. **61**(Pt 12): p. 1719-1726.
93. Chen, M., Yang, Z., Wu, H., Pan, X., Xie, X., and Wu, C., *Antimicrobial activity and the mechanism of silver nanoparticle thermosensitive gel.* International Journal of Nanomedicine, 2011. **6**: p. 2873-2877.
94. Siddhartha, S., Tanmay, B., Arnab, R., Gajendra, S., Ramachandrarao, P., and Debabrata, D., *Characterization of enhanced antibacterial effects of novel silver nanoparticles.* Nanotechnology, 2007. **18**(22): p. 225103.
95. Dror-Ehre, A., Adin, A., Markovich, G., and Mamane, H., *Control of biofilm formation in water using molecularly capped silver nanoparticles.* Water Research, 2010. **44**(8): p. 2601-2609.
96. Lee, Y.-J., Kim, J., Oh, J., Bae, S., Lee, S., Hong, I. S., and Kim, S.-H., *Ion-release kinetics and ecotoxicity effects of silver nanoparticles.* Environmental Toxicology and Chemistry, 2012. **31**(1): p. 155-159.
97. Gajjar, P., Pettee, B., Britt, D., Huang, W., Johnson, W., and Anderson, A., *Antimicrobial activities of commercial nanoparticles against an environmental soil microbe, Pseudomonas putida KT2440.* Journal of Biological Engineering, 2009. **3**(1): p. 9.
98. Sotiriou, G. A. and Pratsinis, S. E., *Antibacterial activity of nanosilver ions and particles.* Environmental Science and Technology, 2010. **44**(14): p. 5649-5654.
99. Park, M. V. D. Z., Neigh, A. M., Vermeulen, J. P., Fonteyne, L. J. J. d. l., Verharen, H. W., Briedé, J. J., Loveren, H. v., and Jong, W. H. d., *The effect of particle size on the cytotoxicity, inflammation, developmental toxicity and genotoxicity of silver nanoparticles.* Biomaterials, 2011. **32**(36): p. 9810-9817.
100. Lebovka, N. I., *Aggregation of charged colloidal particles.* Advances in Polymer Science, 2014. **255**: p. 57-96.
101. Xu, H., Qu, F., Xu, H., Lai, W., Andrew Wang, Y., Aguilar, Z., and Wei, H., *Role of reactive oxygen species in the antibacterial mechanism of silver nanoparticles on Escherichia coli O157:H7.* BioMetals, 2012. **25**(1): p. 45-53.
102. Martinez-Gutierrez, F., Boegli, L., Agostinho, A., Sánchez, E. M., Bach, H., Ruiz, F., and James, G., *Anti-biofilm activity of silver nanoparticles against different microorganisms.* Biofouling, 2013. **29**(6): p. 651-660.
103. Fabrega, J., Zhang, R., Renshaw, J. C., Liu, W.-T., and Lead, J. R., *Impact of silver nanoparticles on natural marine biofilm bacteria.* Chemosphere, 2011. **85**(6): p. 961-966.
104. Wirth, S. M., Lowry, G. V., and Tilton, R. D., *Natural organic matter alters biofilm tolerance to silver nanoparticles and dissolved silver.* Environmental Science and Technology, 2012. **46**(22): p. 12687-12696.
105. Pal, A. and Paul, A. K., *Microbial extracellular polymeric substances: central elements in heavy metal bioremediation.* Indian Journal of Microbiology, 2008. **48**: p. 49-64.
106. Mah, T.-F. C. and O'Toole, G. A., *Mechanisms of biofilm resistance to antimicrobial agents.* Trends in Microbiology, 2001. **9**(1): p. 34-39.
107. Jefferson, K. K., *What drives bacteria to produce a biofilm?* FEMS Microbiology Letters, 2004. **236**(2): p. 163-173.

108. Uhlich, G. A., Gunther, N. W., Bayles, D. O., and Mosier, D. A., *The CsgA and Lpp proteins of an Escherichia coli O157:H7 strain affect HEp-2 cell invasion, motility, and biofilm formation.* Infection and Immunity, 2009. **77**(4): p. 1543-1552.
109. Czaczyk, K. and Myszka, K., *Biosynthesis of extracellular polymeric substances (EPS) and its role in microbial biofilm formation.* Polish Journal of Environmental Studies, 2007. **16**(6): p. 799-806.
110. Frade, J. P. and Arthington-Skaggs, B. A., *Effect of serum and surface characteristics on Candida albicans biofilm formation.* Mycoses, 2011. **54**(4): p. e154-e162.
111. Hoffman, L. R., D'Argenio, D. A., MacCoss, M. J., Zhang, Z., Jones, R. A., and Miller, S. I., *Aminoglycoside antibiotics induce bacterial biofilm formation.* Nature, 2005. **436**(7054): p. 1171-1175.
112. Kaplan, J. B., *Antibiotic-induced biofilm formation.* The International Journal of Artificial Organs, 2011. **34**(9): p. 737-751.
113. Schreiber, F. and Szewzyk, U., *Environmentally relevant concentrations of pharmaceuticals influence the initial adhesion of bacteria.* Aquatic Toxicology, 2008. **87**(4): p. 227-233.
114. Lazazzera, B. A., *Lessons from DNA microarray analysis: the gene expression profile of biofilms.* Current Opinion in Microbiology, 2005. **8**(2): p. 222-227.
115. Beloin, C. and Ghigo, J.-M., *Finding gene-expression patterns in bacterial biofilms.* Trends in Microbiology, 2005. **13**(1): p. 16-19.
116. Wilkinson, D. A., Chacko, S. J., Vénien-Bryan, C., Wadhams, G. H., and Armitage, J. P., *Regulation of flagellum number by FliA and FlgM and role in biofilm formation by Rhodobacter sphaeroides.* Journal of Bacteriology, 2011. **193**(15): p. 4010-4014.
117. Mikkelsen, H., Sivaneson, M., and Filloux, A., *Key two-component regulatory systems that control biofilm formation in Pseudomonas aeruginosa.* Environmental Microbiology, 2011. **13**(7): p. 1666-1681.
118. Fux, C. A., Costerton, J. W., Stewart, P. S., and Stoodley, P., *Survival strategies of infectious biofilms.* Trends in Microbiology, 2005. **13**(1): p. 34-40.
119. Trémoulet, F., Duché, O., Namane, A., Martinie, B., and Labadie, J. C., *Comparison of protein patterns of Listeria monocytogenes grown in biofilm or in planktonic mode by proteomic analysis.* FEMS Microbiology Letters, 2002. **210**(1): p. 25-31.
120. Laspidou, C. S. and Rittmann, B. E., *A unified theory for extracellular polymeric substances, soluble microbial products, and active and inert biomass.* Water Research, 2002. **36**(11): p. 2711-2720.
121. Flemming, H.-C. and Wingender, J., *The biofilm matrix.* Nature Reviews Microbiology, 2010. **8**: p. 623-633.
122. Donlan, R. M., *Biofilms: microbial life on surfaces.* Emerging Infectious Disease, 2002. **8**(9): p. 881-890.
123. Flemming, H.-C. and Wingender, J., *Relevance of microbial extracellular polymeric substances (EPSs) Part 1 Structural and ecological aspects.* Water Science and Technology, 2001. **43**: p. 1-8.

124. Flemming, H.-C., Neu, T. R., and Wozniak, D. J., *The EPS matrix: the house of biofilm cells.* Journal of Bacteriology, 2007. **189**(22): p. 7945-7947.
125. Jiao, Y., Cody, G. D., Harding, A. K., Wilmes, P., Schrenk, M., Wheeler, K. E., Banfield, J. F., and Thelen, M. P., *Characterization of extracellular polymeric substances from acidophilic microbial biofilms.* Applied and Environmental Microbiology, 2010. **76**(9): p. 2916-2922.
126. Lazarova, V. and Manem, J., *Biofilm characterization and activity analysis in water and wastewater treatment.* Water Research, 1995. **29**(10): p. 2227-2245.
127. Azeredo, J. and Oliveira, R., *The role of exopolymers produced by Sphingomonas paucimobilis in biofilm formation and composition.* Biofouling: The Journal of Bioadhesion and Biofilm Research, 2000. **16**(1): p. 17 - 27.
128. Jahn, A., Griebe, T., and Nielsen, P. H., *Composition of Pseudomonas putida biofilms: accumulation of protein in the biofilm matrix.* Biofouling: The Journal of Bioadhesion and Biofilm Research, 1999. **14**(1): p. 49 - 57.
129. Neu, T. R. and Lawrence, J. R., *Lectin-binding-analysis in biofilm systems.* Methods in Enzymology, 1999. **310**: p. 145-152.
130. Whitchurch, C. B., Tolker-Nielsen, T., Ragas, P. C., and Mattick, J. S., *Extracellular DNA required for bacterial biofilm formation.* Science, 2002. **295**(5559): p. 1487-.
131. Schurr, M. J., *Which bacterial biofilm exopolysaccharide is preferred, Psl or alginate?* Journal of Bacteriology, 2013. **195**(8): p. 1623-1626.
132. Nilsson, M., Chiang, W.-C., Fazli, M., Gjermansen, M., Givskov, M., and Tolker-Nielsen, T., *Influence of putative exopolysaccharide genes on Pseudomonas putida KT2440 biofilm stability.* Environmental Microbiology, 2011. **13**(5): p. 1357-1369.
133. Khan, S. S., Srivatsan, P., Vaishnavi, N., Mukherjee, A., and Chandrasekaran, N., *Interaction of silver nanoparticles (SNPs) with bacterial extracellular proteins (ECPs) and its adsorption isotherms and kinetics.* Journal of Hazardous Materials, 2011. **192**(1): p. 299-306.
134. Costerton, J. W., Cheng, K. J., Geesey, G. G., Ladd, T. I., Nickel, J. C., Dasgupta, M., and Marrie, T. J., *Bacterial biofilms in nature and disease.* Annual Review of Microbiology, 1987. **41**(1): p. 435-464.
135. Hunt, S., *Diversity of biopolymer structure and its potential for ion-binding applications*, in *Immobilisation of ions by bio-sorption*, H. Eccles and S. Hunt, Editors. 1986, Ellis Horwood Ltd.: West Sussex, United Kingdom. p. 15-46.
136. Joshi, N., Ngwenya, B. T., and French, C. E., *Enhanced resistance to nanoparticle toxicity is conferred by overproduction of extracellular polymeric substances.* Journal of Hazardous Materials, 2012. **241–242**(0): p. 363-370.
137. Davies, D. G., Parsek, M. R., Pearson, J. P., Iglewski, B. H., Costerton, J. W., and Greenberg, E. P., *The involvement of cell-to-cell signals in the development of a bacterial biofilm.* Science, 1998. **280**(5361): p. 295-298.
138. Hassett, D. J., Ma, J.-F., Elkins, J. G., McDermott, T. R., Ochsner, U. A., West, S. E. H., Huang, C.-T., Fredericks, J., Burnett, S., Stewart, P. S., McFeters, G., Passador, L., and Iglewski, B. H., *Quorum sensing in Pseudomonas aeruginosa controls expression of catalase and superoxide*

dismutase genes and mediates biofilm susceptibility to hydrogen peroxide. Molecular Microbiology, 1999. **34**(5): p. 1082-1093.

139. Xie, H., Cook, G. S., Costerton, J. W., Bruce, G., Rose, T. M., and Lamont, R. J., *Intergeneric communication in dental plaque biofilms.* Journal of Bacteriology, 2000. **182**: p. 7067-7069.
140. Spoering, A. L. and Lewis, K., *Biofilms and planktonic cells of Pseudomonas aeruginosa have similar resistance to killing by antimicrobials.* Journal of Bacteriology, 2001. **183**(23): p. 6746-6751.
141. Stewart, P. S., *Mechanisms of antibiotic resistance in bacterial biofilms.* International Journal of Medical Microbiology, 2002. **292**(2): p. 107-113.
142. Keren, I., Shah, D., Spoering, A., Kaldalu, N., and Lewis, K., *Specialized persister cells and the mechanism of multidrug tolerance in Escherichia coli.* Journal of Bacteriology, 2004. **186**(24): p. 8172-8180.
143. Stewart, P. S. and Franklin, M. J., *Physiological heterogeneity in biofilms.* Nature Reviews Microbiology, 2008. **6**(3): p. 199-210.
144. Høiby, N., Bjarnsholt, T., Givskov, M., Molin, S., and Ciofu, O., *Antibiotic resistance of bacterial biofilms.* International Journal of Antimicrobial Agents, 2010. **35**(4): p. 322-332.
145. González, A., Mombo, S., Leflaive, J., Lamy, A., Pokrovsky, O., and Rols, J.-L., *Silver nanoparticles impact phototrophic biofilm communities to a considerably higher degree than ionic silver.* Environmental Science and Pollution Research, 2014: p. 1-13.
146. Habash, M. B., Park, A. J., Vis, E. C., Harris, R. J., and Khursigara, C. M., *Synergy of silver nanoparticles and aztreonam against Pseudomonas aeruginosa PAO1 biofilms.* Antimicrobial Agents and Chemotherapy, 2014. **58**(10): p. 5818-5830.
147. Monds, R. D. and O'Toole, G. A., *The developmental model of microbial biofilms: ten years of a paradigm up for review.* Trends in Microbiology, 2009. **17**(2): p. 73-87.
148. Ghafoor, A., Hay, I. D., and Rehm, B. H. A., *Role of Exopolysaccharides in Pseudomonas aeruginosa Biofilm Formation and Architecture.* Applied and Environmental Microbiology, 2011. **77**(15): p. 5238-5246.
149. Martínez-Gil, M., Quesada, J. M., Ramos-González, M. I., Soriano, M. I., de Cristóbal, R. E., and Espinosa-Urgel, M., *Interplay between extracellular matrix components of Pseudomonas putida biofilms.* Research in Microbiology, 2013. **164**(5): p. 382-389.
150. Nelson, K. E., Weinel, C., Paulsen, I. T., Dodson, R. J., Hilbert, H., Martins dos Santos, V. A. P., Fouts, D. E., Gill, S. R., Pop, M., Holmes, M., Brinkac, L., Beanan, M., DeBoy, R. T., Daugherty, S., Kolonay, J., Madupu, R., Nelson, W., White, O., Peterson, J., Khouri, H., Hance, I., Lee, P. C., Holtzapple, E., Scanlan, D., Tran, K., Moazzez, A., Utterback, T., Rizzo, M., Lee, K., Kosack, D., Moestl, D., Wedler, H., Lauber, J., Stjepandic, D., Hoheisel, J., Straetz, M., Heim, S., Kiewitz, C., Eisen, J., Timmis, K. N., Düsterhöft, A., Tümmler, B., and Fraser, C. M., *Complete genome sequence and comparative analysis of the metabolically versatile Pseudomonas putida KT2440.* Environmental Microbiology, 2002. **4**(12): p. 799-808.

151. Mulfinger, L., Solomon, S. D., Bahadory, M., Jeyarajasingam, A. V., Rutkowsky, S. A., and Boritz, C., *Synthesis and study of silver nanoparticles.* Journal of Chemical Education, 2007. **84**(2): p. 322-325.
152. Sule, P., Wadhawan, T., Carr, N. J., Horne, S. M., Wolfe, A. J., and Prüβ, B. M., *A combination of assays reveals biomass differences in biofilms formed by Escherichia coli mutants.* Letters in Applied Microbiology, 2009. **49**(3): p. 299-304.
153. Masuko, T., Minami, A., Iwasaki, N., Majima, T., Nishimura, S.-I., and Lee, Y. C., *Carbohydrate analysis by a phenol–sulfuric acid method in microplate format.* Analytical Biochemistry, 2005. **339**(1): p. 69-72.
154. Horne, S. and Prüß, B., *Global gene regulation in Yersinia enterocolitica: effect of FliA on the expression levels of flagellar and plasmid-encoded virulence genes.* Archives of Microbiology, 2006. **185**(2): p. 115-126.
155. Schmittgen, T. D. and Livak, K. J., *Analyzing real-time PCR data by the comparative C_T method.* Nature Protocols, 2008. **3**: p. 1101-1108.
156. Jung, W. K., Koo, H. C., Kim, K. W., Shin, S., Kim, S. H., and Park, Y. H., *Antibacterial activity and mechanism of action of the silver ion in Staphylococcus aureus and Escherichia coli.* Applied and Environmental Microbiology, 2008. **74**(7): p. 2171-2178.
157. Bourven, I., Costa, G., and Guibaud, G., *Qualitative characterization of the protein fraction of exopolymeric substances (EPS) extracted with EDTA from sludge.* Bioresource Technology, 2012. **104**(0): p. 486-496.
158. Vu, B., Chen, M., Crawford, R., and Ivanova, E., *Bacterial extracellular polysaccharides involved in biofilm formation.* Molecules, 2009. **14**(7): p. 2535-2554.
159. Saldaña, Z., Xicohtencatl-Cortes, J., Avelino, F., Phillips, A. D., Kaper, J. B., Puente, J. L., and Girón, J. A., *Synergistic role of curli and cellulose in cell adherence and biofilm formation of attaching and effacing Escherichia coli and identification of Fis as a negative regulator of curli.* Environmental Microbiology, 2009. **11**(4): p. 992-1006.
160. Barnhart, M. M. and Chapman, M. R., *Curli biogenesis and function.* Annual Review of Microbiology, 2006. **60**(1): p. 131-147.
161. Diaz, E., Haaf, H., Lai, A., and Yadana, J., *Role of alginate in gentamicin antibiotic susceptibility during the early stages of Pseudomonas aeruginosa PAO1 biofilm establishment.* Journal of Experimental Microbiology and Immunology, 2011. **15**: p. 71-78.
162. Anderl, J. N., Zahller, J., Roe, F., and Stewart, P. S., *Role of nutrient limitation and stationary-phase existence in Klebsiella pneumoniae biofilm resistance to ampicillin and ciprofloxacin.* Antimicrobial Agents and Chemotherapy, 2003. **47**(4): p. 1251-1256.
163. Rodrigues, D. F. and Elimelech, M., *Toxic effects of single-walled carbon nanotubes in the development of E. coli biofilm.* Environmental Science and Technology, 2010. **44**(12): p. 4583-4589.
164. Liang, Z., Li, W., Yang, S., and Du, P., *Extraction and structural characteristics of extracellular polymeric substances (EPS), pellets in autotrophic nitrifying biofilm and activated sludge.* Chemosphere, 2010. **81**(5): p. 626-632.

165. Golovina, N. B. and Kustov, L. M., *Toxicity of metal nanoparticles with a focus on silver.* Mendeleev Communications, 2013. **23**(2): p. 59-65.
166. Angel, B. M., Batley, G. E., Jarolimek, C. V., and Rogers, N. J., *The impact of size on the fate and toxicity of nanoparticulate silver in aquatic systems.* Chemosphere, 2013. **93**(2): p. 359-365.
167. Ellis, B. D., Butterfield, P., Jones, W. L., McFeters, G. A., and Camper, A. K., *Effects of carbon source, carbon concentration, and chlorination on growth related parameters of heterotrophic biofilm bacteria.* Microbial Ecology, 2000. **38**: p. 330-347.
168. Miqueleto, A. P., Dolosic, C. C., Pozzi, E., Foresti, E., and Zaiat, M., *Influence of carbon sources and C/N ratio on EPS production in anaerobic sequencing batch biofilm reactors for wastewater treatment.* Bioresource Technology, 2010. **101**(4): p. 1324-1330.
169. Aswathanarayan, J. B. and Vittal, R. R., *Attachment and biofilm formation of Pseudomonas fluorescens PSD4 isolated from a dairy processing line.* Food Science and Biotechnology, 2014. **23**(6): p. 1903-1910.
170. Dufour, D., Leung, V., and Lévesque, C. M., *Bacterial biofilm: structure, function, and antimicrobial resistance.* Endodontic Topics, 2012. **22**: p. 2-16.
171. Colvin, K. M., Gordon, V. D., Murakami, K., Borlee, B. R., Wozniak, D. J., Wong, G. C. L., and Parsek, M. R., *The Pel polysaccharide can serve a structural and protective role in the biofilm matrix of Pseudomonas aeruginosa.* PLoS ONE, 2011. **7**(e1001264).
172. Herigstad, B., Hamilton, M., and Heersink, J., *How to optimize the drop plate method for enumerating bacteria.* Journal of Microbiological Methods, 2001. **44**(2): p. 121-129.
173. Lowry, O., Rosebrough, N., Fan, A., and Randall, R., *Protein measurement with the folin phenol reagent.* The Journal of Biological Chemistry, 1951. **193**: p. 265-275.
174. Heydorn, A., Nielsen, A. T., Hentzer, M., Sternberg, C., Givskov, M., Ersboll, B. K., and Molin, S., *Quantification of biofilm structures by the novel computer program COMSTAT.* Microbiology, 2000. **146**(10): p. 2395-2407.
175. Klausen, M., Heydorn, A., Ragas, P., Lambertsen, L., Aaes-Jørgensen, A., Molin, S., and Tolker-Nielsen, T., *Biofilm formation by Pseudomonas aeruginosa wild type, flagella and type IV pili mutants.* Molecular Microbiology, 2003. **48**(6): p. 1511-1524.
176. Cao, B., Shi, L., Brown, R. N., Xiong, Y., Fredrickson, J. K., Romine, M. F., Marshall, M. J., Lipton, M. S., and Beyenal, H., *Extracellular polymeric substances from Shewanella sp. HRCR-1 biofilms: characterization by infrared spectroscopy and proteomics.* Environmental Microbiology, 2011. **13**(4): p. 1018-1031.
177. Hu, X.-b., Xu, K., Wang, Z., Ding, L.-l., and Ren, H.-q., *Characteristics of biofilm attaching to carriers in moving bed biofilm reactor used to treat vitamin C wastewater.* Scanning, 2013. **35**(5): p. 283-291.
178. Bensadoun, A. and Weinstein, D., *Assay of proteins in the presence of interfering materials.* Analytical Biochemistry, 1976. **70**(1): p. 241-250.

179. Khan, S. S., Mukherjee, A., and Chandrasekaran, N., *Impact of exopolysaccharides on the stability of silver nanoparticles in water.* Water Research, 2011. **45**(16): p. 5184-5190.
180. Xue, Z., Sendamangalam, V. R., Gruden, C. L., and Seo, Y., *Multiple roles of extracellular polymeric substances on resistance of biofilm and detached clusters.* Environmental Science and Technology, 2012. **46**: p. 13212-13219.
181. Hamanaka, D., Onishi, M., Genkawa, T., Tanaka, F., and Uchino, T., *Effects of temperature and nutrient concentration on the structural characteristics and removal of vegetable-associated Pseudomonas biofilm.* Food Control, 2012. **24**: p. 165-170.
182. Rescalli, E., Saini, S., Bartocci, C., Rychlewski, L., de Lorenzo, V., and Bertoni, G., *Novel physiological modulation of the Pu promoter of TOL plasmid: Negative regulatory role of the TurA protein of Pseudomonas putida in the response to suboptimal growth temperatures.* Journal of Biological Chemistry, 2004. **279**(9): p. 7777-7784.
183. Sauer, K., Cullen, M. C., Rickard, A. H., Zeef, L. A. H., Davies, D. G., and Gilbert, P., *Characterization of Nutrient-Induced Dispersion in Pseudomonas aeruginosa PAO1 Biofilm.* Journal of Bacteriology, 2004. **186**(21): p. 7312-7326.
184. Chambless, J. D., Hunt, S. M., and Stewart, P. S., *A three-dimensional computer model of four hypothetical mechanisms protecting biofilms from antimicrobials.* Applied and Environmental Microbiology, 2006. **72**(3): p. 2005-2013.
185. Alasonati, E. and Slaveykova, V. I., *Effects of extraction methods on the composition and molar mass distributions of exopolymeric substances of the bacterium Sinorhizobium meliloti.* Bioresource Technology, 2012. **114**(0): p. 603-609.
186. Ostermeyer, A.-K., Kostigen Mumuper, C., Semprini, L., and Radniecki, T., *Influence of bovine serum slbumin and alginate on silver nanoparticle dissolution and toxicity to Nitrosomonas europaea.* Environmental Science and Technology, 2013. **47**(24): p. 14403-14410.
187. Chen, X. and Schluesener, H. J., *Nanosilver: A nanoproduct in medical application.* Toxicology Letters, 2008. **176**(1): p. 1-12.
188. Fabrega, J., Luoma, S. N., Tyler, C. R., Galloway, T. S., and Lead, J. R., *Silver nanoparticles: Behaviour and effects in the aquatic environment.* Environment International, 2011. **37**(2): p. 517-531.
189. Nowack, B. and Bucheli, T. D., *Occurrence, behavior and effects of nanoparticles in the environment.* Environmental Pollution, 2007. **150**(1): p. 5-22.
190. Feng, Q. L., Wu, J., Chen, G. Q., Cui, F. Z., Kim, T. N., and Kim, J. O., *A mechanistic study of the antibacterial effect of silver ions on Escherichia coli and Staphylococcus aureus.* Journal of Biomedical Materials Research, 2000. **52**(4): p. 662-668.
191. Lok, C., Ho, C., Chen, R., He, Q., Yu, W., Sun, H., Tam, P., Chiu, J., and Che, C., *Proteomic analysis of the mode of antibacterial action of silver nanoparticles.* Journal of Proteome Research, 2006. **5**: p. 916-924.

192. Yang, X., Gondikas, A. P., Marinakos, S. M., Auffan, M., Liu, J., Hsu-Kim, H., and Meyer, J. N., *Mechanism of silver nanoparticle toxicity is dependent on dissolved silver and surface coating in Caenorhabditis elegans.* Environmental Science and Technology, 2011. **46**(2): p. 1119-1127.
193. Greulich, C., Braun, D., Peetsch, A., Diendorf, J., Siebers, B., Epple, M., and Köller, M., *The toxic effect of silver ions and silver nanoparticles towards bacteria and human cells occurs in the same concentration range.* RSC Advances, 2012. **2**: p. 6981-6987.
194. Maurer-Jones, M. A., Mousavi, M. P. S., Chen, L. D., Buhlmann, P., and Haynes, C. L., *Characterization of silver ion dissolution from silver nanoparticles using fluorous-phase ion-selective electrodes and assessment of resultant toxicity to Shewanella oneidensis.* Chemical Science, 2013. **4**(6): p. 2564-2572.
195. El Badawy, A. M., Luxton, T. P., Silva, R. G., Scheckel, K. G., Suidan, M. T., and Tolaymat, T. M., *Impact of Environmental Conditions (pH, Ionic Strength, and Electrolyte Type) on the Surface Charge and Aggregation of Silver Nanoparticles Suspensions.* Environmental Science and Technology, 2010. **44**(4): p. 1260-1266.
196. Xiu, Z.-m., Zhang, Q.-b., Puppala, H. L., Colvin, V. L., and Alvarez, P. J. J., *Negligible particle-specific antibacterial activity of silver nanoparticles.* Nano Letters, 2012. **12**(8): p. 4271-4275.
197. Binaeian, E., Safekordi, A. A., Attar, H., Saber, R., Chaichi, M. J., and Kolagar, A. H., *Comparative toxicity study of two different synthesized silver nanoparticles on the bacteria Vibrio fischeri.* African Journal of Biotechnology, 2012. **11**(29): p. 7554-7564.

APPENDIX

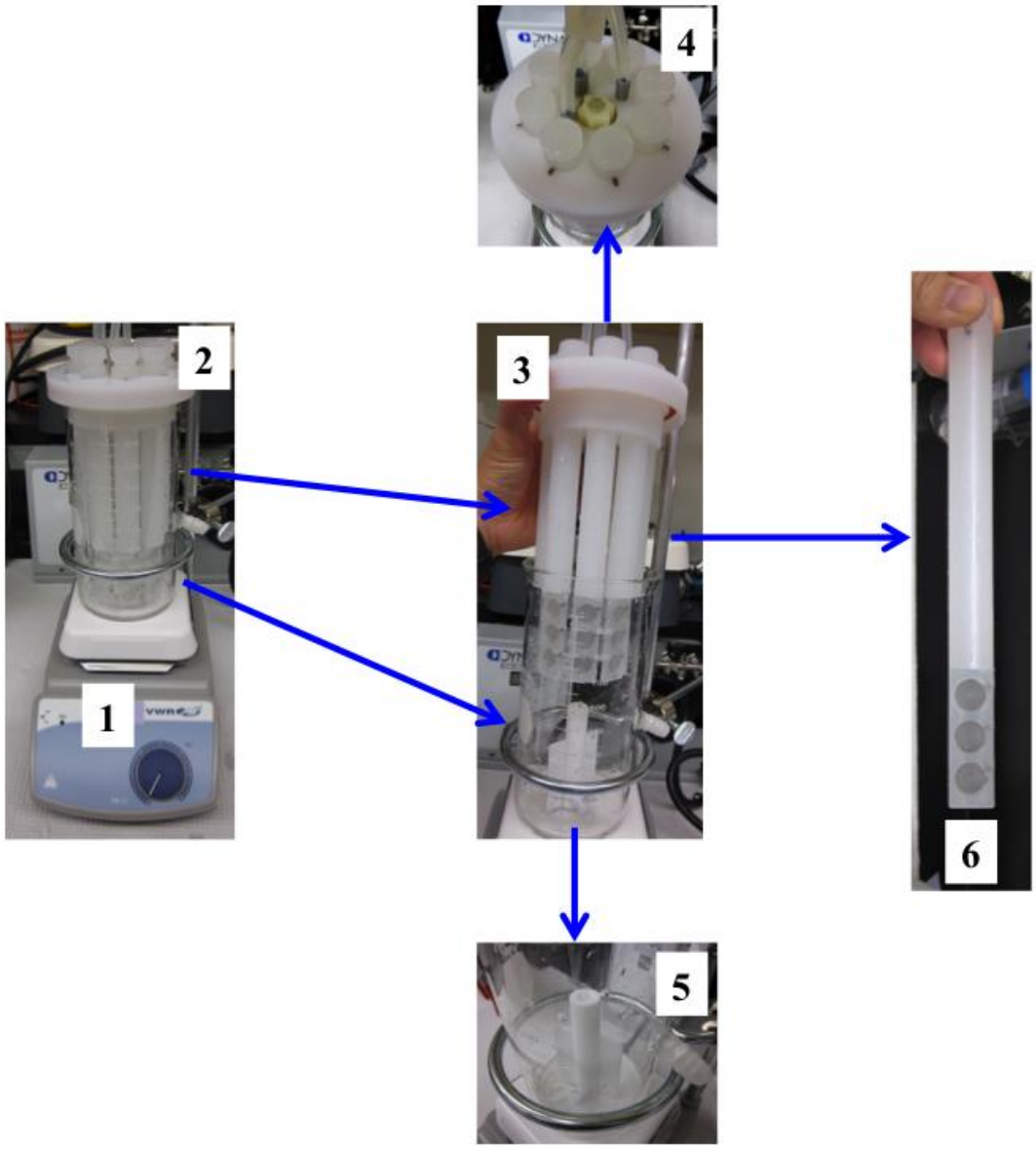

Figure A-1 CDC reactor and its compartments: (1) Stirrer; (2) Glass reactor; (3) Top compartment of the reactor; (4) Top compartment holding eight polystyrene rods and air inlets; (5) Baffle attached with a magnetic bar; and (6) Rod containing three polystyrene coupons.

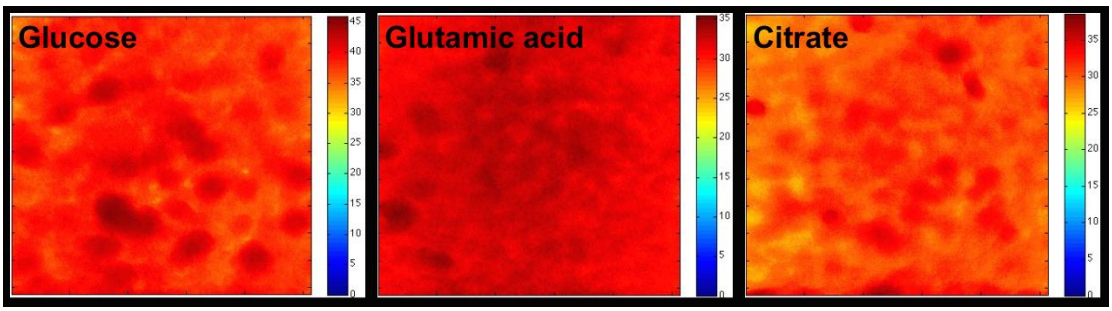

Figure A-2 The processed images of biofilms forming in different carbon sources obtained from COMSTAT software. More red intensity shows more biomass of biofilms.

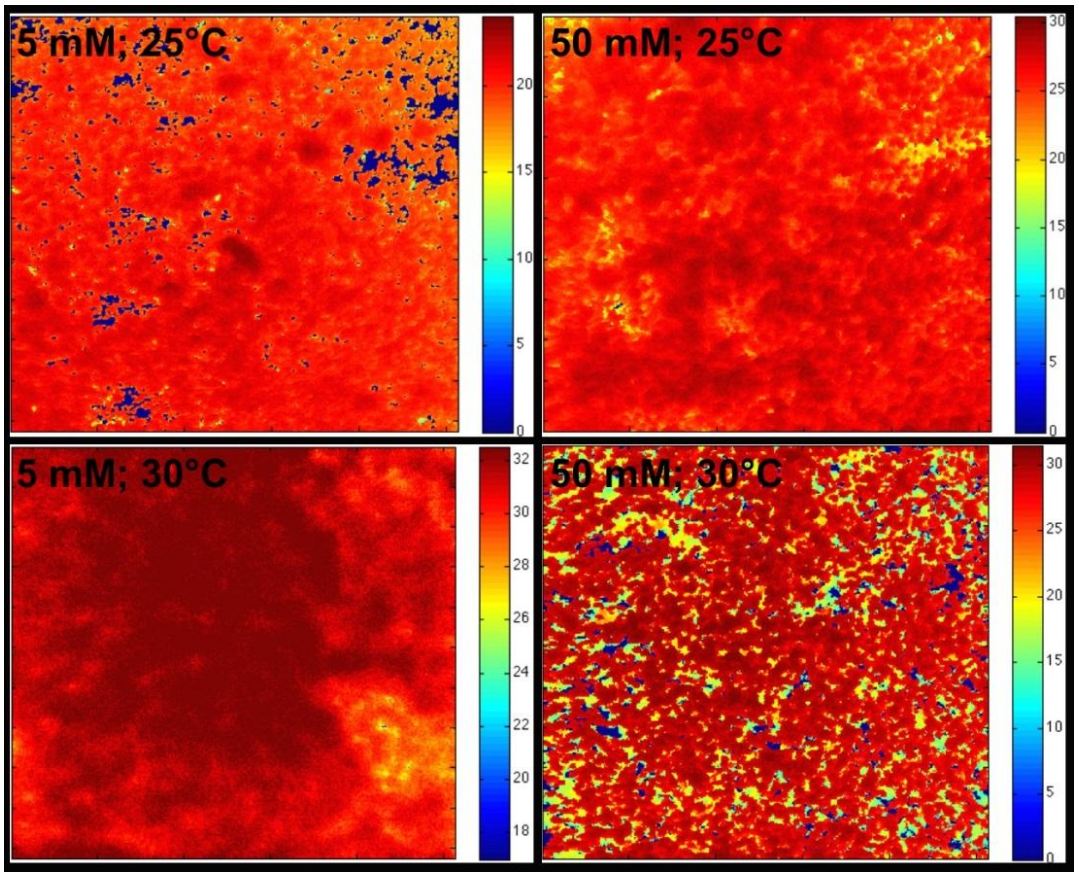

Figure A-3 The processed images of biofilms forming in different carbon concentrations and temperatures obtained from COMSTAT software. More red intensity shows more biomass of biofilms.

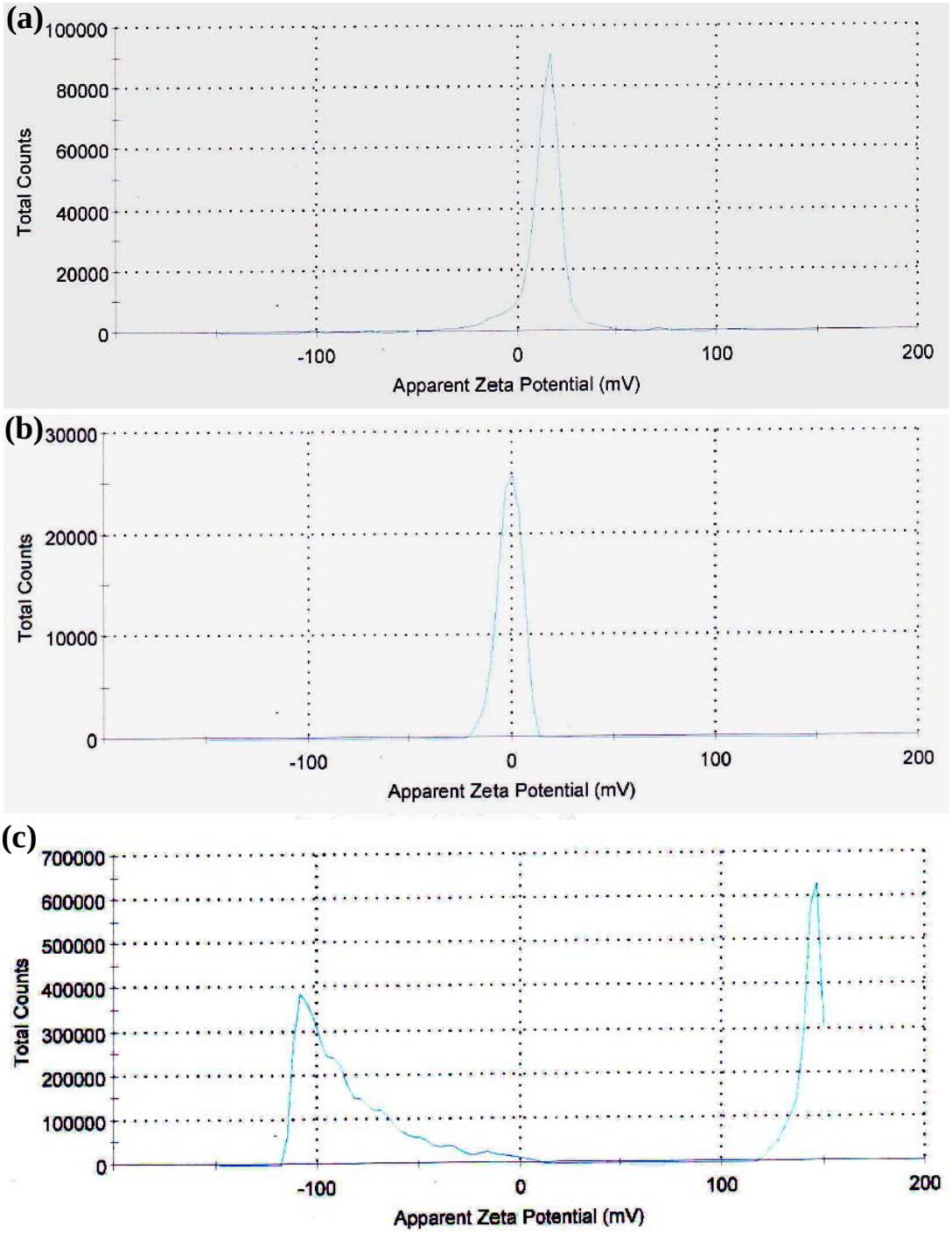

Figure A-4 Zeta potential distributions: (a) AgNPs#1; (b) AgNPs#2; and (c) AgNPs#3. The AgNPs were synthesized by using the molar ratio of BH_4^-/Ag^+ at 0.1. Two peaks of the zeta potentials show highly negative and positive charges in the AgNP solution.

Table A-1 The statistical differences (*p* value) of total carbohydrate and total protein between biofilms forming in glucose, glutamic acid, and citrate analyzed by the multiple *t*-test.

	Glucose vs. glutamic acid	Glucose vs. citrate	Glutamic acid vs. citrate
Total carbohydrate	0.079	0.179	0.304
Total protein	0.003*	0.001*	0.004*

**p* value less than 0.05 = statistical difference

Table A-2 FTIR spectrum and possible functional groups in EPS of biofilms forming in glucose, glutamic acid, and citrate. The spectrum is shown as a wavelength number (cm^{-1}).

Functional group	Glucose	Glutamic acid	Citrate
O–H (carboxylic acids)	3289	3287	3287
C–H (alkane)	2958	2955	2957
	2927	2926	2926
	2875	2873	2875
	2857	2856	2856
*	2372	2365	2365
C=O (carbonyl)	1657	1657	1657
	1651	1652	1651
N–H (amine)	1538	1538	1538
*	1452	1453	1454
	1395	1390	1367
	1239	1270	1269
	1078	1240	1242
	991	1079	1083
	917	987	986
	865		855

*The spectra that could not be identified were left as blank. The spectra less than 1500 cm^{-1} are defined as fingerprint area, which is caused by complex deformation of molecules.

Table A-3 Statistical differences (*p* value) of physical characteristics between biofilms forming in glucose, glutamic acid, and citrate analyzed by the multiple *t*-test.

Characteristics	Glucose vs. glutamic acid	Glucose vs. citrate	Glutamic acid vs. citrate
Thickness (μm)	0.006*	0.0003*	0.019*
Biomass volume ($\mu m^3/ \mu m^2$)	0.192	0.011*	0.100
Surface to volume ratio ($\mu m^3/ \mu m^{2)}$	0.952	0.262	0.483
Roughness coefficient	0.002*	0.527	0.935

**p* value less than 0.05 = statistical difference

Table A-4 Statistical differences (*p* value) of physical characteristics between biofilms forming 5 and 50 mM of glucose analyzed by the multiple *t*-test.

Characteristics	25°C	30°C
	5 mM vs. 50 mM	5 mM vs. 50 mM
Thickness (μm)	0.342	0.0007*
Biomass volume ($\mu m^3/ \mu m^2$)	0.024*	0.018*
Surface to volume ratio ($\mu m^3/ \mu m^{2)}$	0.042*	0.034*
Roughness coefficient	0.439	0.050

**p* value less than 0.05 = statistical difference

Table A-5 Statistical differences (*p* value) of physical characteristics between biofilms forming in 25 and 30°C analyzed by the multiple *t*-test.

Characteristics	5 mM	50 mM
	25°C vs. 30°C	25°C vs. 30°C
Thickness (μm)	0.012*	0.010*
Biomass volume ($\mu m^3/ \mu m^2$)	0.067	0.001*
Surface to volume ratio ($\mu m^3/ \mu m^{2)}$	0.071	0.023*
Roughness coefficient	0.122	0.076

**p* value less than 0.05 = statistical difference

Table A-6 Statistical differences (*p* value) of physical characteristics of biofilms before and after 0.25% EDTA treatment analyzed by the multiple *t*-test.

Characteristics	Before vs. after EDTA treatment			
	5 mM; 25°C	5 mM; 30°C	50 mM; 25°C	50 mM; 30°C
Thickness (μm)	0.004*	0.049*	0.0002*	0.024
Biomass volume ($\mu m^3/ \mu m^2$)	0.006*	0.007*	0.001*	0.226
Surface to volume ratio ($\mu m^3/ \mu m^{2)}$	0.009*	0.003*	0.002*	0.876
Roughness coefficient	0.043*	0.015*	0.011*	0.439

**p* value less than 0.05 = statistical difference

VITA

Pumis Thuptimdang was born in Trang, Thailand. He grew up in Yala before attending high school at Hatyaiwittayalai School in Songkhla. In 2003, Pumis entered the Faculty of Science at Chulalongkorn University (CU). He received the Bachelor of Science (General Science) in 2007. Then, he went for a graduate study in Environmental Management at the International Program in Hazardous Substance and Environmental Management, CU, where he had a chance to conduct his Master research at Chia-Nan University of Pharmacy and Science in Tainan, Taiwan. Pumis was able to publish part of his research in Environmental Science and Pollution Research journal under the title 'Degradation of o-toluidine by fluidized-bed Fenton process: statistical and kinetic study.' After he obtained the Master of Science in 2009, he immediately continued to pursue for the Doctoral degree in Environmental Management at the same program. This time, he got an opportunity to travel to North Dakota State University in Fargo, ND, USA to conduct his research for four years. Part of his doctoral research was published in Journal of Hazardous Materials under the title 'Effect of silver nanoparticles on Pseudomonas putida biofilms at different stages of maturity.' Pumis obtains the Doctor of Philosophy degree in 2015.